

AN ABSTRACT OF THE THESIS OF

Jacqueline Frizenschaf for the degree of Master of Science in
Civil Engineering presented on April 29, 1988

Title: Hydraulic Influences on Pool Morphology --
A Laboratory Investigation

Abstract approved: Redacted for Privacy

A flume study was conducted to investigate the influences of changing hydraulic conditions on the bed morphology of a scoured pool.

During a simulated storm runoff event, responses of the pool were tested under different conditions: clearwater flow, sediment supply at steady rates, and two different sediment mixtures of the pool material between two fixed riffles. Bedload transport in this modelled riffle-pool-riffle sequence was measured to better understand the transport system in a gravel-bed stream.

In addition, an attempt was made to verify the hypothesis of 'competence reversal' between the upstream riffle and subsequent pool. This hypothesis tries to explain areal sorting mechanisms in pools and riffles.

Significant influences on the scour shape of a pool are the quantity and quality of the upstream sediment supply and the grain size distribution of the bed material itself. Higher sediment input into the riffle-pool-riffle system results in shallower pools. Vertical velocity profiles, approaching logarithmic profiles similar to those

on the riffle, are then characteristic. Negative and zero bottom velocities are predominant for those pools shaped under clearwater conditions. The equilibrium scour depth in the case of a heterogeneous bed with a protecting surface layer of coarse particles (armour layer) might be a misleading indicator of the actual scour processes. Partial armouring in the pool can cause deeper local scour than in a non-armoured bed. The total volume of scoured material, however, might still be less than in the case of a non-armoured bed. Hence, even though the depth of a scoured pool can be larger in an armoured bed, less bed material might be transported out of the system.

Under steady flow and steady sediment feed conditions, bedload transport occurs in an unsteady, pulse-wise pattern. Sediment piles up within the pool and moves downstream in waves.

'Competence reversal' could not be verified in the conducted experiments. Under the modelled flow conditions, bottom and mean velocities in the pool never exceeded those on the riffle -- one possible condition for competence reversal. The analysis of other hydraulic parameters also did not indicate any possible reversal.

A more detailed investigation of increasing turbulence with increasing discharge in the pool is suggested. This could be a main driving force for large particle transport from the pool onto the downstream riffle during different flow conditions.

**HYDRAULIC INFLUENCES ON POOL MORPHOLOGY —
A LABORATORY INVESTIGATION**

by

Jacqueline Frizenschaf

A THESIS

submitted to

Oregon State University

in partial fulfillment of
the requirements for the
degree of

MASTER OF SCIENCE

Completed April 29, 1988

Commencement June 1989

APPROVED:

Redacted for Privacy

Professor of Civil Engineering in charge of major

Redacted for Privacy

Head of Department of Civil Engineering

Redacted for Privacy

Dean of Graduate School

Date thesis is presented April 29, 1988

Typed by Carol Phelps for Jacqueline Frizenschaf

To my mother
who made this all possible

ACKNOWLEDGEMENTS

I would like to express my appreciation to Dr. Peter C. Klingeman for his encouragement to begin this project and for his help throughout the study, especially during the final phase of writing.

My personal thanks go to my Master's examination committee members Dr. Robert L. Beschta and Dr. Jonathan D. Istok, who both helped me to further develop ideas and supported me with suggestions. I am especially thankful to Cheng-Chang Huang for the numberless discussions we had throughout the study. His advice was of great importance to me. Words of thanks go also to Habibollah Matin, who was willing to help me with the HEC-6 computer program. I am grateful to Andrew M. Brickman, who constantly helped me maintain the equipment and my morale, when both seemed to break down.

The research on which this study is based was financed in part by the United States Department of the Interior, Geological Survey, through the Oregon Water Resources Research Institute.

Last but not least, I want to thank the special person in my life, Jeffrey D. Connor who gave me the necessary support throughout this study and encouragement for my final exam.

TABLE OF CONTENTS

<u>Chapter</u>		<u>Page</u>
I	INTRODUCTION.....	1
	Purpose and objectives of the laboratory investigation.....	2
	Experimental approach.....	3
	Organization of the thesis.....	4
II	LITERATURE REVIEW.....	7
	The formation of pools and riffles in gravel-bed rivers.....	8
	The concept of unit stream power and the law of least time rate of energy expenditure.....	9
	Nomenclature and classification schemes of different pool and riffle units.....	13
	Hypothesis of competence reversal and areal sorting mechanisms.....	16
	Bedload transport.....	25
	Summary.....	27
III	LABORATORY EXPERIMENTATION.....	29
	Experimental approach.....	29
	Prototype information for the experimental design.....	30
	Preliminary calculations for the experimental set up.....	31
	Experimental design.....	36
	Runs and measurements.....	36
	Overview.....	36

<u>Chapter</u>	<u>Page</u>
Velocities.....	41
Flow Patterns.....	42
Bed morphology.....	43
Bedload transport.....	44
Summary.....	46
IV RESULTS AND INTERPRETATION.....	48
Overview.....	48
Bed morphology changes.....	50
Clearwater scour for a homogeneous bed.....	50
Comparison of clearwater scour for a homogeneous and a heterogeneous bed.....	54
Sediment feed test runs.....	63
Bed scour with sediment supply from upstream.....	67
Description of scour shapes in run 3 and comparison with clearwater shapes in run 1.....	67
Comparison of scour shapes for homogeneous and heterogeneous beds when sediment is supplied to the system.....	73
Bedload transport.....	75
Comparison of bedload output rates in the clearwater experiments.....	78
Comparison of bedload output rates in the experiments with sediment feed.....	81
Relationship between bedload transport rates and maximum scoured volumes.....	89
Competence reversal.....	93
Hydraulic characteristics of the modelled riffle-pool-riffle sequence.....	94

<u>Chapter</u>	<u>Page</u>
Froude number.....	97
Hydraulic radius.....	99
Velocity reversal.....	101
Considerations about shear stress reversal calculations.....	106
V SUMMARY AND CONCLUSIONS.....	115
Bed morphology changes.....	115
Competence reversal hypothesis.....	120
VI IMPLICATIONS AND RECOMMENDATIONS.....	124
Some implications of the research.....	124
Recommendations for future research.....	126
VII BIBLIOGRAPHY.....	128
APPENDIX A: Oak Creek field site data.....	133
APPENDIX B: Laboratory sediment characteristics.....	134
APPENDIX C: Bedload transport calculations using the HEC-6 computer program.....	135
APPENDIX D: Experimental data.....	141

LIST OF FIGURES

<u>Figure</u>		<u>Page</u>
1	Classification schemes for pools after Sullivan (1986)	15
2	Low and high water surface slopes in a riffle-pool-riffle sequence	17
3	Mean bottom velocities for a pool and riffle versus discharge after Keller (1971)	19
4	Mean bottom velocities for a pool and riffle versus discharge after Richards (1978)	19
5	Hydraulic parameters in a riffle-pool-riffle sequence over a range of discharges after Lisle (1979)	22
6	Water channel used in the experiment	37
7	Riffle-pool-riffle sequence modelled in the experiment	38
8	Model hydrograph used in the experiment	39
9	Composite scour shapes for run 1	52
10	Superimposed velocity profiles for run 1	55
11	Comparison of scour shapes for runs 1 and 4	56
12	Partial armour layer formation in the pool (view looking downstream from above)	61
13	Superimposed velocity profiles for runs 1d and 4d	62
14	Scour shapes in sediment feed test run 2	64
15	Sediment output rates for run 2	65
16	Comparison of scour shapes for runs 1f and 3f	70
17	Scour shape and velocity profiles for run 1d	71
18	Scour shape and velocity profiles for run 3d	72
19	Comparison of scour shapes for runs 3d and 5d	74
20	Sketched armour layer 'relics' after run 5	76
21	Photograph of armour layer 'relics' after run 5	77

<u>Figure</u>	<u>Page</u>
22 Sediment output rates for runs 1 and 4	79
23 Sediment output rates for run 3	82
24 Sediment output rates for run 5	83
25 Composite scour shapes for run 3e	86
26 Armour layer formation at the smallest discharge	90
27 Bedload transport rates vs. total scour volume over the range of discharges for runs 1, 3, 4, 5	92
28 Flow conditions during the experiments	96
29 Change of Froude numbers in pool and on riffle	98
30 Change of hydraulic radius in pool and on riffle	100
31 Change in arithmetic mean velocities in pool and on riffle	102
32 Change in 0.6-depth 'mean' velocities in pool and on riffle	104
33 Flow visualization in the pool at different depths (flow from right to left; discharge: 5.1 l/sec)	107
34 Bottom shear stresses in pool and on riffle $(\tau = u_*^2 \times \rho)$	112

LIST OF TABLES

<u>Table</u>		<u>Page</u>
1	Scaling ratios and model dimensions	31
2	Critical velocity and discharge for incipient motion	34
3	Values of key hydraulic parameters for different experimental runs	40
4	Sediment feed rates for the experimental runs	46
5	Comparison of scour volumes at increasing discharges during run 1	51
6	Comparison of scour volumes of homogeneous and heterogeneous beds	59
7	Comparison of scour volumes for homogeneous beds with clearwater scour and scour under steady sediment supply	68
8	Comparison of scour volumes for homogeneous and heterogeneous beds under steady sediment supply	73
9	Sediment output rates from homogeneous and heterogeneous clearwater beds	80
10	Sediment output rates from homogeneous and heterogeneous beds under steady sediment supply	84
11	Bottom velocities for a heterogeneous clearwater bed	88
12	Bottom velocities in pool and on riffle	105

HYDRAULIC INFLUENCES ON POOL MORPHOLOGY — A LABORATORY INVESTIGATION

I. INTRODUCTION

Large bedforms in gravel-bed rivers have received attention in different research disciplines. In particular, riffle-pool-riffle systems, typical for river beds composed of heterogeneous mixtures of gravel particles, act as energy dissipators during the self-adjustment process of a stream. These features are important with respect to fish habitat and sediment transport phenomena.

Pools and riffles provide diverse habitat for fish. Fish can be found at different locations, depending on their age, their strength to handle the fluid forces in the system (high velocities, local turbulence, etc.), the presence or lack of coarse spawning gravel, or because of hiding possibilities in deep sections in pools. The hydraulic properties as well as the sediment conditions within a riffle-pool-riffle unit are considered to have a major impact on the distribution of the fish.

Pools and riffles also represent local sinks and sources for the bed material supplied from upstream. Flow magnitude and duration, as well as quantity of sediment input from upstream, define the final shape of a pool as it appears at low flow conditions. This shape further influences the actual 'retention' time for bed material in the pool during high flow events. Empirically developed bedload transport formulas for gravel-bed rivers are often imprecise, since these

large-scale bedforms distort the outcome of laboratory-based predictions.

Several attempts have been made to quantify hydraulic and bed-morphologic processes in riffle-pool-riffle systems. Field work has emphasized the investigation of total bedload transport and sediment distribution within these features. Measurements of 'mean' values for hydraulic parameters such as velocity or water surface slope have served to relate observed phenomena to hydraulic properties. However, field investigations were typically limited by physical restrictions on taking measurements during high flow events. Because of insufficient knowledge of all the variables in a natural system that influence the measured outcomes, several hypotheses have resulted from the gained data sets. Recently, more and more laboratory experiments have concentrated on bedload transport phenomena in riffle-pool-riffle systems -- especially to get more insight into processes occurring during higher flows.

This thesis seeks to contribute to knowledge about the hydraulic influences on the bed morphology of a pool and the role of bedload transport processes. Furthermore, hypotheses established from observations and measurements in the field are addressed and evaluated.

Purpose and objectives of the laboratory investigation

The main purpose of this thesis is to provide more insight into the hydraulic conditions of large-scale features of rivers involving

pool-riffle sequences. These hydraulic conditions are known to influence the bed morphology. A major remaining problem is the quantification of the processes.

One main objective of this thesis is to assess the specific hydraulic conditions within one riffle-pool-riffle sequence. A related objective is to study the morphological scour and deposition processes of the bed. Another research objective is to investigate whether a small-scale flume experiment can be used to verify specific hypotheses established by past field research regarding areal sorting and hydraulic interactions in pools and riffles. Special emphasis is given to the hypothesis of "velocity reversal" at flows around bankfull discharges; this hypothesis has been used to explain sorting mechanisms in pools and riffles (Keller, 1971; Lisle, 1979).

Experimental approach

A flume experiment models a riffle-pool-riffle sequence in a gravel-bed river. By simulating a hydrograph over a partially movable bed (the riffle is fixed), the initial formation of the pool and its ongoing changes during different flow stages can be studied in conjunction with the hydraulic conditions within the pool.

To better understand the scour and deposition processes and the changing hydraulic conditions over a range of discharges, the following factors were examined in detail:

- 1) velocity profiles along the longitudinal riffle-pool-riffle unit (by direct measurement);

- 2) flow patterns within the system (by dye tracing);
- 3) shear stresses as a function of discharge (by calculation);
- 4) bed elevations during scour and deposition processes
(by direct measurement); and
- 5) armouring effects within the pool due to a wider standard deviation of a particular grain size distribution chosen for the pool material (by direct observation).

Organization of the thesis

This thesis is organized in five major sections. A literature review introduces the theoretical background and the practical applications regarding past pool-riffle studies. Concepts which provide a background understanding of the formation processes of pools and riffles in stream systems are described first. This information helps clarify the principal forces that influence changes in channel morphology; it is the basis for analyzing morphological processes occurring during the laboratory experiments. Since the classification of pools and riffles in natural stream systems causes some difficulties, different classification schemes are described and evaluated in order to help categorize the laboratory examination into the complexity of these features. Furthermore, hypotheses are described which try to explain areal sorting mechanisms in pools and on riffles. As mentioned earlier, the examination of these hypotheses is a major objective of this research. Finally, research of bedload transport phenomena related to pool-riffle features in gravel-bed

rivers is cited and the difficulties in prediction approaches are highlighted. In particular, focus is given to the variability of bedload transport in these complex stream systems.

The second major section of this thesis contains theoretical considerations and descriptions regarding the experimental design and set-up of a modelled riffle-pool-riffle sequence in the laboratory. Field data, gathered prior to the actual experiment in connection with preliminary calculations, are explained first. The hydraulic parameters which were chosen as being variable during the different experimental runs are described regarding their importance in a natural setting. The theoretical treatment of the hydraulic characteristics in a riffle-pool-riffle sequence leads to the formulation of expected results from the experiments. Expected results are stated for each described quantity that is measured during the individual runs (velocity, bed elevation change, bedload transport, etc.).

The third major section of this thesis presents the obtained experimental data, followed by data analysis and interpretation. Results are evaluated in comparison with the formulated expected results. The results are treated under two subsections. In the first, bed-morphologic changes are described; in the second, results are presented which relate to verification of the hypothesis of 'competence reversal'. Bed-morphologic changes are interpreted with regard to the two major variables 'bed mixture of the pool material' and 'sediment supply rate from upstream'. The analysis of vertical velocity profiles as well as other hydraulic parameters leads to some

considerations about the theoretical and practical treatment of the 'competence reversal' hypothesis.

In the fourth section of this thesis, major findings of the research are summarized and conclusions are drawn. The conclusions relate the qualitative and partly quantitative results to the findings in the literature.

The last section of this thesis puts the outcomes of this research in perspective to practical applications. The examination and observation of several parameters (discharge, velocities, bed elevation, armouring processes, etc.) and the technical difficulty of measuring others (e.g., shear stresses) resulted in the evaluation of the importance of specific hydraulic conditions. This leads to recommendations for future research. In particular, more detailed investigation is recommended of those parameters which could not be examined during this study but were recognized to provide important insight into the studied phenomena.

II. LITERATURE REVIEW

A literature review will help forward the objectives of this research by highlighting the theoretical considerations, definitions and practical applications reported for pool-riffle studies. The concept of minimum stream power is described in the first section of this chapter. This provides a background understanding of the formation processes of pools and riffles in stream systems. The concept also provides a basis for the identification of an adequate riffle-pool-riffle sequence in nature for modelling in laboratory experiments as part of this thesis. Different classification schemes of various pool and riffle units are compared with each other and evaluated. Their description helps to categorize the laboratory experimentation within the large variety of these features. The sections of this chapter which follow focus on the hydraulic properties within a pool-riffle system. Many field studies and flume experiments have been undertaken with the objective of relating results from morphological observations to theoretical concepts.

This literature review emphasizes studies having hypotheses of special interest for my experiment. I attempted to verify the hypothesis of "Velocity Reversal", first introduced by Keller (1971) or "Competence Reversal", as later renamed and investigated in more detail by Lisle (1979). This hypothesis explains the occurrence of areal sorting mechanisms in pools and riffles. Mean velocities and/or mean shear stresses in the pool are smaller than those at the riffle for small discharges (Breusers, 1975) but increase relatively more

rapidly as discharge increases until they exceed those at the riffle at near-bankfull discharges. This provides the hydraulic conditions for the transport of the larger bed material through the pool onto the downstream riffle during large flows. The reversal theories provide an explanation for the fact that hardly any large bed material is found exposed on the pool bed at low flows. By means of a laboratory study with controlled hydraulic parameters, the occurring changes can be observed in detail.

The formation of pools and riffles in gravel-bed rivers

Several types of bedforms can be distinguished in natural channels. In sand-bedded rivers the presence of dunes, anti-dunes and ripples is dominant. These features are especially prevalent in flatland streams with lower gradients and in streams with very fine sediment supply, where the median diameter of the bed material does not exceed approximately 0.6 mm (Simons and Simons, 1987). In rivers with higher gradients (1% to 4%), coarser bed material occurs and riffles and pools are the typical features. Rivers with slopes greater than 4% show the specific bedforms of cascade and step-pool units (Whittaker and Jaeggi, 1982; Sullivan, 1986). My study focuses on the case of a gravel-bed stream with a channel gradient of 1%.

In various experiments and field observations, several authors (Leopold and Langbein, 1962; Yang, 1971; Cherkauer, 1973) identified that the common reason for the occurrence of such 'deeps' and 'shallows' lies in the self-adjustment process of a natural stream.

This process has been explained by Bagnold (1966) and Yang (1971) by introducing the law of least time rate of energy expenditure.

The following section introduces the theoretical background of these concepts. Understanding the concepts is necessary for generally interpreting the processes that influence the actual formation and shapes of pools and for specifically examining the pool formation in the flume study.

The concept of unit stream power and the law of least time rate of energy expenditure

From season to season and year to year, natural channels are influenced by several forces which change their morphology. High flows with their induced scouring and low flows with deposition processes may alter the channel morphology drastically within short time periods. Channel changes like scour and fill (short-term time scale), bankcut and deposition (intermediate-term time scale) and aggradation and degradation (long-term time scale) are part of typical stream dynamics. If the short-term and intermediate-term changes tend to balance out over the long term, it can be said that the stream is in "dynamic equilibrium". Otherwise, the stream will experience some net change (non-equilibrium) over the long term.

The potential energy (PE) available to make these changes possible is determined by the water's elevation above sea level. This can be expressed by:

$$PE = mgh \text{ [ML}^2\text{T}^{-2}\text{]} \quad [2-1]$$

where:

m = mass of water [M]

g = gravitational acceleration [LT^{-2}]

h = elevation above sea level [L].

On the water's way downstream, this potential energy is progressively converted to kinetic energy (KE), expressed as:

$$KE = 1/2 mV^2 \text{ [ML}^2\text{T}^{-2}\text{]} \quad [2-2]$$

where:

V = velocity [LT^{-1}].

Most of the kinetic energy (approximately 95%) is consumed as heat loss during turbulent mixing within the main flow and along the channel margins (after Morisawa, 1968, see Beschta and Platts, 1986). The remaining energy can be utilized for sediment transport, bed scour and bank erosion (Beschta and Platts, 1986).

In a stream, the availability of energy to do work can be defined by introducing 'unit stream power'. Unit stream power (w) is defined by Bagnold (1966) as the time rate of loss of potential energy per unit mass of water and can be expressed as:

$$w = \rho_g VS \text{ [ML}^{-1}\text{T}^{-3}\text{]} \quad [2-3]$$

where:

ρ_g = density of water [ML^{-3}]

S = energy slope of water [LL^{-1}]

The unit stream power concept provides a basis for understanding the erosive capability of water in an open channel system. Relatively high unit stream power is associated with steep straight channels having uniform cross sections and large hydraulic radii; reduced stream power can be obtained by various morphological changes which decrease the average channel slope or provide roughness elements for energy dissipation (Beschta and Platts, 1986).

Yang (1971) further developed the idea of unit stream power by introducing the law of least time rate of energy expenditure. This states that during the evolution towards its equilibrium condition, a natural stream chooses its course of flow such that the time rate of potential energy expenditure per unit mass of water along its course is a minimum. Yang used the concept of entropy, previously applied to study landscape evolution by Leopold and Langbein (1962), and applied it to a stream system. The minimum value for each stream depends on the external constraints applied to it. The law of least time rate of energy expenditure can be expressed by the equation:

$$(\Delta H/\Delta t)(kY/\Delta t) = f (Q, S_v, C_s, G, \dots) \quad [1-5]$$

which is at a minimum.

Here:

$\Delta H/\Delta t$ = time rate of potential energy expenditure per unit
mass of water in a reach along a stream with
a fall Y

y = fall = change of water elevation across the reach of
stream

t = average time required for a unit mass of water to travel through this reach

k = factor of conversion between energy and fall

f = function of the external constraints applied to the stream;

Q = water discharge

S_v = valley slope

C_s = sediment concentration

G = geological constraints (the geological constraints consider erodibility of the soil, the grain roughness, the stream valley width, etc.).

The value of $\Delta H/\Delta t$ should always be greater than zero along the course of the flow except at the end of the river. In his paper, Yang (1971) showed that the formation of pools and riffles is one way in which a natural stream conforms to the law of least time rate of energy expenditure.

From this literature review, it can be seen that the concept of 'unit stream power' and the 'law of least time rate of energy expenditure' have importance in explaining stream dynamics. The evolution of conceptual research from the early studies of Leopold and Langbein through the phase of Bagnold and Yang has brought us to a better understanding of the theoretical background which explains the ongoing morphological processes.

The flume experiment carried out as part of this thesis will seek to use these concepts to evaluate the morphological changes occurring in the studied stream reach.

Nomenclature and classification schemes of different pool and riffle units

Pool and riffle features are mainly attributed to the meandering behavior of a river as one way to dissipate the energy which is associated with high unit stream powers (Tinkler, 1970; Yang, 1971; Cherkauer, 1973; Richards, 1976a; Thompson, 1986). Nevertheless, these bedforms can also be found in short straight reaches of the channel, behind obstructions, and elsewhere. This implies that "pools are not pools" in the sense of features which all obey the same formation processes or can all be described by similar hydraulic conditions.

During recent years, field biologists and other researchers in the domain of fisheries and wildlife have used approaches that describe these features by emphasizing not only their specific hydraulic parameters (e.g., velocity, flow depth, geomorphological bed form) but also the forming conditions.

Classification of different pool and riffle units is quite useful in providing a better understanding of their hydraulic characteristics. Consideration of the applicable nomenclature will aid in a clearer understanding of the pool type simulated in this study.

Beschta and Platts (1986) give a short overview of the development in the nomenclature process through the last 15 years. They note that two types of pools were distinguished by Keller and Melhorn (1973) in meandering channels. Primary pools are usually found at bends and are always associated with point bars; deep scour

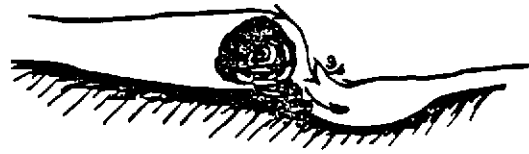
is characteristic for these forms. Secondary pools exhibit less scour and can be found at different locations in streams. Beschta and Platts also give a more detailed classification developed by Bisson, et al. (1982) that recognizes six types of pools:

- 1) secondary pools are found on floodplains when the high waters recede;
- 2) backwater pools exist behind large obstructions along the channel margins (tree stems, root wads, boulders, etc.);
- 3) lateral scour pools are caused by deflection of water at stream bends or by large obstructions;
- 4) plunge pools exist after a main flow has passed over a complete channel obstruction and drops vertically onto the downstream channel bed;
- 5) trench pools form long slots in a stable channel bottom; and
- 6) dammed pools result from a full or partial channel blockage (caused by debris jams, landslides, etc.).

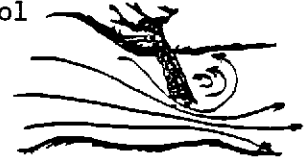
Sullivan (1986) developed a key to identify channel 'units' having similar hydraulic characteristics. Her suggested classification of various pools is illustrated in Figure 1.

For the purpose of my thesis research, it is not necessary to analyze the differences between the various identification approaches in more detail. The flume study emphasizes one riffle-pool-riffle sequence which had been visually identified in the field. An appropriate description of the pool in my physical model is Sullivan's

a) Dammed pool



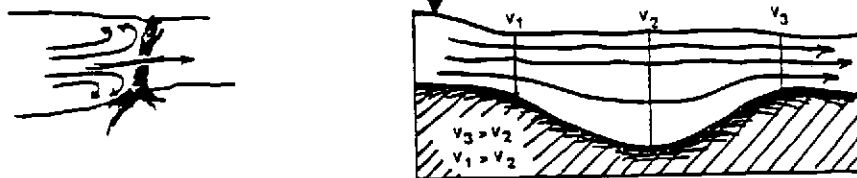
b) Eddy pool



c) Plunge pool



d) Drawdown pool



e) Scour pool



Fig. 1. Classification schemes for pools after Sullivan (1986)

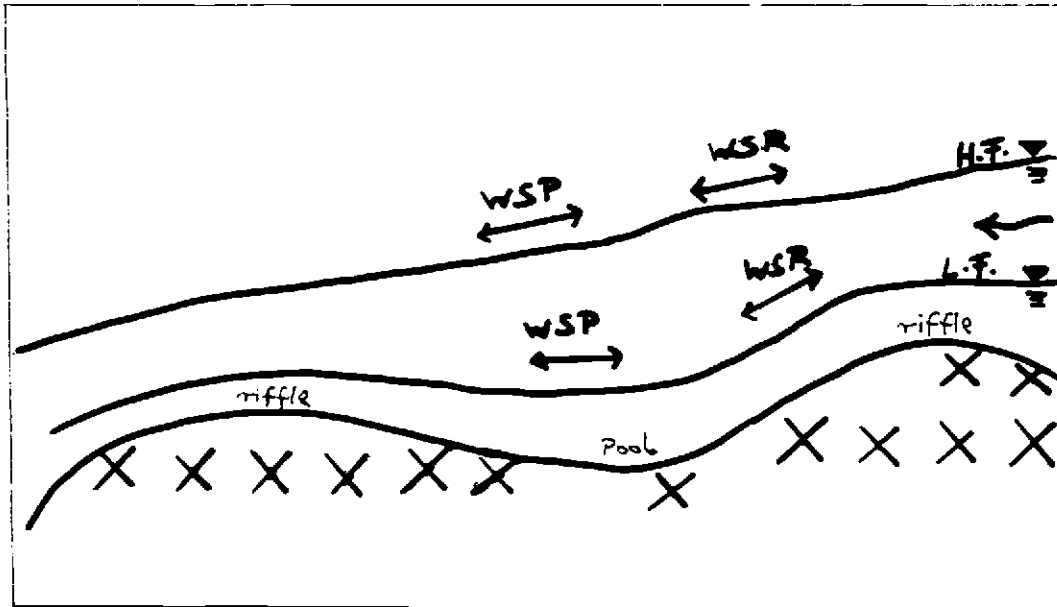
'scour pool', shown in Figure 1e, excluding the logs at the upstream end.

Hypothesis for competence reversal and areal sorting mechanisms

Several recent studies have examined the hypothesis of reversal of competence to transport bedload at a certain discharge near the bankfull condition. This thesis also attempts to test that hypothesis. The perspective provided by the other investigations, which mainly represent field work, will help in understanding this laboratory experiment and in interpreting the results.

The basic considerations for the hypothesis of 'competence reversal' are based on the fact that riffle-pool-riffle units are submerged at high flows. This alters the relative behavior of several hydraulic parameters in pools and riffles. One of these parameters is the water surface slope which is often used in field investigations to estimate the energy slope. The numerical slope value is used in tractive force calculations which are emphasized later in this section. The principal appearance of a riffle-pool-riffle sequence under low flow (L.F.) and high flow conditions (H.F.), as used by the hypothesis, is shown in Figure 2.

The earliest theory considers the reversal of velocity in pools and riffles in particular. The theory states that with increasing discharge the average bottom velocity in a pool increases faster than that on a riffle, until at relatively high flow near bankfull condition the average bottom velocity in the pool exceeds that on a



H.F. = high flow condition

L.F. = low flow condition

WSR = water surface slope above riffle

WSP = water surface slope above pool

→ = direction of flow

Fig. 2. Low and high water surface slopes in a riffle-pool-riffle sequence

riffle. This phenomenon is often also referred to as the convergence phenomenon describing the convergence of the velocities in the riffle and pool towards an intersecting point. The hypothesis was proposed by Keller (1971) as he tried to find an explanation for areal sorting mechanisms of channel material. That is, he attempted to explain the sorting that caused relatively large material to be found on riffles and finer material to be found in pools during low flow conditions. In a field study, Keller measured velocities across pools and riffles during different flow events (1 cfs to 60 cfs). At each flow, the mean velocities for each cross section were then determined for the pools as well as for the riffles. The results, shown in Figure 3, were as follows:

1. At low flow, the bottom velocity in the pools is less than on the adjacent riffles; large bed material cannot be moved onto riffles.
2. With increasing discharge, the bottom velocity in pools increases faster than on riffles; the 'reversal' velocity occurs when the bottom velocity in the pool is equal to that on the riffle.

Keller concluded that at high flows with velocities above the reversal velocity, bed material that can be moved through a riffle and into a pool will be transported quickly through the pool by the greater bottom velocities and tractive forces there; redeposition occurs on the riffle where the velocity and the tractive forces are smaller. Furthermore, at low flow conditions, the largest bedload particles

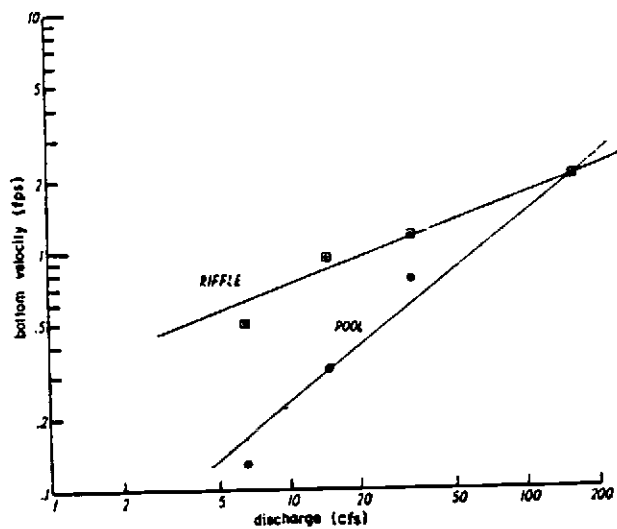


Fig. 3. Mean bottom velocities for a pool and riffle versus discharge after Keller (1971)

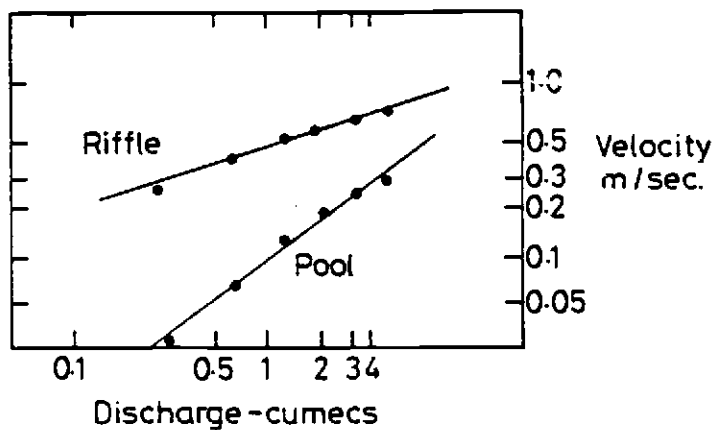


Fig. 4. Mean bottom velocities for a pool and riffle versus discharge after Richards (1978)

will be found on riffles and the relatively finer material will be found in the pools.

To the present time, the hypothesis of velocity reversal has been examined by various researchers with contradictory results. Richards (1978) analyzed a river in Ontario, Canada. By means of a computer model, he simulated hydraulic geometry relations for adjacent riffle and pool cross sections. He obtained tendencies for the changes of mean velocities in pool and riffles with increasing discharges, as shown in Figure 4, and similar to those reported by Keller (1971). However, contrary to Keller, he concluded that the different gradients of the velocity relationships only demonstrate that there may possibly be a convergence phenomenon. A tendency for convergence may reflect a proportionate reduction in the difference between the two sections (pool and riffle), but not necessarily a reduction in the absolute difference. In his flow geometry simulation model, Richards could not clearly prove that an actual equalization of depth, mean velocity or surface gradient through the studied reach would occur at higher discharges. He added, however, that the results applied only to mean velocity, and that there may be a more rapid convergence for bed shear stress because it incorporates the changes in depth and slope.

Lisle (1979) used field data to describe sorting effects of coarse bed material on riffles and finer material in pools based on the reversal hierarchy of mean shear stress at a pool and riffle. Measurements of velocity near the bed as well as calculations of mean shear stresses at different flows allowed him to demonstrate not only the convergence of the competences in pools and riffles, as has been

shown in previous studies, but also an actual reversal of these parameters at flows near bankfull discharge. Results are shown in Figure 5. Lisle used the results of his analysis to explain sorting mechanisms of bed material in the pool-riffle sequence of gravel streams at less than extreme flows.

In their study of bedload transport in a pool-riffle sequence, Campbell and Sidle (1985) tried to relate specific bedload transport patterns to competence reversals between pools and riffles. This reversal or convergence of competence appeared to take place around bankfull discharge, as had been suggested by Keller. However, actual measurements of hydraulic parameters like shear stresses, velocities, etc., had not been conducted during the high flow periods. Mechanisms suggested in other studies (shear stress or velocity reversal, increases in local turbulence intensity, etc.) were accepted without being proved explicitly as appropriate explanations for the bedload transport patterns observed.

A theory which at first seems to contradict the competence reversal hypothesis, or at least to offer an alternative explanation for areal sorting mechanisms, was proposed by Yang in 1971, based on experiments conducted by Bagnold (1954), who studied the dispersion of solid spherical grains in a Newtonian shear flow. The results of his experiments can be understood if we consider the following equation:

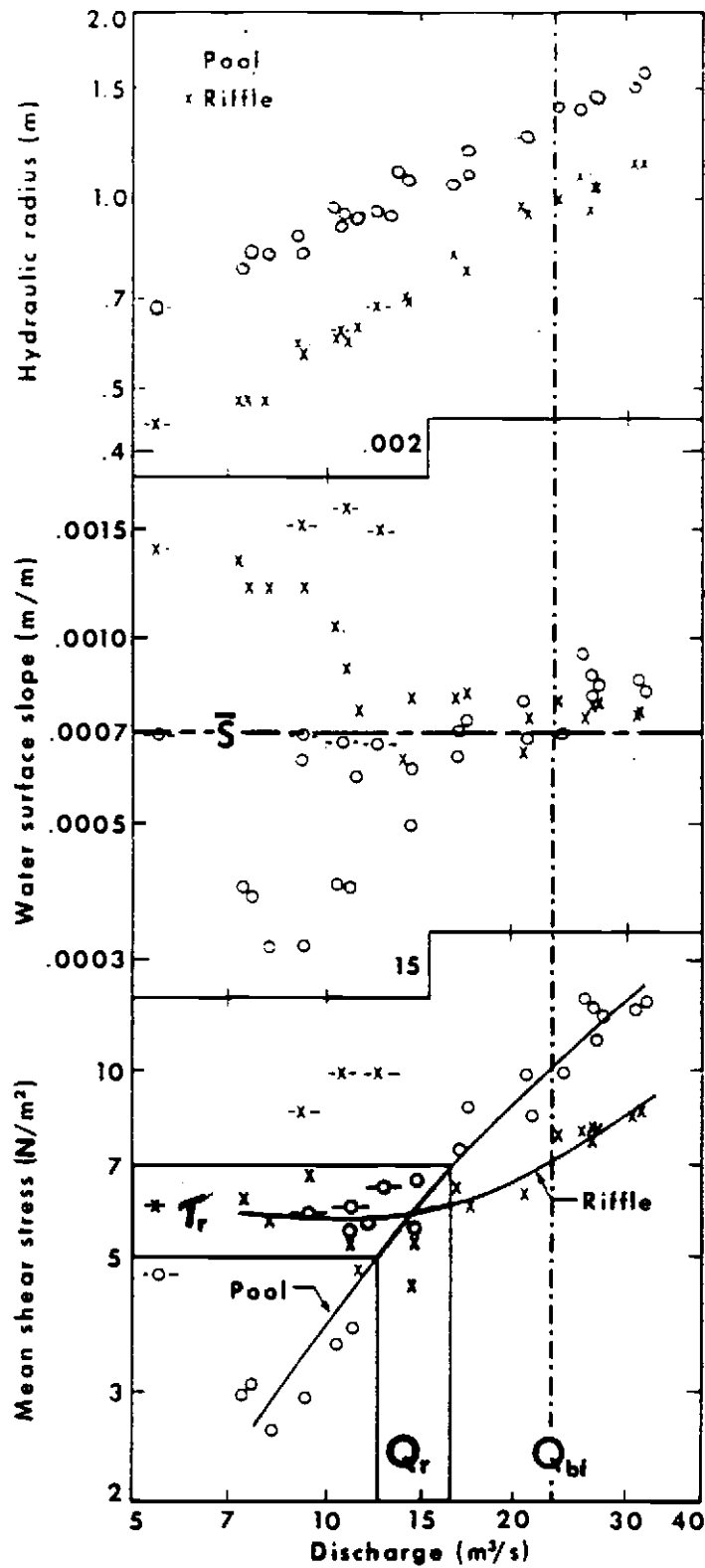


Fig. 5. Hydraulic parameters in a riffle-pool-riffle sequence over a range of discharges after Lisle (1979)

$$P = a \rho \lambda f(\lambda) D^2 (du/dy)^2 \cos \alpha \quad [2.1.]$$

where:

P = repulsive pressure

a = constant

ρ = density of the grain

λ = concentration

D = diameter of the grain

du/dy = velocity gradient

α = some unknown angle determined by the collision conditions (incl. grain rotation)

It states that with an increase in concentration, grain diameter, and/or velocity gradient, an increase will result in the repulsive pressure between the grains of two layers. Accordingly, the higher velocity gradient at the riffle will result in a higher repulsive pressure on the riffle than in the pool. Because of the mobility of the alluvial bed, this difference in pressure will depress the bed surface at the pool and raise it at the riffle to form a concave-convex bed profile. Once this relative movement of the bed surface starts, the difference in velocity gradient between the pool and the adjacent riffle increases and, therefore, amplifies the pressure effect. The repulsive pressure also increases as the grain diameter increases. When grains of mixed sizes are sheared together, the larger grains tend to drift toward the surface. The smaller grains cannot sustain the high shear stress at the riffles due to the

higher velocity there. They will be washed out and deposited in the downstream pool. This theory explains part of the formation of the pool-riffle feature as well as the areal sorting mechanisms of the bedload material.

Since the above studies and the related theories cover only parts of the phenomenon occurring in nature, a combined effect can be assumed to influence the features as they appear in natural channels. This suggestion was also given by Lisle (1979), who attributed the deficiency of a specific size fraction of the surface deposits to dispersive stress and a winnowing effect, which concentrate coarser gravel fractions at the surface of the riffle (see Bagnold, 1954). A study by Whittacker and Jaeggi (1982) also suggests that competence reversal alone does not explain the sorting out of different size fractions within a pool-riffle sequence. In particular, they point out that the reversal mechanism can be seen as one of maintenance of pool-riffle forms; it does not account for a development of these bedforms from an initially plane bed.

As the last contribution to the attempt to explain the pool-riffle feature and the different grain sizes attributed to the pool and riffle, I mention Bagnold's 1980 paper, in which he suggests that the almost universal tendency for streams to form alternating sequences of riffles and pools may be caused by variations in turbulence intensity at alternating regions of converging and diverging flow. This idea has not been emphasized much by other authors, presumably because of the lack of turbulence data, but seems to be an adequate explanation of the phenomenon.

The various theories and field investigations explain more or less satisfactorily the phenomenon of 'reversal competence' under different circumstances. Therefore, investigation of reversal competence is a primary purpose of this thesis.

The theory of velocity reversal was analyzed in this experiment with the help of measured velocity profiles along the entire riffle-pool-riffle section. Other hydraulic parameters were also considered, such as hydraulic radius, energy slope and mean shear stress. This could lead to a comparison with the controversial field results. This section of the literature review has consequently lead us to a better understanding of the possibilities for additional studies that might contribute to the present theories.

Bedload transport

Since half of the experimental runs undertaken in this research investigated the effect of sediment transport on the resulting morphological and hydraulic conditions, a closer look at field and flume studies done for the specific case of pool-riffle systems will help to put this work into perspective.

Bedload is defined as the part of the total sediment load which is not transported in suspension. Bedload transport, herein, describes the movement of this material near or on the bed (Vanoni, 1975). The material that is initially immobile on the bottom of the channel starts to move when the forces that resist the entraining action of the flowing water are exceeded by hydrodynamic forces. The

calculation of these critical values is extremely difficult because the process of incipient motion is influenced by a wide range of factors.

For example:

$$\text{incipient motion} = f(\text{sediment forces, fluid forces})$$

where:

$$\text{sediment forces} = f(\text{particle sizes, specific weight, fall velocity, depositional arrangement, etc.})$$

$$\text{fluid forces} = f(\text{temperature, discharge, velocity, turbulence, etc.})$$

Several formulas have been developed to calculate total bedload transport. Each is based on differing assumptions and different critical criteria involving discharge, tractive force, relative roughness (ratio of grain diameter to depth of flow), etc. Three of these formulas are briefly discussed in Appendix C in connection with calculations of bedload transport rates for use in the research experiments.

Natural rivers are high-energy, unsteady and nonuniform systems. The flow in most streams is gradually varied rather than uniform; this is particularly true for streams with coarse gravel bed material (Richards, 1978). High temporal and spatial variability of bedload transport has therefore been found by several researchers (Milhous, 1973; Jackson, 1980; Klingeman and Emmett, 1982; Campbell and Sidle, 1985; Whittaker, 1987). Bedload transport equations developed from steady-state hydraulic considerations consequently do not appear to apply to these natural conditions (Vanoni, 1975) and accurate

predictions turn out to be difficult. Furthermore, transport in a gravel-bottomed stream may occur for only a small percentage of time and may consist of pulse-wise downstream movement with long residence times at single locations (Beschta, 1987). Some of these locations are represented by pool-riffle sequences themselves. In this project, bedload transport occurring in the riffle-pool-riffle unit was examined, as will be described in Chapter IV. Results from field work reveal interesting outcomes in this respect. Campbell and Sidle (1985) quantified net scour and deposition in one riffle-pool-riffle sequence over the period of four storms and obtained differing results, depending on the magnitude of the storm. The same pool was scoured during relatively high flows whereas deposition occurred at storms of lower magnitude. This leads to the expectation that changing hydraulic properties at various high flows influence the transport phenomena within the riffle-pool-riffle system in an important way. The different runs in the flume experiment examined these changes.

Summary

This literature review has identified general concepts related to the formation of pools and riffles in natural stream systems. Some difficulties in arriving at an "objective" nomenclature were shown as well. The hypothesis of "competence reversal" in combination with areal sorting theories was stressed so as to explain important morphological and hydraulic influences on the existence and

maintenance of pool-riffle features. The reported results from field and flume studies, together with the choice of the measured hydraulic parameters, influenced the planning of the current study. This laboratory experimental work tries to represent a link in the present state of the findings and theories, which have been mainly obtained by field work. It was therefore intended to model a situation which simulated natural events like storm runoff going through the system and bedload transport occurring at specific rates. Parameters similar to those for recent field studies were measured in the flume. The following chapter introduces the experiment as it was planned, set up and finally conducted.

III. LABORATORY EXPERIMENTATION

Experimental approach

The experiment was undertaken in two steps. The first step consisted of finding an adequate riffle-pool-riffle sequence in nature. This was done to get a better idea of the dimensions a riffle-pool-riffle feature could have in a short, straight channel reach. It was not the objective of this thesis, however, to accurately simulate the prototype situation, but rather to justify the dimensions used in the experimental set up. In the first section of this chapter, the collection of the necessary field data is therefore described. Furthermore, the theoretical modelling approaches used to conduct a geometric similarity study are listed. Finally, the preliminary hydraulic calculations for the flume experiment which follow from the theoretical modelling approaches are explained. The chosen riffle-pool-riffle sequence was then reconstructed in a laboratory flume.

The second step was to run several experiments with the physical model by changing the hydraulic parameters at each run. The section titled "Runs and Measurements" explains in detail the single steps of the conducted experiments.

After the selection of the design discharges is described, an overview is given over the specific runs. The theoretical background for the various hydraulic and morphological interactions is then

developed; this includes short technical descriptions of each apparatus which was used in the experiment.

The theoretical considerations described in each paragraph lead to some expected results for the flume experiment. At the end of each paragraph some anticipated results are mentioned. Expectations are formulated for the critical discharges for incipient motion, shapes of velocity profiles at different locations within the studied system and kinds of velocity patterns to be anticipated. Possible morphological changes and bedload transport patterns are finally described.

Prototype information for the experimental design

In order to model a riffle-pool-riffle unit in a flume, actual dimensional data were gathered from a prototype situation (Oak Creek in the McDonald Forest, Corvallis, Oregon). A riffle-pool-riffle sequence was found in a 30-meter straight stretch 40 meters upstream of the inlet to the concrete field flume which is part of the OSU Water Resources Research Institute facilities at Oak Creek. The straightness of the natural unit could be easily modelled in a relatively narrow flume. The fact that the pool itself did not extend laterally to the shores (and therefore undercutting of the banks was not present) indicated that during higher flows, pool scouring is not interrupted by the channel banks.

The longitudinal profile as well as the cross section of the pool were surveyed.

A pebble count was made by sampling 100 particles across the riffle during low flow conditions. The resulting mean grain size diameter (D50) was 8 cm. From Milhous' work in Oak Creek (1973) the D50 of the pool sediment to be modelled was obtained as follows:

$$(D50 \text{ armour layer} + D50 \text{ subarmour layer})/2.$$

$$(6 \text{ cm} + 2 \text{ cm})/2 = 4 \text{ cm}$$

The surveying data from the Oak Creek site are given in Appendix A.

Preliminary calculations for the experimental set-up

For modelling purposes, the classical approaches for physical models were applied (Yalin, 1971; Novak and Cabelka, 1981). The surveyed stretch in Oak Creek could be scaled down to one tenth of the original feature (prototype/model = L = 10:1). The prototype channel slope of 1% was directly transferred to the model. The calculated dimensions for the undistorted model are shown in Table 1.

Table 1. Scaling ratios and model dimensions

parameter	scaling ratio: prototype/model	values used for the experiment
length	[L] = 10.0	pool length: 1 m D50(riffle): 0.01 m D50(pool): 0.004 m
velocity	[L ^{0.5}] = 3.16	
discharge	[L ^{2.5}] = 316.23	Q _{max} : 7.6 l/sec

The highest discharge was calculated based on the highest possible flow in the flume. The value of 7.6 l/sec corresponds to an event in Oak Creek of $2.4 \text{ m}^3/\text{sec}$ (or 85 cfs), a moderate storm runoff that causes some sediment transport.

To determine the starting discharges for the experiment to use, preliminary calculations were made of incipient motion conditions for sediment mixtures with different D_{50} 's before the actual study was conducted. However, the calculated values of critical discharge, mean velocity and shear stress were considered to be only initial guesses, since the set-up of the experiment already implied some possible deviation due to eventual local turbulences induced by the fixed riffle structure upstream. The calculations are based on Shields' approach to identifying incipient motion conditions in a homogeneous bed (Vanoni, 1975). The step-wise calculation uses the following equations:

1. calculation of the value 'A' = $d_s / \nu [0.1(v_s/v-1)gd_s]^{1/2}$ [3-1]

where:

d_s = mean size of sediment [L]

ν = kinematic viscosity of fluid [L^2T^{-1}]

v_s = specific weight of sediment grains [$ML^{-2}T^{-2}$]

v = specific weight of fluid [$ML^{-2}T^{-2}$]

g = acceleration of gravity [LT^{-2}];

2. obtaining the value for the dimensionless shear stress from the Shields diagram and calculating the critical shear stress τ_* :

$$\tau_* = \tau / ((v_s - v)d_s) \quad [3-2]$$

therefore:

$$\tau_o = \tau_* ((v_s - v)d_s) \quad [ML^{-1}T^{-2}]$$

where:

$$\tau_o = \text{bed shear stress } [ML^{-1}T^{-2}];$$

3. obtaining the value for the critical shear velocity u_* from the Shields diagram:

$$R_* = u_* d_s / v \quad [3-3]$$

therefore:

$$u_* = R_* v / d_s \quad [LT^{-1}]$$

where:

$$R_* = \text{boundary Reynolds number};$$

4. calculating the hydraulic radius R from the equation of mean shear stress:

$$\tau = vRS \quad [ML^{-1}T^{-2}] \quad [3-4]$$

therefore:

$$R = \tau / (vS) \quad [L]$$

where:

$$\tau = \text{mean shear stress}$$

$$R = \text{hydraulic radius}$$

$$S = \text{channel/energy slope } [LL^{-1}];$$

5. calculating the depth from the hydraulic radius

6. obtaining the mean velocity based on the assumption of a logarithmic velocity profile:

$$u = 5.75 u_* \log(30 R/k) \quad [3-5]$$

where:

$$k = \text{van Karman constant (value=0.4)}$$

7. calculating the critical discharge based on the dimensions of the flume:

$$Q = wdu \quad [L^3T^{-1}] \quad [3-6]$$

where:

$$w = \text{channel (flume) width [L]}$$

$$d = \text{flow depth [L]}$$

$$u = \text{mean velocity [LT}^{-1}\text{]}$$

Table 2 gives incipient motion results obtained for sediment mixtures with D50s of 3 mm and 4 mm.

The two sediment mixtures which were actually chosen for the experiment both had the same D50 of 3.3 mm.

Table 2. Critical velocity and discharge for incipient motion

D50 <mm>	critical mean velocity u_{cr} <m/sec>	critical discharge Q_r <l/sec>
3	0.052	0.8
4	0.081	2.5

The expected critical discharge for incipient motion was therefore approximately 0.8 l/sec. The first mixture contained relatively homogeneous material while the second mixture was chosen with a larger standard deviation around the median, representing more heterogeneous sediment. For heterogeneous mixtures, however, the calculated critical values might not be very accurate. According to Gessler (1975), the largest shear stress a sediment mixture can withstand is determined by the summation of the contributions of each individual grain rather than one "characteristic" grain size like D50 or D75, as suggested by other researchers. He attributes this to the occurrence of armour layer formation of different thicknesses which may change the value of the "effective" grain size. I consider this aspect as a further reason for a possible inaccuracy regarding the prediction of incipient motion.

The grain size distribution curves of the two mixtures are given in Appendix B.

Discharge was measured volumetrically. Maximum relative measurement errors were in the range of 1% to 8%. Relative error in this case is to be understood as the error arising between two obtained experimental values (Chapra, 1985):

$$e = [(\text{present discharge}) - (\text{previous discharge})] / [\text{present discharge}]$$

Experimental design

The Oak Creek riffle-pool-riffle sequence was modelled in a 2.5 m long and a 0.1 m wide flume at a scale ratio of 10:1. The fixed upstream and downstream riffles provided riffle grain sizes of 10.25 mm (3/8 in). The distance between the two riffles was 1 m. The slope in the flume was 1%. The space between the two riffles was filled with pool material to provide a plane initial bed. Figure 6 shows the overall sketch of the flume-setup, Figure 7 gives a more detailed close-up picture of the riffle-pool-riffle sequence.

The measurements in all experimental runs were made along the longitudinal center line in the flume in order to omit side wall effects. These measurements and the organisation of the experimental runs are described in the following section.

Runs and measurements

Overview

Each experimental run consisted of the simulation of a hydrograph for a storm runoff event. The highest discharge used represented the peak discharge of the hydrograph. The rising limb was divided into four discharge steps, the falling limb into three. The resulting hydrograph used in the model can be seen in Figure 8.

Separate discharge 'units' were then used in step-by-step fashion with each treated like a steady flow situation. The discharge was

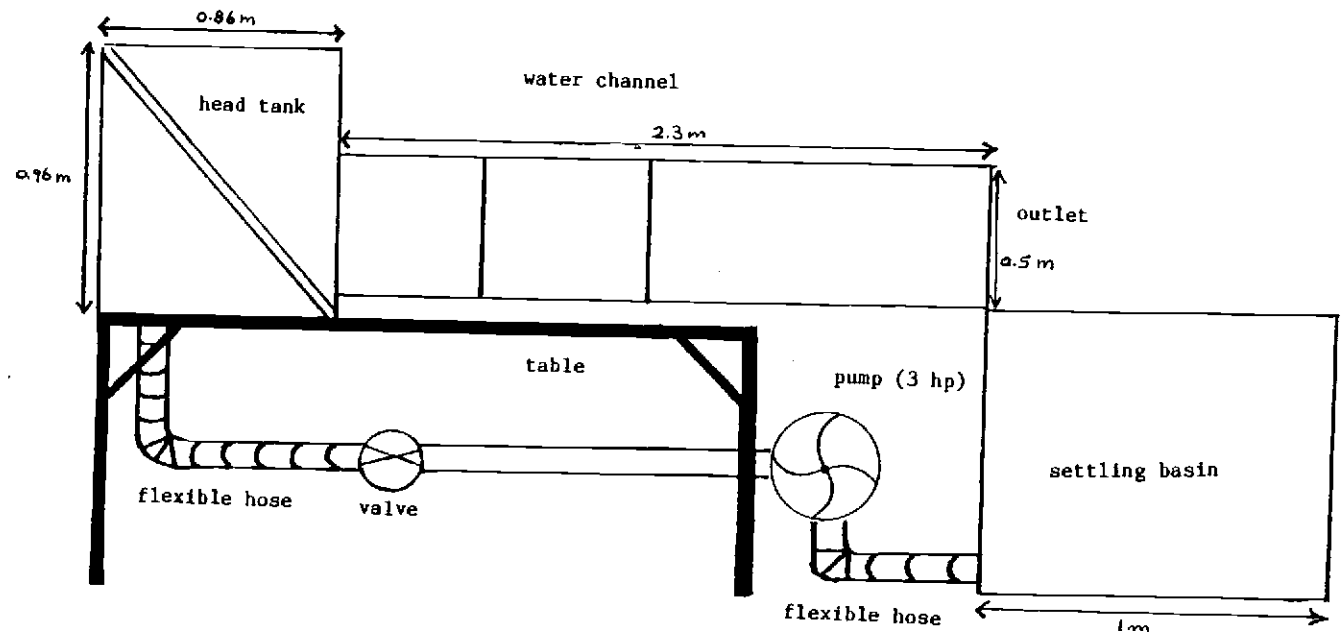


Fig. 6. Water channel used in the experiment

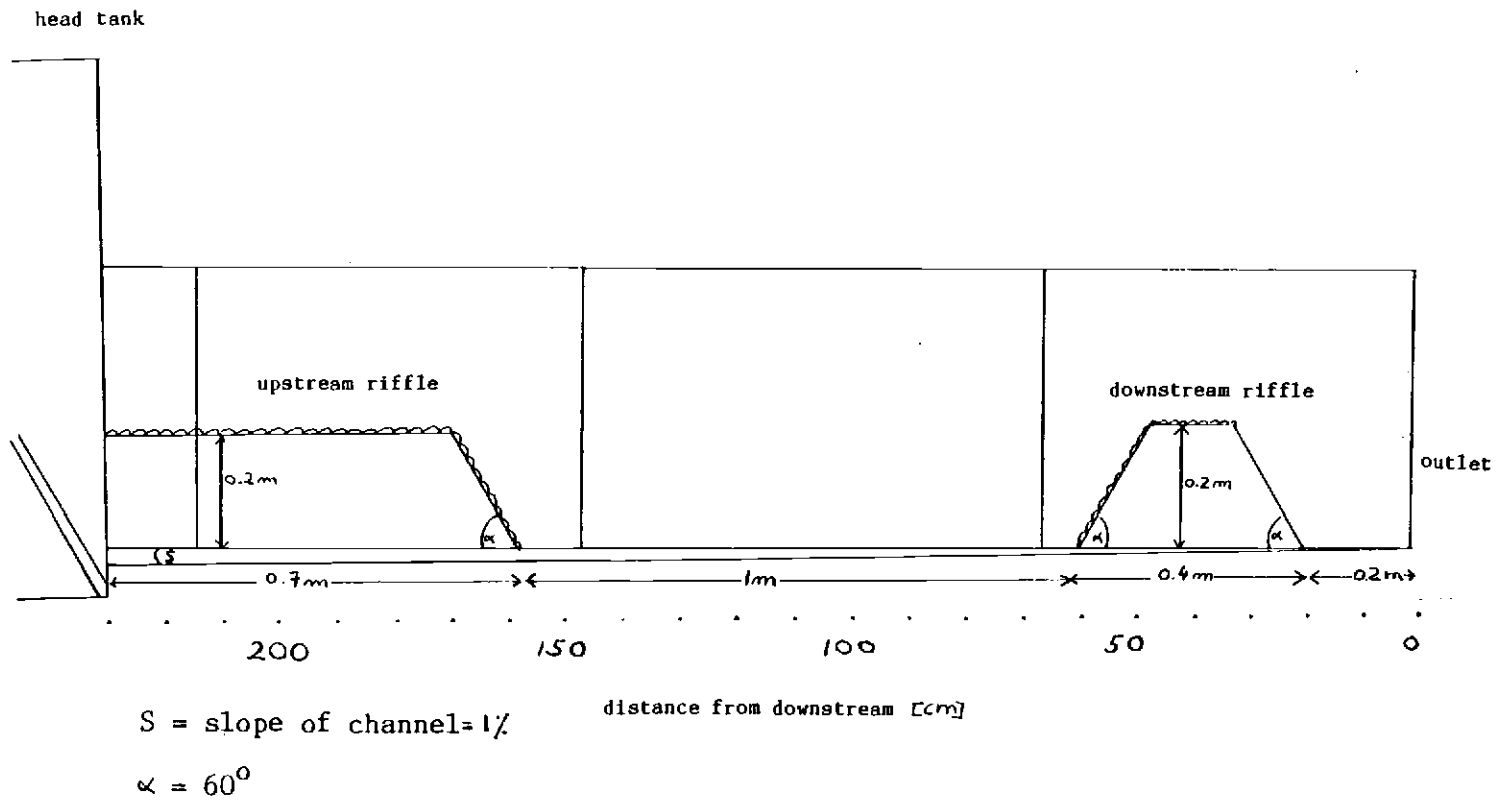
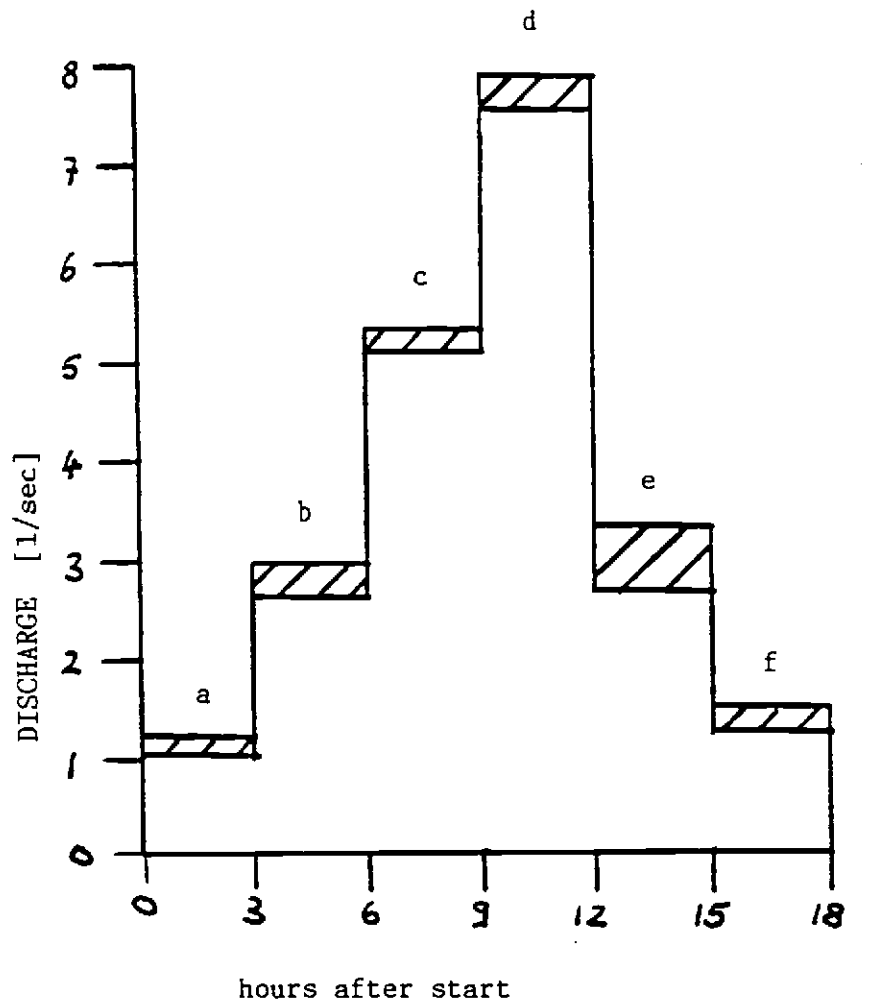


Fig. 7. Riffle-pool-riffle sequence modelled in the experiment



 = range of differences in discharges
for the same discharge step

a, b, c, d, e, f = discharge steps during the simulated storm runoff event

Fig. 8. Model hydrograph used in the experiment

held at a specific value until the scour and deposition processes reached 'equilibrium'; equilibrium was determined as the point where the absolute change of the bed elevation approached an asymptotic limit of zero change. Three hours seemed to be long enough to reach the 'equilibrium bed' condition for each discharge.

The runs were conducted such that hydraulic and bed morphology changes during a storm event could be investigated by changing key parameters. Table 3 shows the different runs and the specific test conditions. Run 2 is not shown here because it was a sediment feed test run, as is explained later in more detail.

The same slope was maintained during all runs, the D50 of the pool material was also held fixed. Runs 1 and 3 represent one experiment "unit"; both examined the situation of a relatively homogeneous bed, run 1 under clearwater conditions and run 3 under the condition of steady sediment supply at specific rates over the whole

Table 3. Values of key hydraulic parameters for different experimental runs

	run 1	run 3	run 4	run 5
slope [%]	1	1	1	1
D50 [mm] of pool sediment*	3.3	3.3	3.3	3.3
pool sediment size uniformity	homo- geneous	homo- geneous	hetero- geneous	hetero- geneous
sediment supply from upstream	none (clearwater)	feed	none (clearwater)	feed
discharge	varied in steps	varied in steps	varied in steps	varied in steps

* see Appendix B for particle size gradation curves

test period. Runs 4 and 5 represent the second experimental "unit", showing eventual effects of a more heterogeneous bed material in the pool. As for the first unit, these experiments were conducted under clearwater and sediment supply conditions. The sediment supplied to the pool from upstream at the riffle matched in size that placed in the pool initially.

Water temperature was held between 18°C to 22°C.

Velocities

A mini-propeller flowmeter ('Micropropeller Velocity Flowmeter', model No.15, type BIDEK, Hydrel Copenhagen) was used to measure velocities at various depths. The instrument had a propeller with a diameter of 1 cm, which allowed measuring velocities close to the bed as well as gaining detailed information about velocity distributions normal to the bed.

Approximately uniform flow conditions existed for the two riffles in the flume study. Uniform flow is characterized by the constant depth, water area, velocity and discharge at every section of the channel reach and by parallel energy line, water surface and channel bottom. In other words, the flow lines are parallel to each other. The velocity distribution in such a case is said to become stable when the turbulent boundary layer is fully developed (Chow, 1959). In this turbulent boundary layer, the distribution can be shown to be approximately logarithmic (Chow 1959):

$$v = 2.5 u_* \ln(y/y_0) \text{ [LT}^{-1}\text{]} \quad [3-7]$$

where:

u_* = shear velocity which varies with the boundary
friction $\text{[LT}^{-1}\text{]}$

y = water depth [L]

y_0 = constant of integration.

Equation [3-7] is widely known as the Prandtl-Van Karman universal-velocity-distribution-law.

Recognizing that the application of this law is very limited in natural systems, other approaches have been developed to describe the actual velocity situation more adequately. Most of such research is descriptive in nature: velocity profiles are measured and curves are then developed to fit the actual data. Breusers (1975) computed such velocity profiles in scour holes within boundaries. The boundaries are similar to the 'riffle boundary' in this flume experiment, so that the velocity data from the scour hole (which corresponds to the pool) can be compared later with my experimental results.

Flow patterns

Besides velocity distribution curves, the visualizing of the flow field gives additional information about the fluid behavior at different locations in the studied section. Since the miniflow meter used in the experiments neither measured flow direction nor turbulence intensity, flow paths were instead documented by dye application to

the system. Turbulence "bursts", eddy formation, etc., could be identified at different depths and various distances within the pool. What seems to be a difficult technique to apply in natural stream systems turns out to be an extremely useful tool in a flume experiment.

The flow patterns in the pool were visualized at each discharge step within a hydrograph run. Fluorescent dye showed the streaklines which describe fixed points through which fluid particles have passed during a specific time interval (Goldstein, 1983).

Bed morphology

Within each run the bed elevations were recorded after 'equilibrium' was reached. A point gage was used in order to obtain precise results.

Several researchers investigated changes in the pool-riffle morphology after large storms had passed the system. In connection with field studies of sediment transport, Campbell and Sidle (1985) reported the filling of pools at moderate high flows while extreme high flows were recognized to scour the pool. The flume study conducted by Jackson and Beschta (1984) shows that increased sand delivery fills the pools. This can also be expected for material which is generally finer than the riffle material applicable to this flume study. For the case of aggradation in an entire channel, Lisle (1982) found that the response is a decrease in bar relief and that pool sections became more riffle-like in their hydraulic

characteristics. These characteristics were expected to possibly occur during steady-state sediment feed in runs 3 and 5. All these studies suggest that some major transformation processes occur in pool-riffle systems which are quantitatively influenced in their final shape, depending on different flow stages as well as bedload supply. Since this experiment investigated the quantitative changes a pool is exposed to under different circumstances, results can be compared with the existing field data. The resulting shapes of the formed pool in this study will be discussed in Chapter IV.

Bedload transport

This section describes the procedures applied for measuring and evaluating bedload transport in the modelled system.

The question of how sediment transport occurs in a fully turbulent flow situation in a riffle-pool-riffle sequence was examined. As previously discussed in the literature review, it seemed to be likely that sediment transport would not occur in a regular, steady pattern (Milhous, 1973; Vanoni, 1975; Jackson, 1980; Klingeman and Emmett, 1982; Campbell and Sidle, 1985). During the controlled experiment, sediment samples could be taken within short time periods while the flow magnitude was constant. Sediment output was therefore integrated over short time intervals at each discharge step and recorded. In order to catch the washed-out sediment, a fine-meshed wire basket was fixed at the outlet of the flume. Sediment trapped in this basket was then dried and weighted. This procedure allowed the

analysis of the short-term distribution of sediment transport rates as well as the relative amount of sediment transport at specific discharges compared to the actual total bedload output.

Bedload transport was expected to occur in pulses, or at least in a non-regular pattern, due to the pool which acts as a temporary sediment "sink" (Beschta, 1987). The actual quantitative bedload output under the condition of the clearwater experiment and under the condition of a steady sediment feed rate was therefore investigated.

In order to get a qualitative idea of how different sediment supply rates applied at the same water discharge would alter the riffle-pool-riffle system in the flume, two test runs were conducted (runs 2a and 2b). At a discharge of 3.02 l/sec, the following two sediment feed rates were applied: 3.14 kg/hr and 15.71 kg/hr. The first rate was chosen using the final clearwater scour shape of the bed obtained at 2.75 l/sec (run 1b). The total volume of sediment output integrated over three hours was calculated. This volume was then fed back into the system over a three hour period. In the second run (run 2b) a rate five times the first rate was applied. The results of the two test runs (see Chapter IV) lead to the conclusion that sediment feed at changing rates strongly influences the hydraulic properties within the pool. In order to use comparable sediment feed rates for the various discharges in the experiment, calculations were made of the bedload transport rates. This was done with the commercially available U.S. Army Corps of Engineers Hydrologic Engineering Center HEC-6 mainframe computer program as modified

for microcomputer use by Matin (1986). A brief description of the program, the formulas used for the purpose of this study, and the output list are given in Appendix C of this thesis.

The resulting values for the sediment feed rates for the specific discharges (with a D50 of 3.3 mm) are listed in Table 4. Mean values were taken from the results of three calculation methods.

For the reason of mechanically simple application, slightly different feed rates were actually used (the calibration of an automatic sediment feeding system turned out to be unreliable and the values were unreproducible, so I decided to feed the sediment manually at known rates).

Summary

This chapter has described the methods and techniques to experimentally model a natural riffle-pool-riffle sequence in a straight channel reach. The examination of the hydraulic conditions inducing clearwater scour as well as scour during steady sediment

Table 4. Sediment feed rates for the experimental runs

discharge [l/sec]	mean calculated sed. feed rate [kg/hr]	finally applied sed. feed rate [kg/hr]
1.1	1.0	1.57
2.8	7.5	9.43
5.3	26.0	28.30
7.6	32.0	33.00

input were recognized as being important study subjects. The results of the different experimental runs are reported in the following chapter.

IV. RESULTS AND INTERPRETATION

Overview

The first objective of this study was to investigate hydraulic influences on the bed morphology of a riffle-pool-riffle sequence. The second objective was to verify the hypothesis of 'competence reversal' which tries to explain areal sorting mechanisms in these small-scale systems. Chapter II clarified hydraulic concepts such as 'unit stream power', 'the law of least time rate of energy expenditure' and the hypothesis of 'competence reversal'. Chapter III described the physical model used to simulate a storm event in a riffle-pool-riffle sequence and to investigate its effects on the pool morphology. This chapter contains a description of the experimental results. The treatment of the results is separated into two major sections: changes in bed morphology and findings related to the competence reversal hypothesis.

The section on observed changes in bed morphology presents an analysis of the clearwater and the sediment feed experiments. Under clearwater conditions and using a homogeneous bed, the pool shapes reached a certain depth at each flow. This depth was compared with the case of clearwater flow over a heterogeneous bed. The coarser bed material in the latter case was thought to develop a protective layer at discharges below the general incipient motion condition for this layer. Therefore, armouring effects in the heterogeneous bed were expected to result in a shallower scour depth. In these experiments a

limited armour layer formed at relatively low discharges (around 1 to 2 l/sec) and broke up at higher discharges (3 to 7.8 l/sec). The difference in final pool shape between a homogeneous and heterogeneous bed was only significant for the clearwater experiments. This can be seen in figures presented later that compare the scour depths for the different test conditions. The sediment feed experiments simulated the case where bedload transport occurs at a steady flow. The sediment feed rate and the morphological 'history' of the pool influenced the final shape of the pool. This was true both for the case of the homogeneous bed and the heterogeneous bed.

Furthermore, the results of the bedload transport through the system are analyzed. Incipient motion conditions in the experiment matched those calculated previously. Unsteady bedload transport occurred during the steady flow steps. A more irregular pattern of bedload output was found when sediment was fed to the system. The possible reasons for these results are described in the corresponding section in more detail.

The second section of this chapter covers the results relating to the hypothesis of "competence reversal" which was introduced in the literature review. The trends for pool and riffle velocities at different depths over the range of the studied discharges were compared with trends suggested by the hypothesis. Various considerations concerning the calculation of shear stresses in the flume experiment explain why it was difficult to come to a direct comparison with the existing hypothesis.

Bed morphology changes

As noted in the literature review, the shape of stream beds is influenced by many forces. This study identifies significant influences on bed morphology changes of one riffle-pool-riffle sequence modelled in a flume.

Each experimental run, spanning a hydrograph runoff event, was started with a plane bed. This is indicated as 'initial bed' on the graphs. Each discharge step during a run was treated like a steady flow situation. At each discharge step, bed elevation changes and velocity profiles at several locations within the studied system were recorded. The complete data set, including the tables and figures corresponding to each run, is given in Appendix D. In the following sections of this chapter, only those figures are presented which illustrate the text description.

Clearwater scour for a homogeneous bed

Several general patterns of bed scour were identified in the clearwater experiments. The details of the hydraulic conditions for run 1 (homogeneous bed) are given here. This detailed description leads to a comparison with the heterogeneous bed (run 4) in the next section.

Incipient motion of the homogeneous bed material ($D_{50} = 3.3$ mm) was determined visually at the start of run 1 by three trials in which

discharge slowly increased. Incipient motion occurred at a discharge of approximately 0.75 l/sec. This corresponds well with the calculated value of 0.8 l/sec (see Chapter III).

Figure 9 gives an overview of the bed elevations and pool shapes for all the discharge steps during run1. The pool shape changes in the following pattern, according to the discharges to which it is exposed. The first noticeable pool change is the increase in depth and the downstream shifting of the deepest section with each discharge step. The discharge just above the incipient motion condition causes a very shallow pool. With increased discharges, the pool gets deeper and extends farther downstream. Table 5 shows some of the scour dimensions.

Table 5. Comparison of scour volumes at increasing discharges during run 1

Run	Discharge <l/s>	greatest depth in pool <m>	distance from d/s* end <m>	ratio of depth change **	scour volume <m ³ >	increase in volume <%>	ratio of volume change ***
1a	1.09	-0.0210	1.64	-	7.58E-04	-	-
1b	2.75	-0.1128	1.42	5.4	5.60E-03	639.0	7.4
1c	5.31	-0.1313	1.30	1.2	9.86E-03	76.1	1.8
1d	7.60	-0.1583	1.20	1.2	1.48E-02	50.2	1.5

* downstream

** depth for this run divided by depth for previous run

*** volume for this run divided by volume for previous run

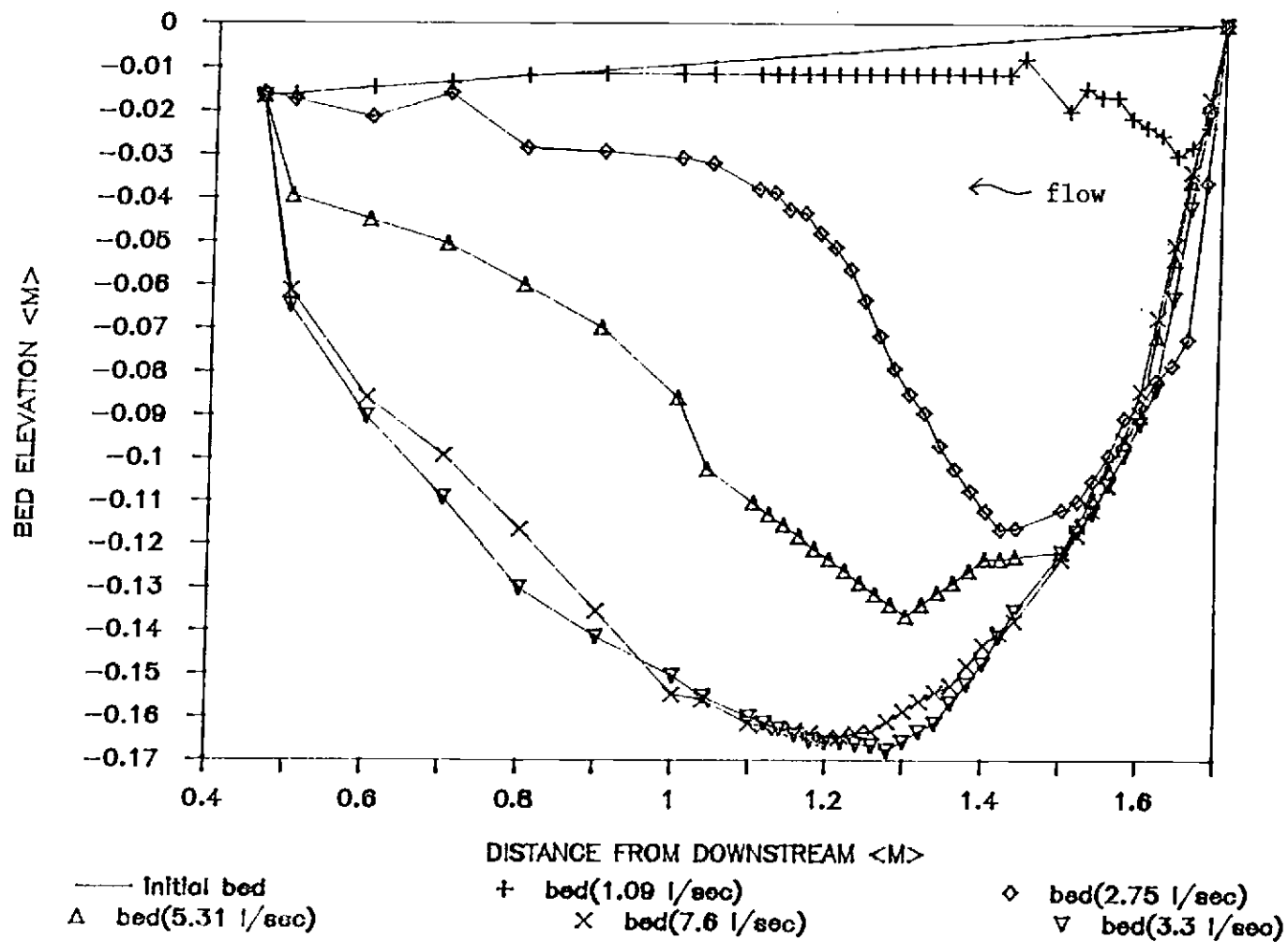


Fig. 9. Composite scour shapes for run 1

A remarkable increase in scour depth and volume occurs at the second discharge step. The discharge was increased by approximately the factor of two, which caused an increase in pool depth by the factor of 5.4 and an increase in bed scour volume of 639 % (factor 7.4)! For the two next higher discharges, however, the depth only increased by a factor of 1.2, even though the discharges increased by factors of 1.9 and 1.5, respectively. This pattern was also found in other runs, as is shown later. It seems to explain the fact that, at the lower discharges, the incipient motion condition is only reached to a limited extent. Local supercritical flow at the interface of the fixed riffle (with coarse gravel) and the pool (with finer bed material) could have caused local scour effects that affected the actual scour shape of the pool. A 'break-through' apparently occurred at a flow of 2.75 l/sec. The incipient motion condition was exceeded and the system responded with a spontaneous bedload output and deep scour.

Interesting is the fact that the bed shape does not change any more on the recession limb of the hydrograph. Figure 9 shows that the pool shape at 3.3 l/sec (run 1e) is similar to the shape formed by the highest flow. This suggests that, at these high flows, a natural pool with limited upstream sediment supply maintains its 'high' flow scour shape throughout the following low flow period. Some abrupt rearrangement of pool material occurred at the end of the last discharge in this run (run 1f, 1.66 l/sec), after equilibrium conditions had been observed. This occurrence is unexplained but

repeated itself during some other runs as well (see Appendix D for graphs).

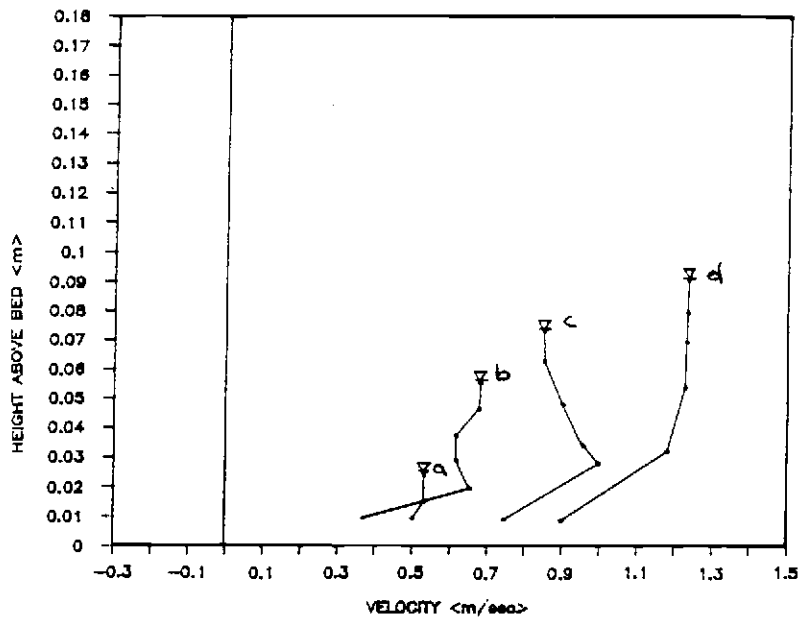
The velocity profiles for the upstream riffle and pool are shown in Figure 10. These demonstrate the following two tendencies throughout one hydrograph run: at the riffle (Figure 10a), the vertical velocity distribution is relatively uniform but increases in magnitude with flow; at the deepest location in the pool for each discharge step, the vertical velocity profile has a strong gradation. Negative flows near the bottom indicate that the flow direction has changed, causing the flow to move upstream along the pool bottom.

Comparison of clearwater scour for a homogeneous and a heterogeneous bed

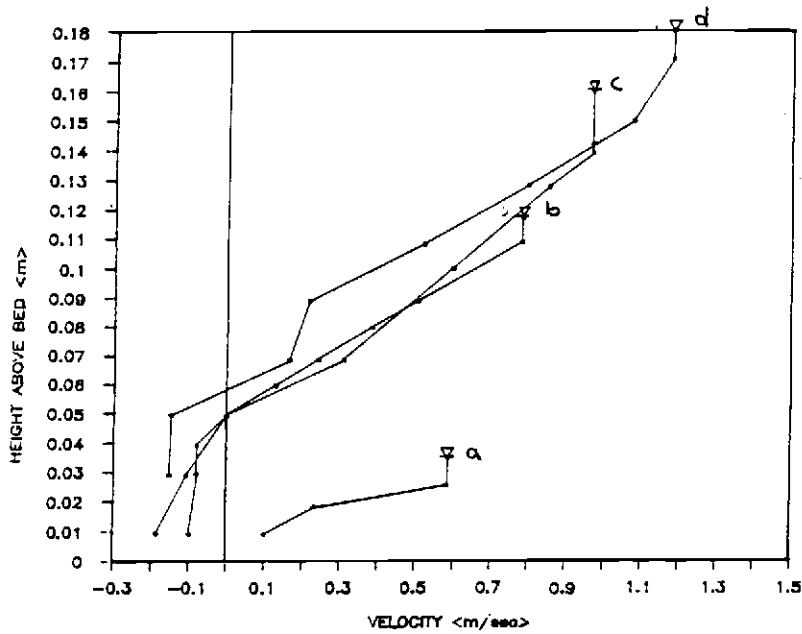
In the design of this experiment, differences in bed material composition were hypothesized to influence changes in bed morphology. The results of an experimental comparison of the effect of homogeneous and heterogeneous material are described here. Specifically, the comparison is made between run 1 and run 4 (the two clearwater runs), the former having a uniform pool sediment and the latter having heterogeneous material. Both sediment mixtures had a median grain size diameter of 3.3 mm.

In Chapter III, I formulated the expectation that an armour layer could act as a protective shield against further erosion. Figure 11

a) riffle



b) pool



discharge steps: a ~ 1.1 l/sec
 b ~ 3.0 l/sec
 c ~ 5.3 l/sec
 d ~ 7.6 l/sec
 e ~ 3.0 l/sec
 f ~ 1.3 l/sec

Fig. 10. Superimposed velocity profiles for run 1

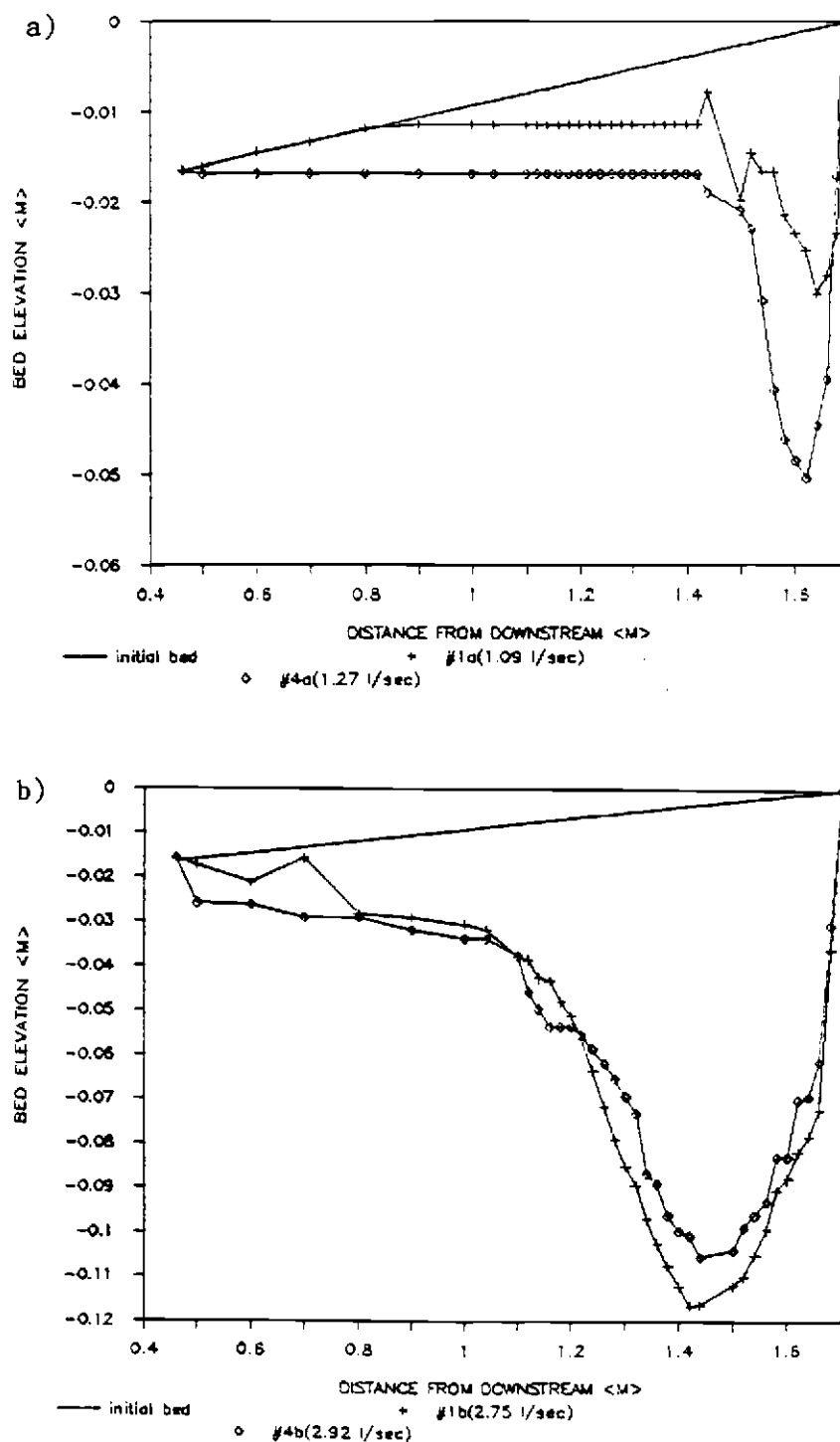


Fig. 11. Comparison of scour shapes for runs 1 and 4

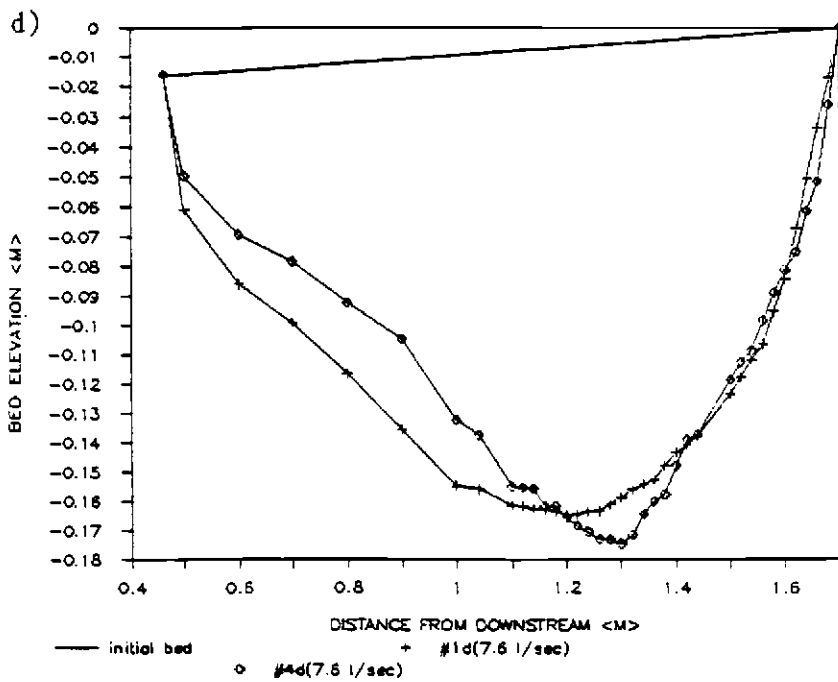
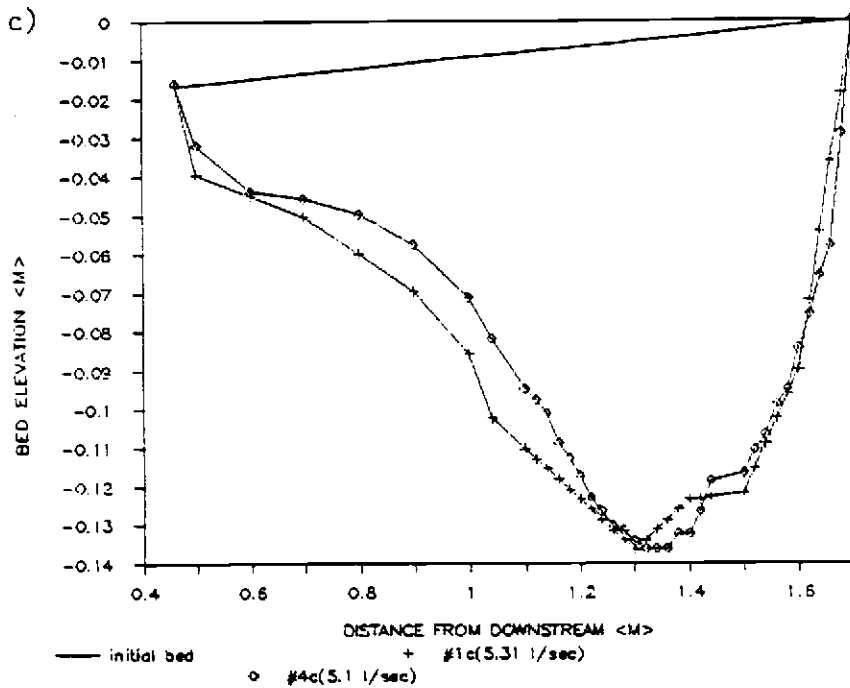


Fig. 11. (continued)

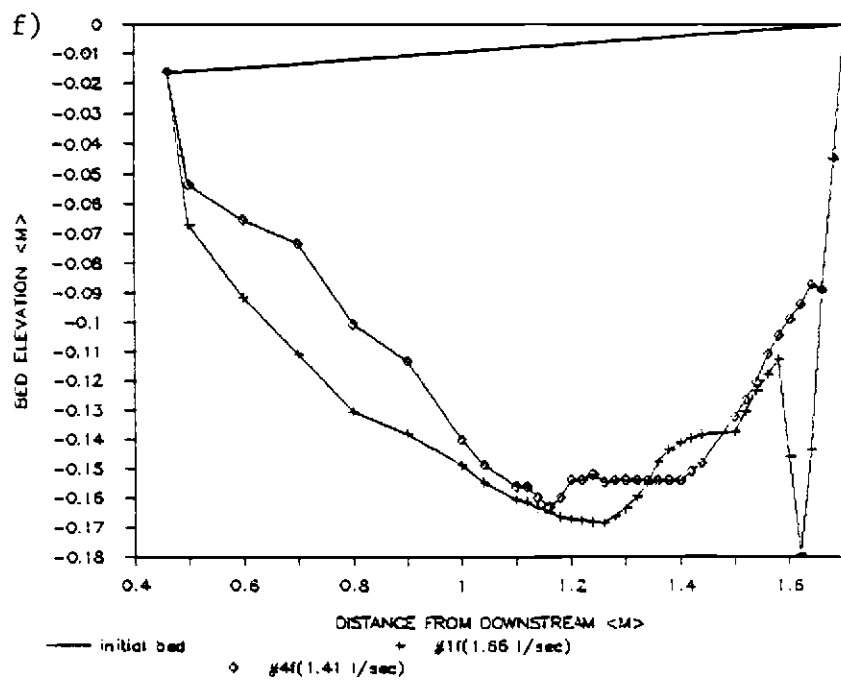
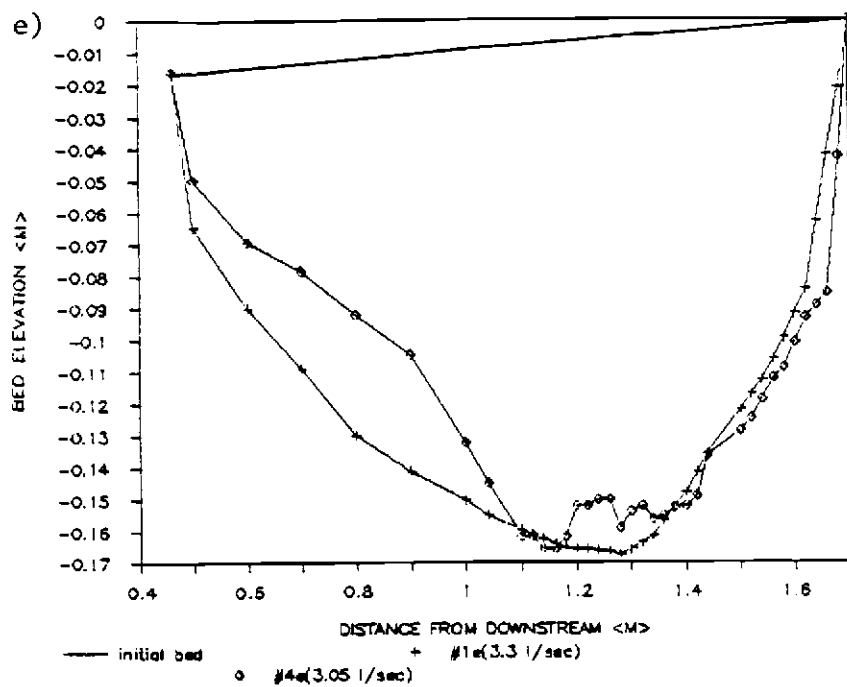


Fig. 11. (continued)

gives a comparison of the differences in the scoured bed for the two runs.

Except for the scour shapes formed at the lowest discharges (run 1: 1.09 l/sec; run 4: 1.27 l/sec), the scoured volume for the heterogeneous bed is always smaller than the scoured volume for the homogeneous bed (see Table 6). After the peak discharge was reached (runs 1d and 4d), the scour volume in the armoured bed stayed approximately 10 % smaller than for the non-armoured bed. The greatest difference in pool depth occurred over the downstream half of each pool. This phenomenon, which occurs most noticeably at higher flows, can be explained by observations during the experiment: the upstream halves of the pools (nearest to the upstream riffle) did not show any stable armour layer. The bed material there was completely disturbed throughout each discharge step. Midway along the pool, however, stabilizing of the bed configuration started. Imbricated coarser material was found on the up-slope side and continued downstream beyond the end of the pool.

Table 6. Comparison of scour volumes of homogeneous and heterogeneous clearwater beds

Discharge step	Run 1 scoured volume $\langle m^3 \rangle$	Run 4 scoured volume $\langle m^3 \rangle$	Volume difference, run 4-run 1 $\langle \% \rangle$	Volume ratio, run 4/run 1
a	7.58E-04	1.61E-03	112.6	0.47
b	5.60E-03	5.58E-03	-0.3	1.00
c	9.86E-03	9.18E-03	-6.9	1.07
d	1.48E-02	1.32E-02	-11.1	1.12
e	1.48E-02	1.32E-02	-10.5	1.12
f	1.49E-02	1.33E-02	-11.0	1.12

This observation is analogous to results of a flume experiment conducted by Harrison in 1950 (see Vanoni, 1975). He identified the collection of coarser sediment particles at the base of dunes. Despite the fact that only a portion of the bed surface was covered by armour particles, he noticed a significant decrease in sediment discharge compared to the non-armoured beds. Harrison also observed that these particles were arranged in a shingle pattern. This corresponds to the observations in this flume study as can be seen in Figure 12.

The establishment of a stable armour layer appeared to have two effects: inhibiting further erosion and, at the same time, concentrating the erosional forces locally towards the center of the pool. This caused deeper erosion, resulting in a more V-shaped pool (longitudinally) compared to the U-shape of the homogeneous bed (see Figures 11c and 11d). The combined effect of armouring and locally deeper erosion can be directly compared in Figure 11d, where the applied discharges for runs 1 and 4 are identical. However, velocity distribution curves for this case, shown in Figure 13, suggest different flow conditions of the bed but not necessarily higher erosional forces at the bottom of the armoured bed.

As mentioned earlier for run 1f, a sudden rearrangement of the pool material near the upstream riffle took place in run 4f (see Figure 11f).

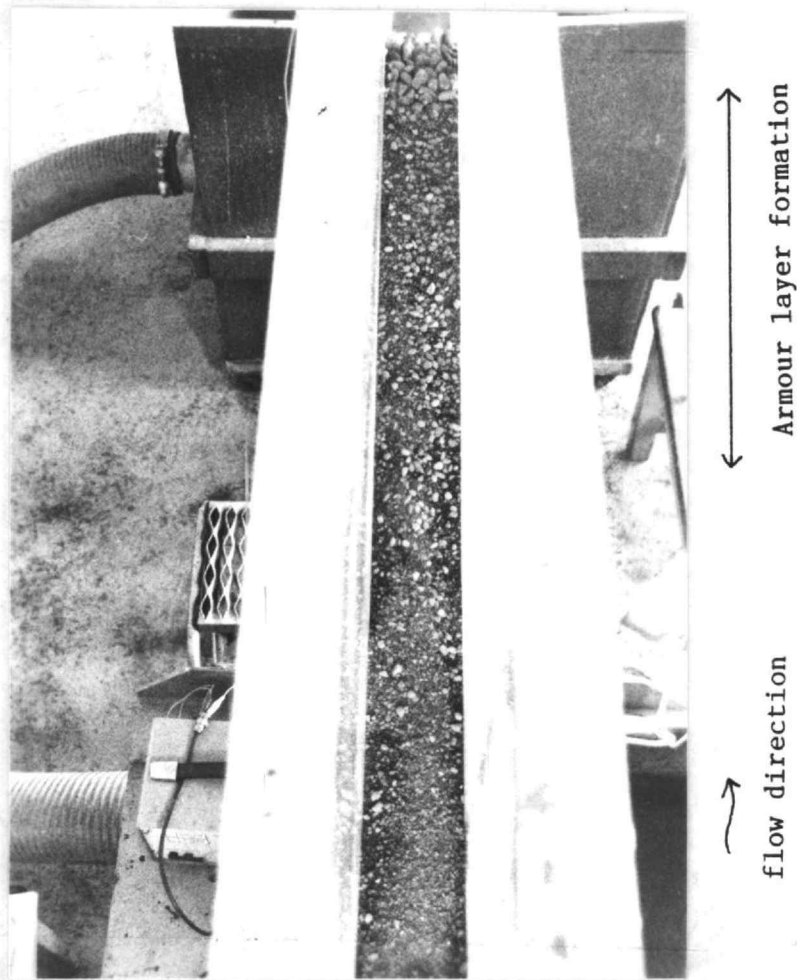
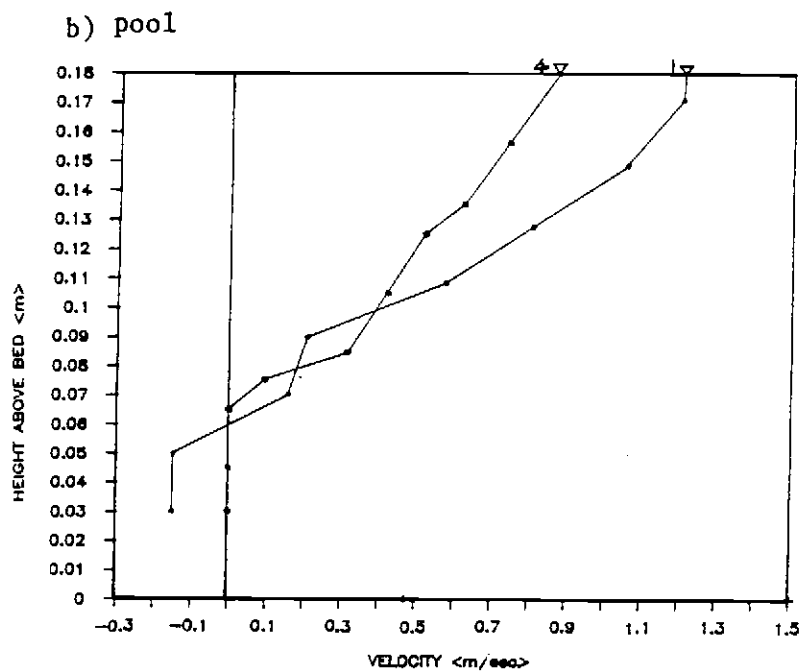
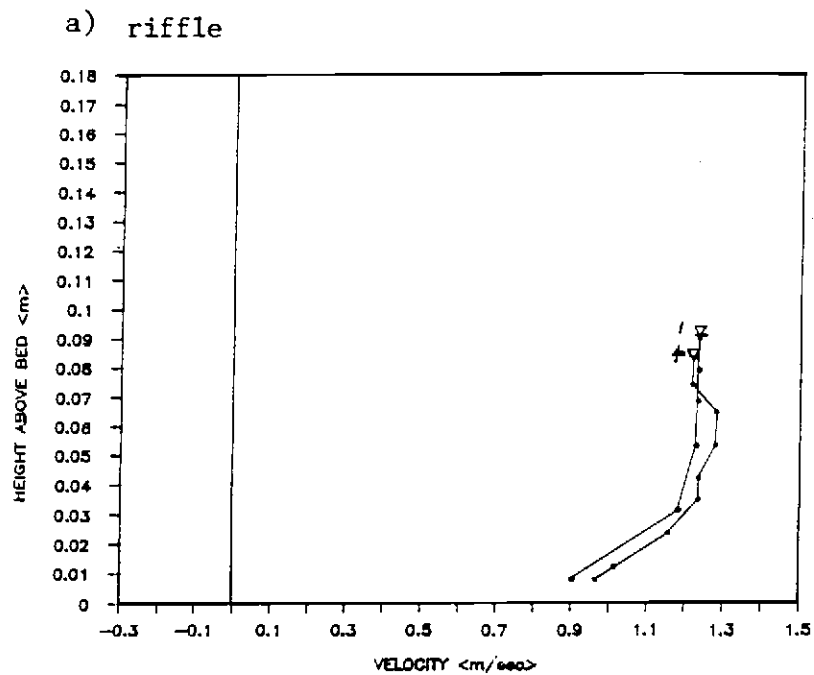


Fig. 12. Partial armour layer formation in the pool
(view looking downstream from above)



1 = run 1d

4 = run 4d

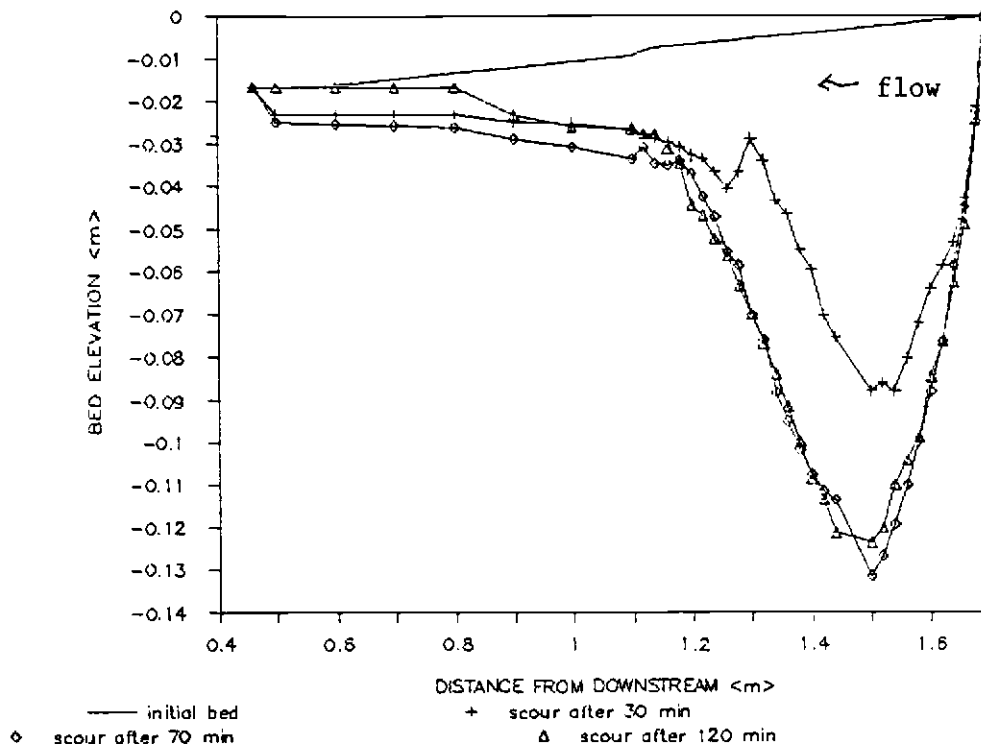
Fig. 13. Superimposed velocity profiles for runs 1d and 4d

Sediment feed test runs

The description and quantitative analysis of the clearwater experiments illustrated the influence of different flow conditions and bed material composition on the scour shapes of a pool during a simulated storm flow event. Clearwater runoff events may occur in natural stream systems under specific conditions (for example, in supply-limited steep mountain streams). More commonly, however, is the situation where sediment enters the pool-riffle 'unit' due to bedload transport from upstream. To get an idea of the magnitude of changes that can possibly be induced by different sediment supply rates, two sediment feed test runs were conducted prior to the experimental runs. Hence, before the results of the actual experiments are described, the outcomes and conclusions from the sediment test runs are presented. They help understand the choice of the specific sediment feed rates in the actual experiments.

In the two test runs, sediment was applied at steady rates until equilibrium was reached. The sediment feed rates were 3.14 kg/hr in the first run (run 2a) and 15.72 kg/hr in the second run (run 2b). The choice of the rates was explained in Chapter III. As can be seen in Figure 14a (run 2a), the shape of the bed changed during the observed time period. During the first half hour the bed was scoured to a depth of 8.5 cm below the initial bed. After 120 minutes, a further increase in depth to 12.1 cm occurred and the bed shape then stabilized for the rest of the three-hour period. Figure 15 shows the sediment output rates from the pool during the course of runs 2a and 2b.

a) Run 2a:



b) Run 2b:

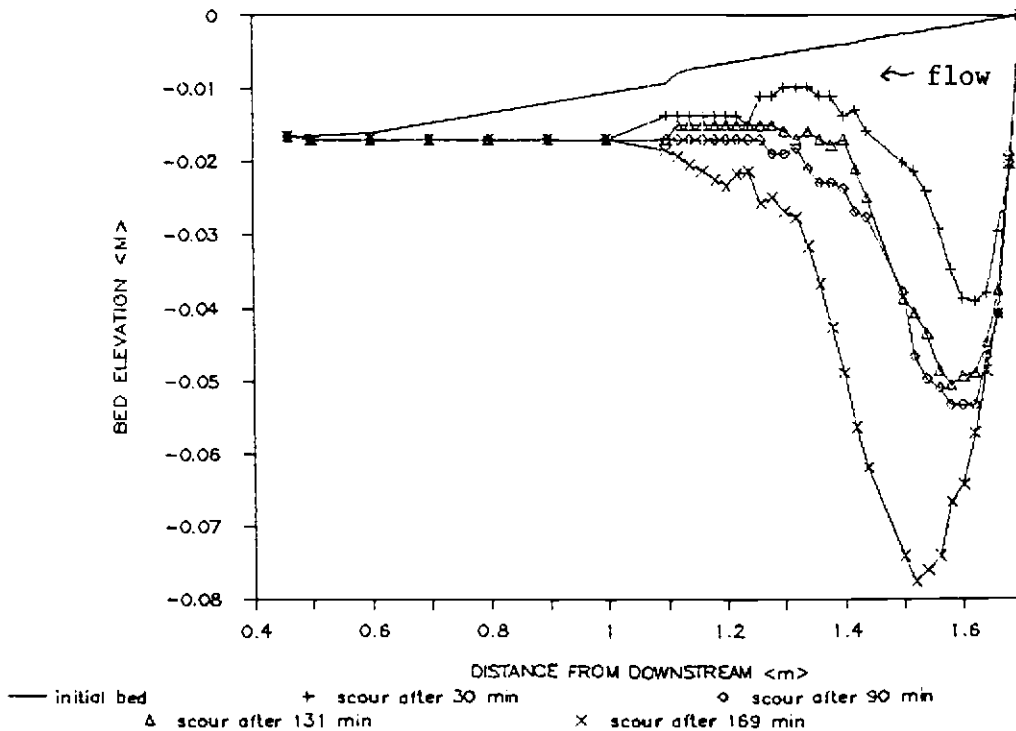
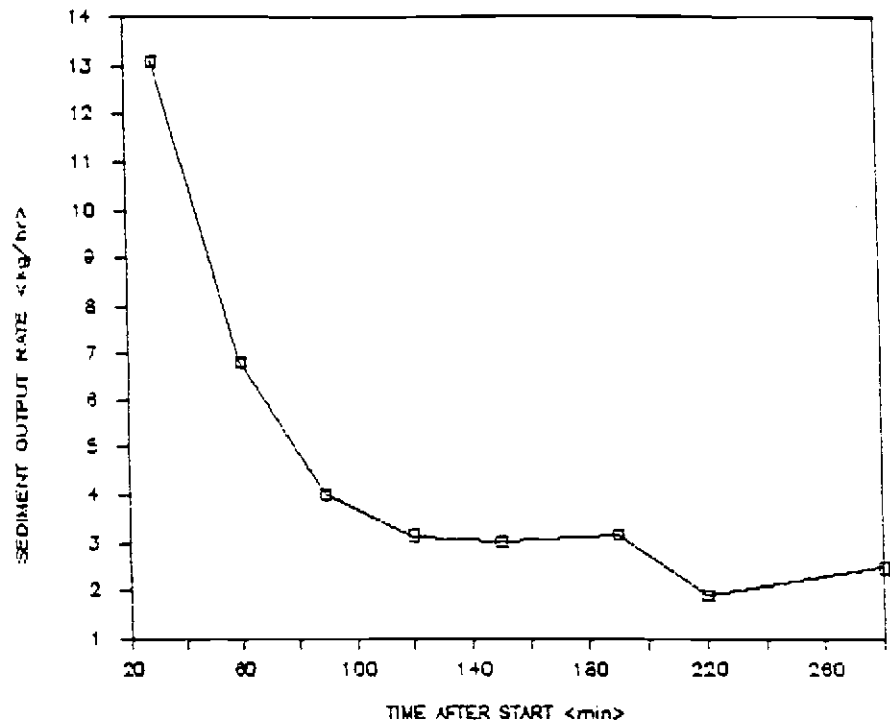


Fig. 14. Scour shapes in sediment feed test run 2

a) Run 2a:
(sed. feed: 3.14 kg/hr)



b) Run 2b:
(sed. feed: 15.72 kg/hr)

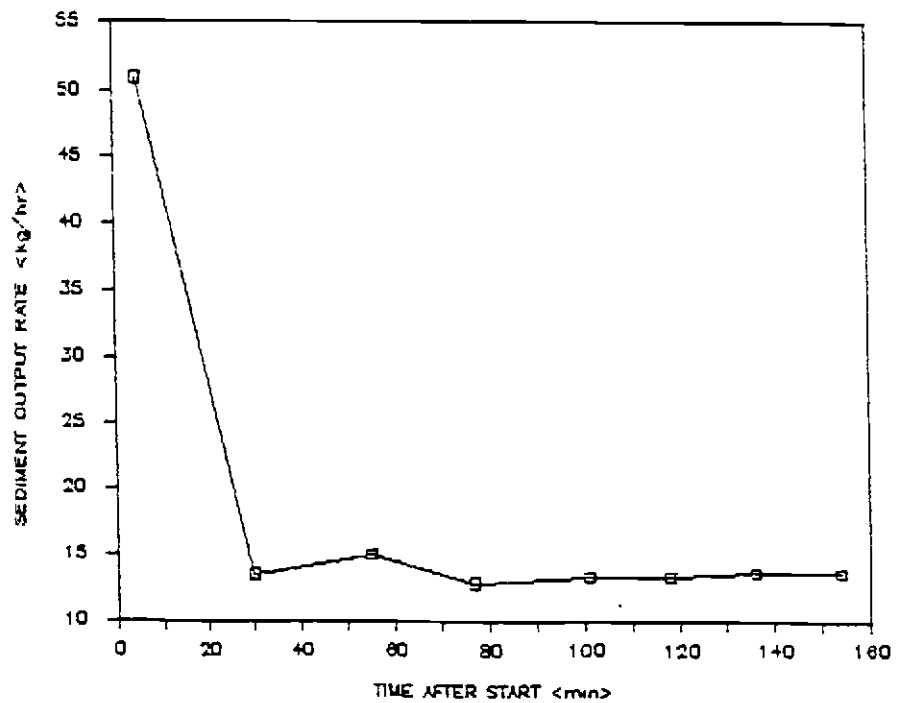


Fig. 15. Sediment output rates for run 2

These show that an 'equilibrium' is eventually reached after about 60 to 90 minutes. The time when the 'equilibrium' bed shape is obtained does not coincide exactly with the time when an 'equilibrium' sediment output rate occurs. This is discussed later.

Comparing the maximum scour depths of the final bed in run 2a (12.1 cm, Figure 14a) with the one obtained in run 1b (11.28 cm, Figure 9), both having the same moderate discharge, a strong similarity can be seen. Therefore, scour processes did not seem to be inhibited by introduction of sediment from upstream at the chosen rate. This leads to the conclusion that the chosen sediment feed rate was lower than that necessary to cause changes in the pool hydraulics and to cause sediment deposition (or less net scour).

In the second test run, a sediment rate five times as high as the first was applied to the system (15.72 kg/hr). The pool hydraulics were changed sufficiently that much energy was consumed in transporting the additional sediment rather than in scouring the bed. Therefore, only a relatively shallow scour bed could be shaped by the flow (maximum scour depth: 7.52 cm). An equilibrium situation (sediment transport capacity equals erosional capacity) was reached approximately one hour after the start (Figure 15b).

The outcome of the two test runs illustrates that the pool scour condition equilibrates faster at a higher sediment feed rate. Furthermore, an increase of the sediment load by the factor of five decreases the water scour depth by 33%.

The results of test run 2 lead to the conclusion that bedload transport in general buffers the 'final' scour depth of a pool. Also, the rate of sediment supply significantly influences the magnitude of change in the pool shape.

To choose initial sediment feed rates to quantify this effect, it seemed reasonable to choose rates which correspond to calculated bedload transport rates for the specific grain size distributions. This attempts to match the situation in nature where bedload transport occurs upstream of the observed riffle and consumes some of the flow energy otherwise available for pool scour.

Bed scour with sediment supply from upstream

An important objective of this research was to identify the impact of sediment transport on bed morphology changes in the modelled riffle-pool-riffle sequence. Run 3 (homogeneous bed) and run 5 (heterogeneous bed) repeated run 1 and run 4 with the addition of simulated bedload transport from upstream of the riffle. The grain size distribution of the the sediment that was supplied from upstream was identical to the pool material.

Description of scour shapes in run 3 and comparison with clearwater shapes in run 1

Comparison of the experiments involving a homogeneous bed with clearwater scour (run 1) and scour during sediment supply (run 3)

showed that scour volumes and shapes were quite different (see Table 7).

Comparing the scour volumes for the two runs, the differences (expressed in percent and as volume ratios) become more significant with time during the hydrograph run. The pool shapes on the recession limb of the hydrograph (represented by discharge steps e and f) reveal particularly important differences. Figure 9 showed that the high flow-scour shape in run 1 is maintained during the recession limb of the hydrograph. With sediment feed, however, the pool starts filling in again as discharge decreases after high flow. If the sediment supply stays constant over time during each discharge step, as done in the experiment, the pool attempts to reach that shape which corresponds to the specific equilibrium condition. The scoured volume at the lowest recession limb discharge in run 3 (1.29 l/sec) is approximately 15 times smaller than the volume scoured in run 1 (at 1.66 l/sec). In fact, the pool is approaching its original shape

Table 7. Comparison of scour volumes for homogeneous bed with clearwater scour and scour under steady sediment supply

Run	Run 1 scoured volume $\langle m^3 \rangle$	Run 3 scoured volume $\langle m^3 \rangle$	Volume difference, run 3-run 1 $\langle \% \rangle$	Volume ratio, run 3/run 1
a	7.58E-04	9.85E-04	30.0	0.77
b	5.60E-03	2.57E-03	-54.1	2.18
c	9.86E-03	5.41E-03	-45.1	1.82
d	1.48E-02	9.74E-03	-34.2	1.52
e	1.48E-02	3.65E-03	-75.3	4.05
f	1.49E-02	9.73E-04	-93.5	15.36

corresponding to the similar discharge step on the rising limb of the hydrograph. This striking difference can be seen in Figure 16 where the two pool shapes are superimposed.

Velocity profiles for run 1d and run 3d are given in Figure 17 and 18. Comparison reveals significant differences in the hydraulic conditions. These runs have the highest discharge and are representative of the observed differences at other discharges. Abrupt directional changes characterize the velocity patterns in run 3d. While velocities in run 1d were steadily increasing from the bottom to the water surface, low or zero-velocity regions interrupted this regular pattern in the case of run 3d. This could be due to several factors which have impact on the hydraulics in this bedload transporting system. It is clear that hydraulic measurements can only capture a single incident during the dynamic process of bedload transport; they represent only 'point' measurements. This results from the pulse-wise transport of the sediment (described later). Observations during the experimental runs showed that sediment was carried through the pool with high velocities only at certain times; the same location was exposed to low velocities some time later during the same discharges. Readjustment of the hydraulic conditions was taking place continuously.

Quantitative errors occurred when measuring the velocity profiles. These errors were caused by the fact that the situation in the flume was not completely two dimensional. Side wall effects were observed during the experiments and led to local distortions of the

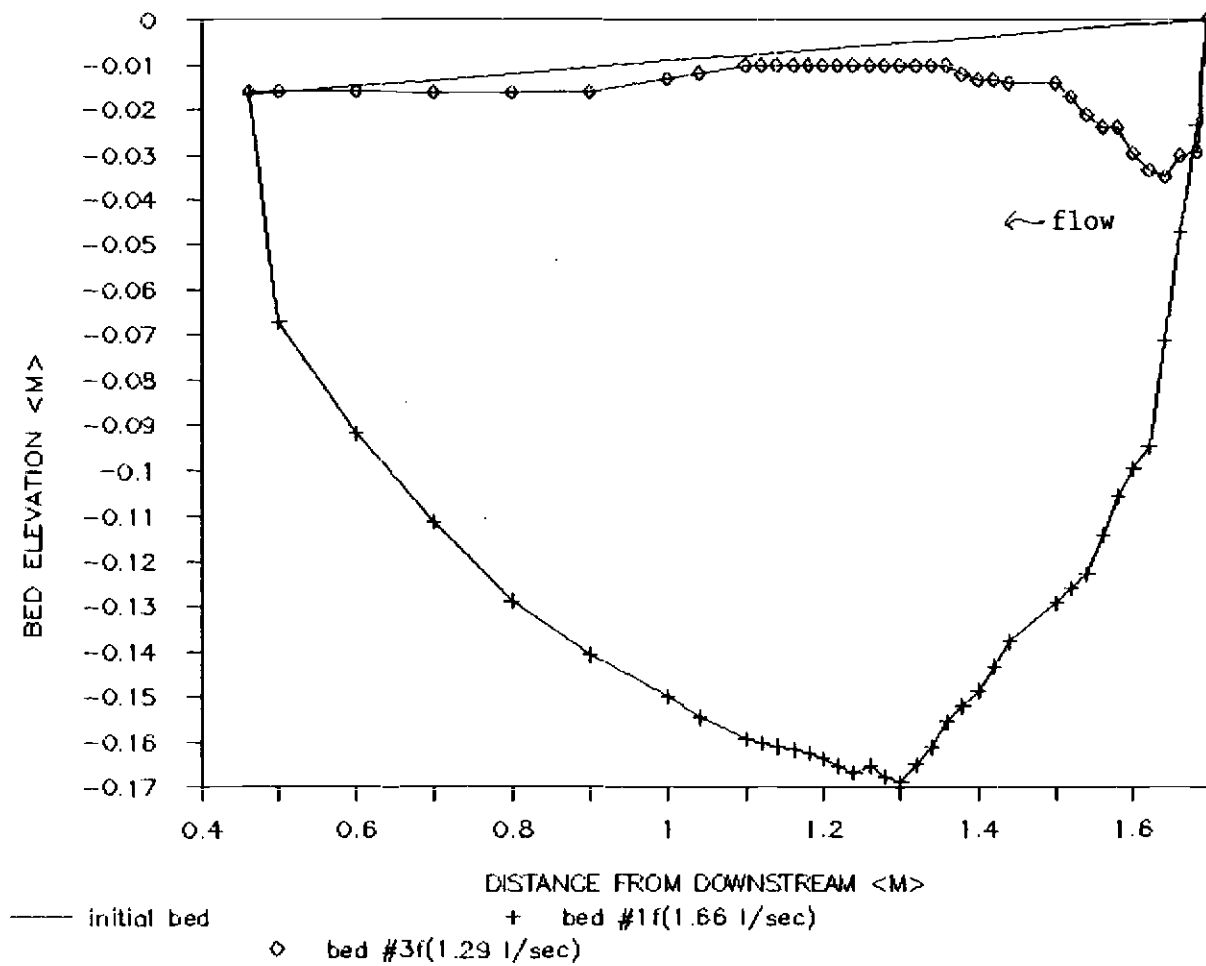


Fig. 16. Comparison of scour shapes for runs 1f and 3f

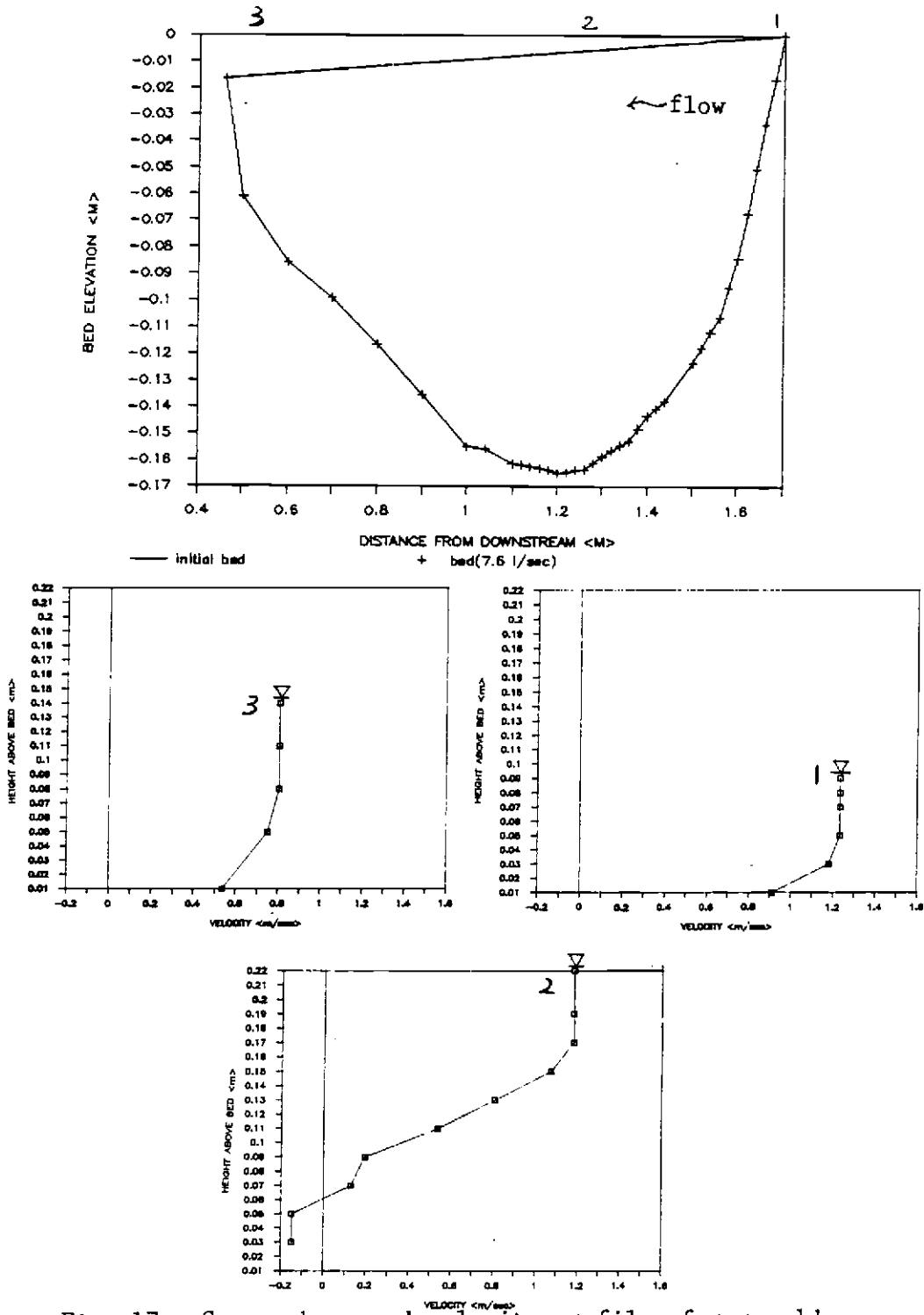


Fig. 17. Scour shape and velocity profiles for run 1d

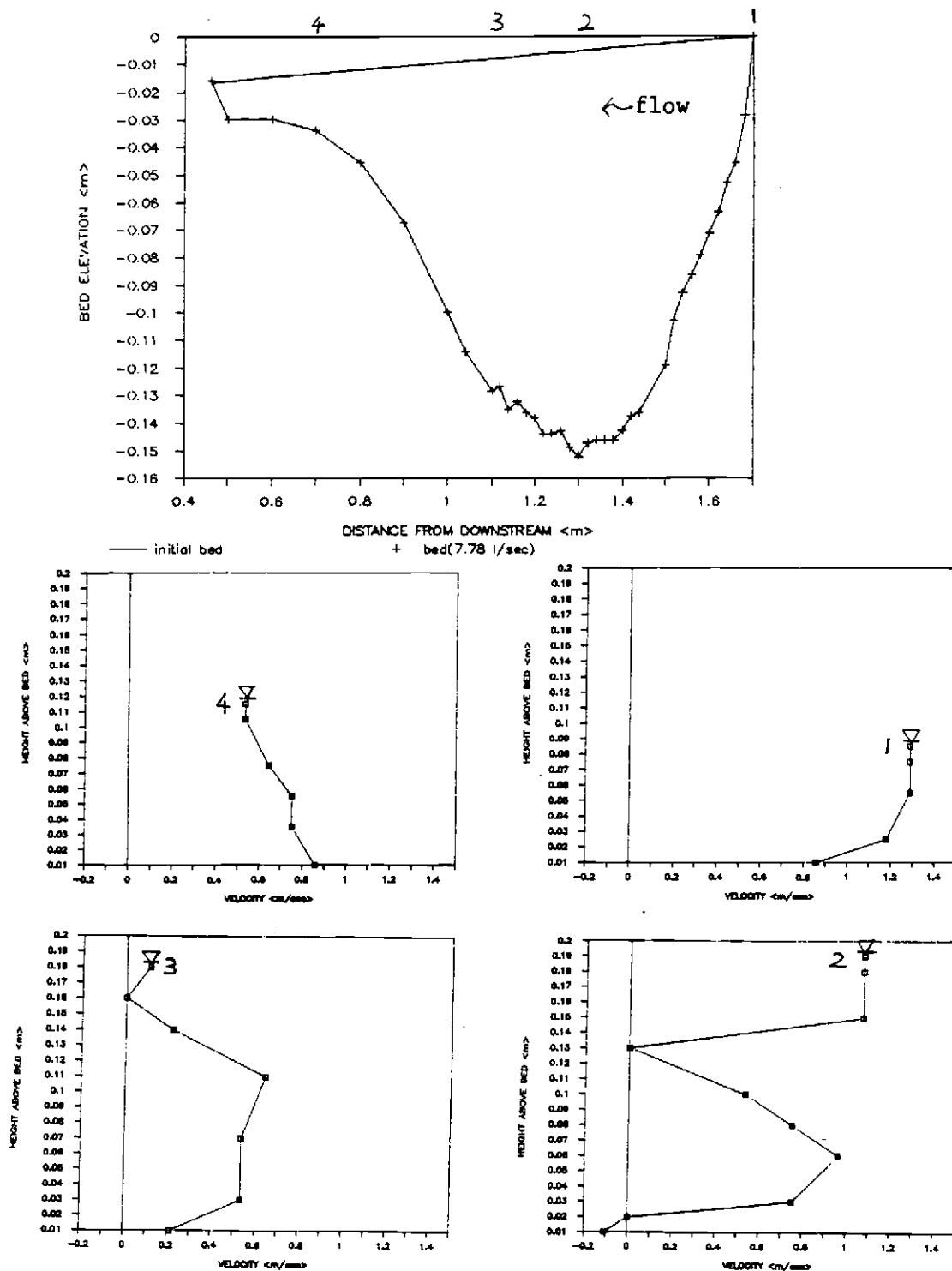


Fig. 18. Scour shape and velocity profiles for run 3d

measurements. The basic trends, however, are not thought to be influenced by these errors.

Comparison of scour shapes for homogeneous and heterogeneous beds when sediment is supplied to the system

In the clearwater case, it was noted that the formation of a partial armour layer resulted in a diminished amount of pool scour. In the following paragraphs, a comparison is made for the case of sediment supply. The results for run 3 (homogeneous bed) and run 5 (heterogeneous bed), in terms of scour volumes, are given in Table 8. Figure 19 illustrates the pool shapes in the case of sediment supply and the highest discharge. The scour in run 5d (armoured bed) exceeds the scour in run 3d (non-armoured bed), contrary to expectation. One possible explanation may be that the incoming heterogeneous bedload may have been more effective in disturbing the armour layer and causing pool scour than would the smaller-sized bedload for

Table 8. Comparison of scour volumes for homogeneous and heterogeneous beds under steady sediment supply

Discharge step	Run 3 scoured volume $\langle m^3 \rangle$	Run 5 scoured volume $\langle m^3 \rangle$	Volume difference, run 5-run 3 $\langle \% \rangle$	Volume ratio, run 5/run 3
a	9.85E-04	9.10E-04	-7.7	1.08
b	2.57E-03	2.82E-03	9.5	0.91
c	5.41E-03	6.68E-03	23.4	0.81
d	9.74E-03	1.16E-02	19.1	0.84
e	3.65E-03	3.55E-03	-2.6	1.03
f	9.73E-04	1.47E-03	51.2	0.66

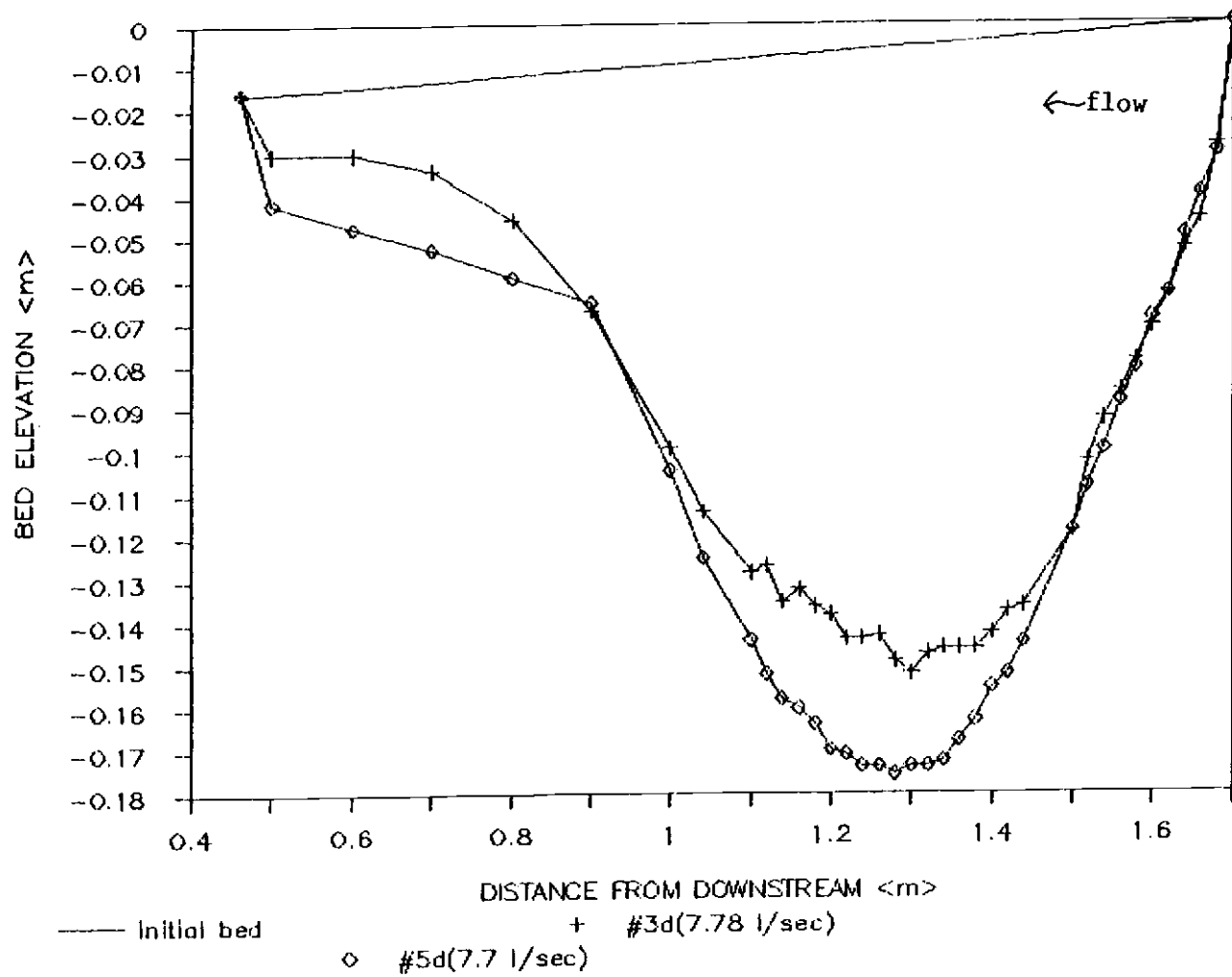


Fig. 19. Comparison of scour shapes for runs 3d and 5d

homogeneous sediment supply and pool material. It may be that the larger particles in the heterogeneous bedload are less supported by the fluid than are the other particles, allowing greater impact on the stationary particles on the pool bottom.

Nevertheless, residual armour layers could be seen in the bed at the end of run 5. Figure 20 illustrates the armour 'relicts' from the different discharge steps as they appeared at the end of run 5. Coarser layers could be identified which traced the 'historical' pool shapes formed by previous discharges. Figure 21 is a photograph showing how these coarse layers appeared in the flume. Historical pool shapes have also been investigated in the field work conducted by O'Connor et al. (1986) who examined the relationship between various historical flood events and the configuration of pool and riffle material. They could establish direct relations between the bigger boulder sizes that formed the riffle features and the magnitude of the storm events. Knowing the principal grain size distribution within a stream system it is possible to reconstruct the shape of the former bed morphology and the magnitude of the responsible storm events.

As in run 3, the velocity profiles for run 5 showed vertical changes in flow direction at a given location.

Bedload transport

In order to analyze the bedload transport phenomena within the modelled riffle-pool-riffle sequence the bedload transport rates of the individual runs were compared with each other. Common to all

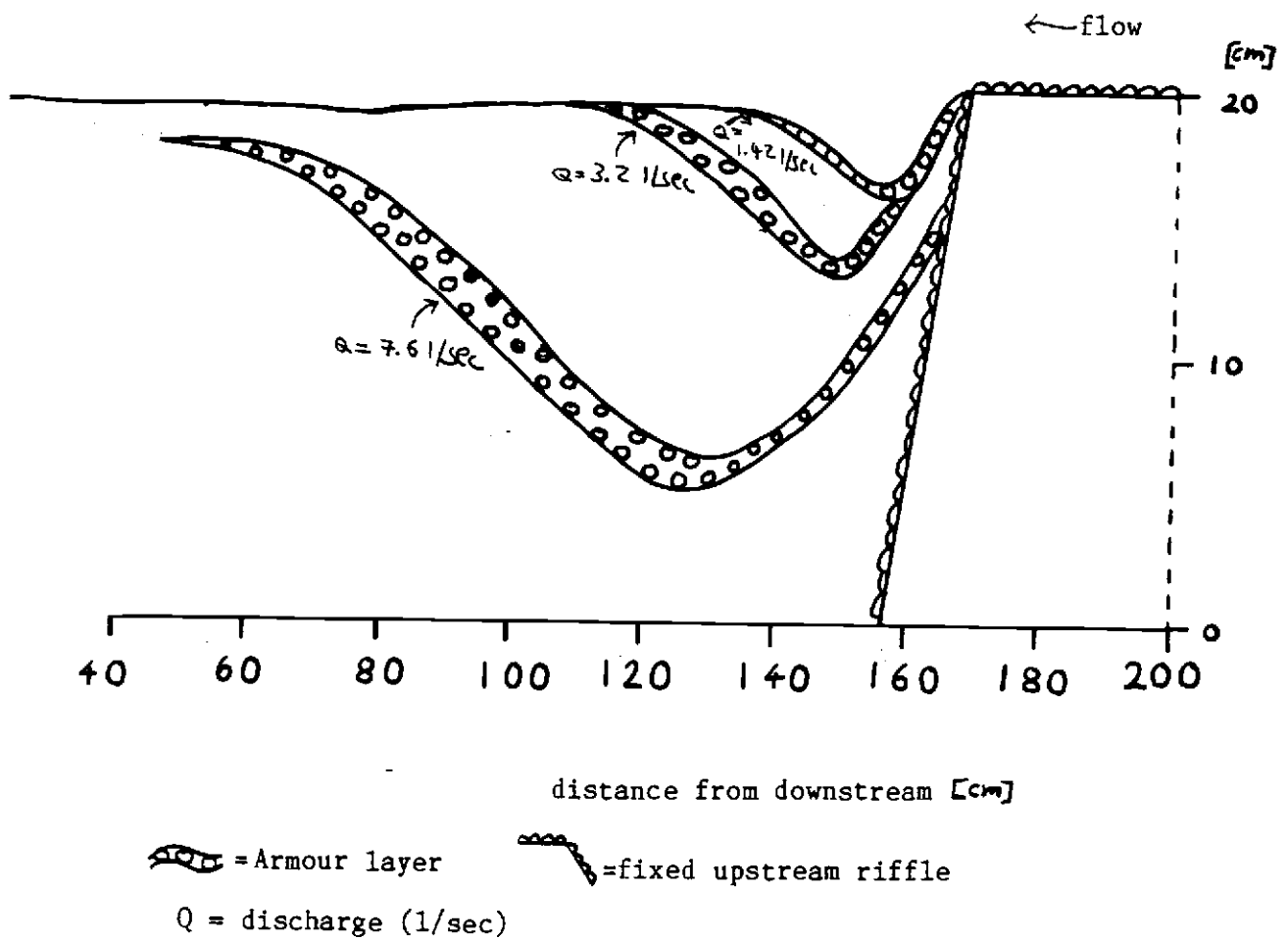


Fig. 20. Sketched armour layer 'relics' after run 5

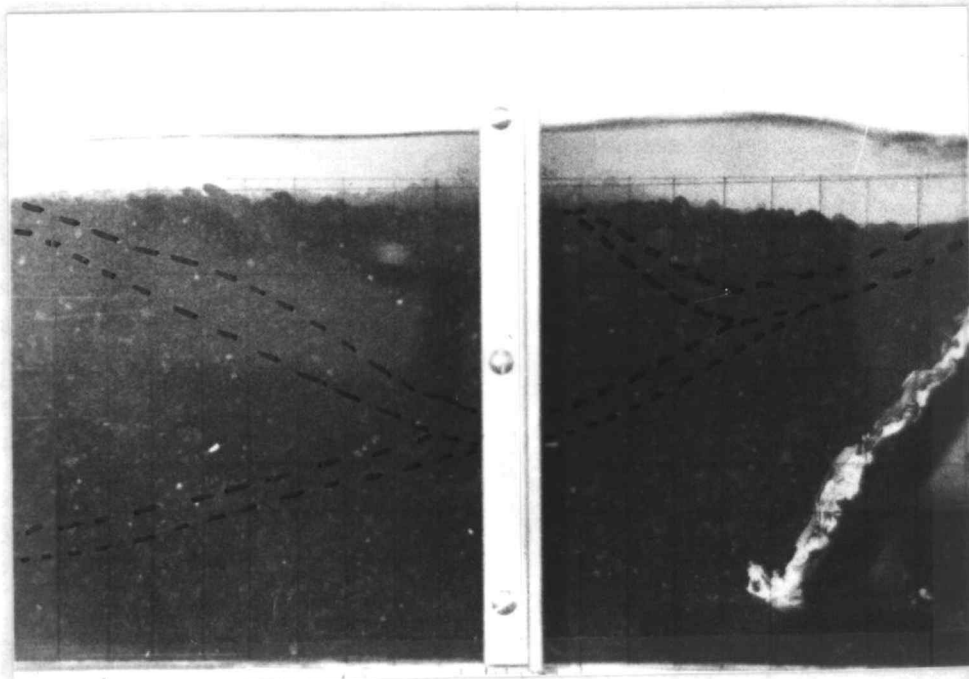


Fig. 21. Photograph of armour layer 'relics' after run 5

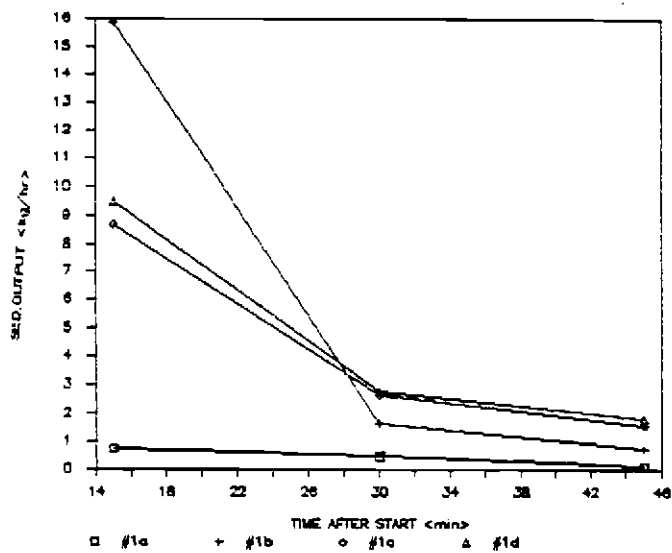
simulated situations under steady flow conditions was the condition of unsteady bedload transport. At each new increase in discharge during one experimental run, the system responded with a spontaneous increase in sediment output. The highest bedload transport rates occurred during the first hour of each discharge step on the rising limb., After this time period of adjustment, sediment output from the system — and therefore bedload transport — showed different patterns, depending on the amount of sediment feed and the bed material size.

Comparison of bedload output rates in the clearwater experiments

Figure 22 summarizes the obtained measurement results for runs 1 and 4. Even though only three consecutive intervals of 15 minutes were sampled in run 1 (homogeneous bed), the trends are comparable with the ones in run 4 (heterogeneous bed). Figure 22 and Table 9 demonstrate the difference in output rates due to protective armouring effects in run 4.

As can be verified on the graphs and in Table 9, the highest output rates during the first half hour are slightly smaller in run 4. The fact that the initial output rate in run 4a exceeds that in run 1a is due to the higher initial discharge (1.27 l/sec in run 4a compared to 1.09 l/sec in run 1a). With the next increases in flow, however, the establishment of a protective armour layer leads to significant decreases in sediment output. It can be seen that the protective effect of the armour layer becomes more important at higher discharges. In particular, the bedload transport rates during the first 15 minutes show remarkable differences: sediment output at a

a) run 1



b) run 4

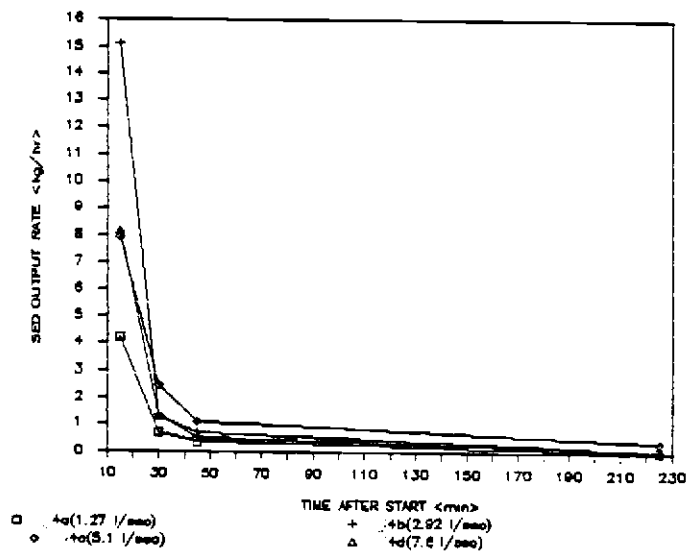


Fig. 22. Sediment output rates for runs 1 and 4

discharge around 3 l/sec (discharge step b) is increased by 4.8% in the case of the non-armoured bed. At subsequent progressively higher discharges, the difference in the increase rate doubles (8.9%) and even triples (13.8%). The protection becomes even more important over a longer time period. After the same discharge step has lasted for 45 minutes, bedload transport in the non-armoured bed is increased by 30% to 60%. Hence, it can be concluded that the establishment of a relative stable layer with coarser material inhibits further erosion even though this layer covers only part of the bed surface (discussed earlier in this chapter).

Table 9. Sediment output rates from homogeneous and heterogeneous clearwater beds

time <min>	output rate run 1a <kg/hr>	output rate run 4a <kg/hr>	difference run 1a- run 4a <%>	output rate run 1b <kg/hr>	output rate run 4b <kg/hr>	difference run 1b- run 4b <%>
15	0.756	4.22	-458.20	15.888	15.13	4.77
30	0.463	0.69	-49.03	1.606	1.34	16.56
45	0.112	0.34	-203.57	0.744	0.48	35.48
225		0.00			0.06	

time <min>	output rate run 1c <kg/hr>	output rate run 4c <kg/hr>	difference run 1c- run 4c <%>	output rate run 1d <kg/hr>	output rate run 4d <kg/hr>	difference run 1d- run 4d <%>
15	8.692	7.92	8.88	9.493	8.18	13.83
30	2.624	2.48	5.49	2.763	1.29	53.31
45	1.532	1.07	30.16	1.792	0.70	60.94
225		0.34			0.03	

Comparison of bedload output rates in the experiments with sediment feed

Figures 23 and 24 demonstrate the different bedload output rates in run 3 (homogeneous bed) and run 5 (heterogeneous bed), respectively, when sediment is supplied from upstream. A striking difference between these rates and the clearwater rates (see Figure 22) becomes obvious immediately: transport occurs with higher variability when sediment is supplied. The example of the highest discharge in run 5 (step d, 7.7 l/sec) illustrates these highly unsteady sediment output rates. It can be seen that the adjustment period toward 'equilibrium' is characterized by high sediment output rates during the first half hour, similar to the clearwater conditions. Other than that, however, bedload transport occurs in pulses of changing magnitude. No decrease in magnitude of those pulses over time can necessarily be concluded from the existing data. Table 10 demonstrates the differences in bedload transport rates between the homogeneous and heterogeneous beds.

These results verify that pools act as temporary sediment 'sinks' which release bulks of sediment in a rhythmic manner (Beschta, 1987; Jackson, 1980, Whittaker, 1987). Some regularity could be identified during high discharge steps like run 3c (5.25 l/sec) and 5c (5.21 l/sec), as well as in run 3d (7.78 l/sec) and 5d (7.7 l/sec). Output pulses occurred in 30-minute intervals in run 3c and run 5c and in

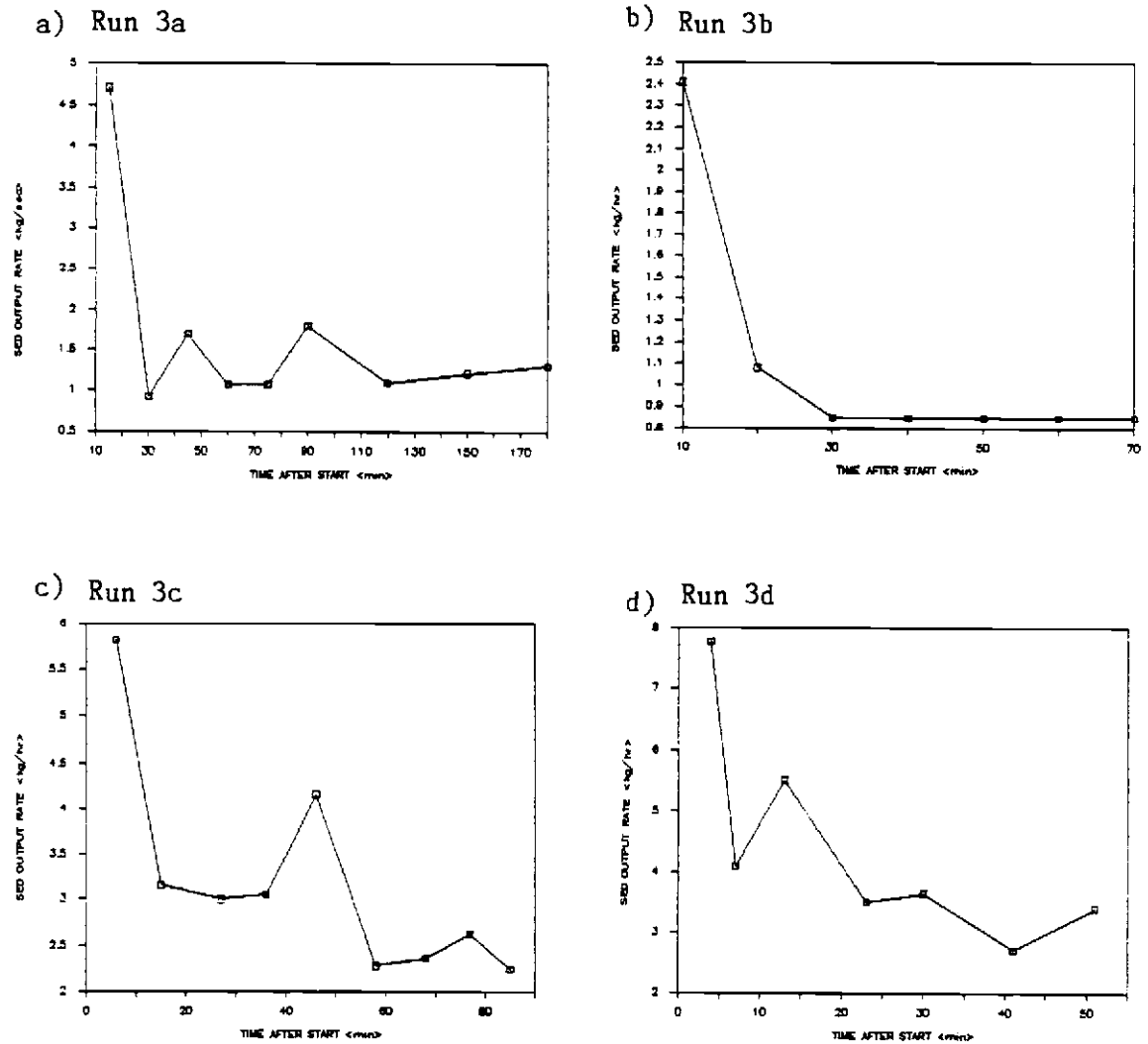


Fig. 23. Sediment output rates for run 3

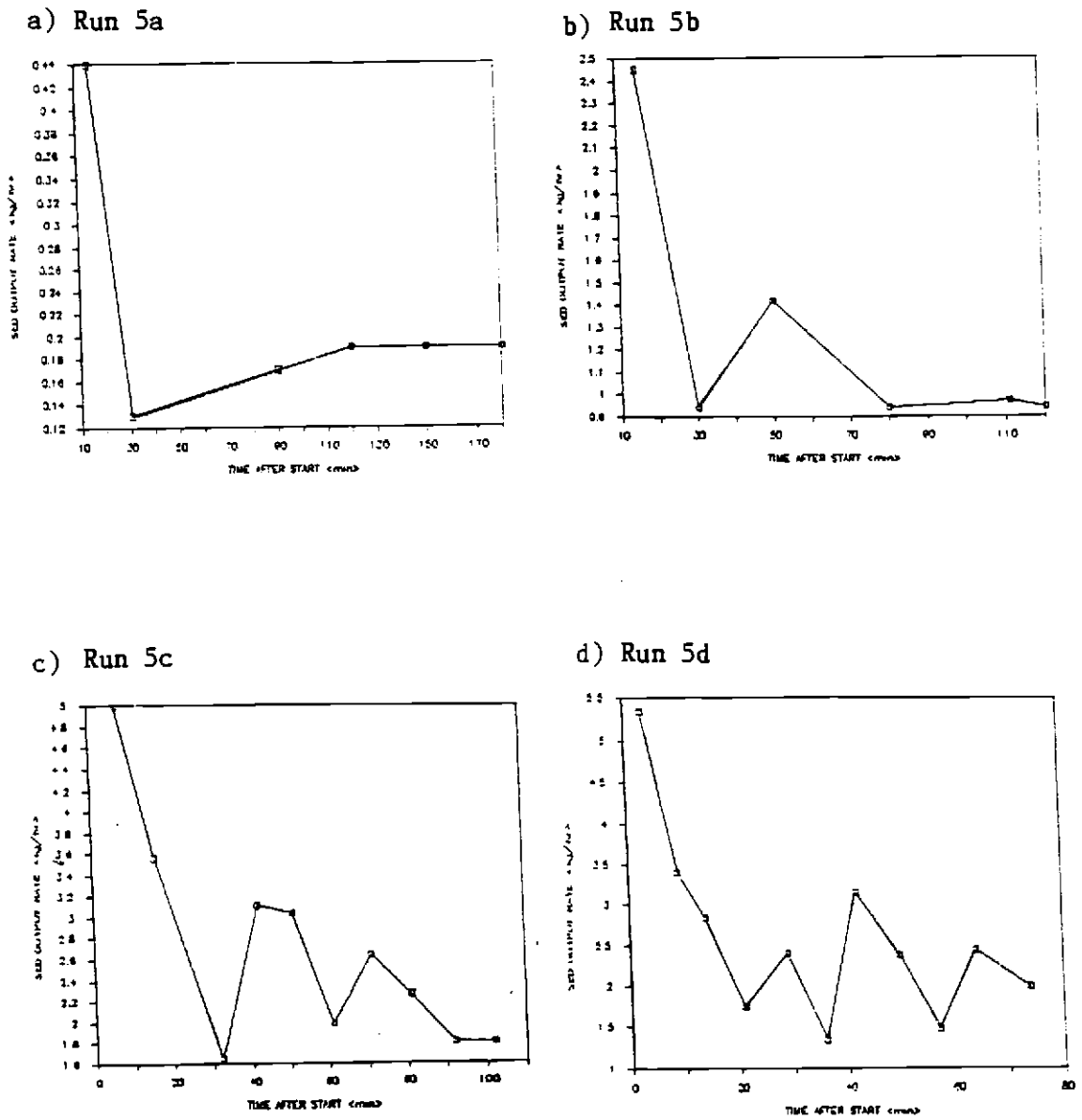


Fig. 24. Sediment output rates for run 5

Table 10. Sediment output rates from homogeneous and heterogeneous beds under steady sediment supply*

time <min>	rate 3a feed: 1.57 kg/hr	rate 5a feed: 1.57 kg/hr	differ. run 5a-3a by <%>	rate 3b feed: 9.43 kg/hr	rate 5b feed: 9.43 kg/hr	differ. run 5b-3b by <%>
15	4.71	0.44	-90.7	2.41	2.45	1.7
30	0.92	0.13	-85.9	0.85	0.94	10.6
60	1.08	0.14	-87.0	0.85	1.25	47.1
90	1.79	0.17	-90.5		0.94	
103	1.09	0.18	-83.5		0.97	
120	1.09	0.19	-82.6		0.94	
150	1.22	0.19	-84.4			
180	1.32	0.19	-85.6			

time <min>	rate 3c feed: 28.3 kg/hr	rate 5c feed: 28.3 kg/hr	differ. run 5c-3c by <%>	rate 3d feed: 33 kg/hr	rate 5d feed: 33 kg/hr	differ. run 5d-3d by <%>
15	3.14	3.56	13.4	5.50	2.82	-48.7
30	3.04	1.65	-45.7	3.64	2.39	-34.3
60	2.28	1.98	-13.2	3.39	2.43	-28.3
90	2.24	1.80	-19.6			
103	2.87	1.80	-37.3			
120	1.53					
150	3.49					
180	2.56					

time <min>	rate 3e feed: 9.43 kg/hr	rate 5e feed: 9.43 kg/hr	differ. run 5e-3e by <%>
15	0.52	0.82	57.7
30	0.63	0.82	30.2
60	1.04	0.82	-21.2
90	0.82	0.85	3.7
103	0.83		
120	0.93		
150	0.85		
180	0.85		

*rates given in kg/hr

20-minute intervals in run 3d and run 5d. Several authors traced the path of these sediment bulks in pool-riffle systems over time and tried to predict mean pulse intervals and relate them to bedform dimensions (see discussion section in Whittaker, 1987 and in Tacconi and Billi, 1987). From the results of this study, it could be concluded that at higher discharges pulses occur in shorter time intervals than at lower discharges. Figure 25 illustrates one reason for the occurrence of these transport rate-pulses. In the case of run 3e (2.77 l/sec), the change in pool shape is traced over time. Under steady sediment supply the pool, which was scoured during high flow conditions, started to refill. The additional sediment first accumulated as a bulk at the deepest spot in the pool (see 'bed after 5 min' in Figure 25). As time proceeded, the bulk was built up higher and higher and moved downstream. When the end of the pool was reached (the pool had filled to its 'equilibrium' scour hole), the whole sediment bulk was split into smaller units which kept on moving further downstream as sediment waves. These waves, trapped in the sediment catcher at the outlet of the flume, resulted in higher bedload transport rates. The movement of sediment waves has been reported by Whittaker (1987). He argued that bulk inputs of sediment were quickly spread into long low waves. In this experiment, the sediment waves were not restricted to bulk inputs but occurred under steady sediment input conditions. As pointed out by Reid (see discussion section in Whittaker, 1987) it is likely that the magnitude and frequency of sediment pulses varies in a natural system from river

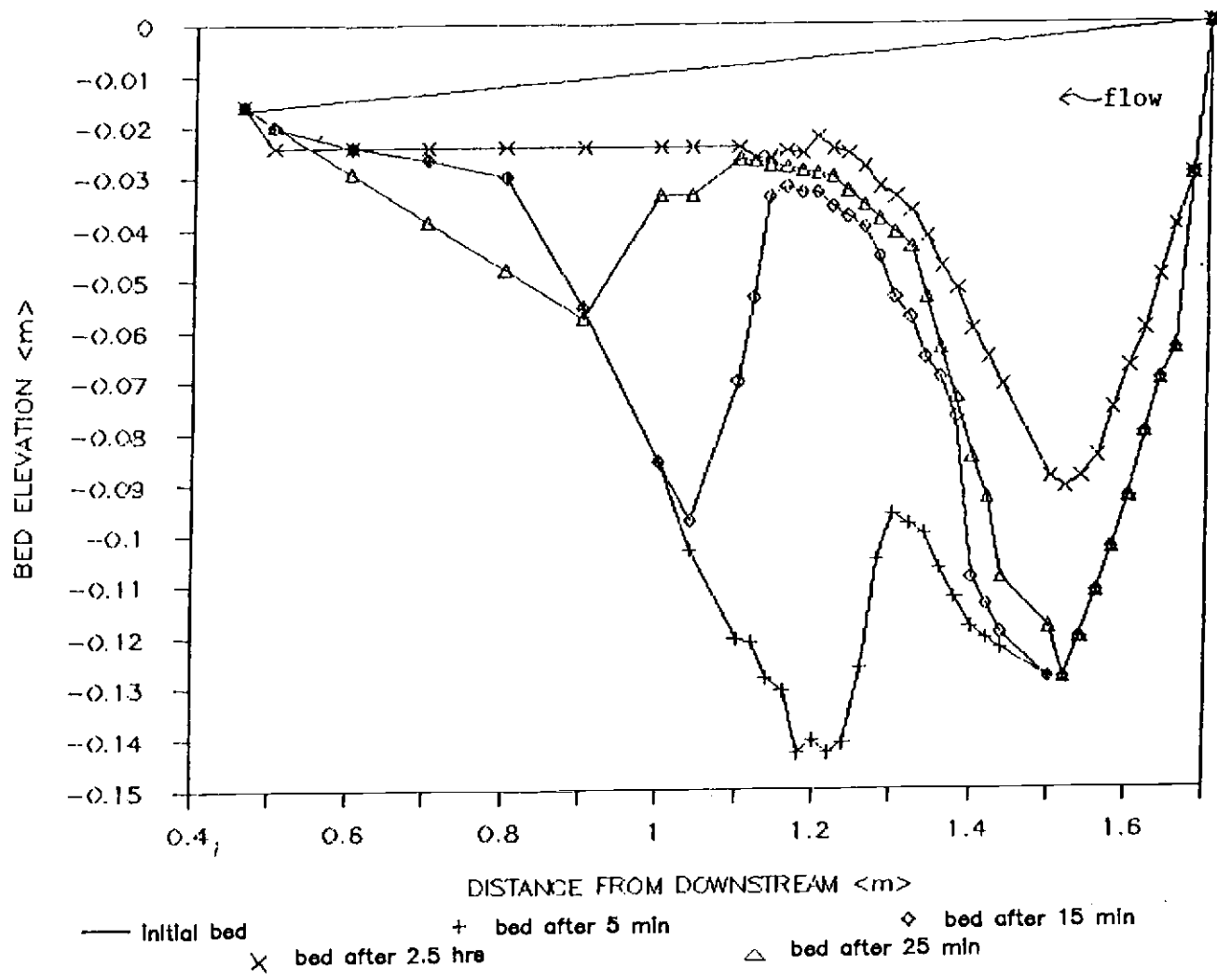


Fig. 25. Composite scour shapes for run 3e

to river. The task of finding some 'common' values will, therefore, often be unsuccessful.

In the sediment experiments, differences between armoured and non-armoured bed material could not be identified. However, it seems to be highly speculative to exclude such differences. Higher percentages of larger particle sizes in the bed material mixture could alter conditions completely.

The question then arises how the armouring effects can be explained with regard to the characteristics of the chosen sediment mixture in the experiments. First, several conditions have to be checked which allow the formation of an armour layer in the first place. Sutherland (1987) reviews the various suggestions of hydraulic 'prerequisites' for armouring processes to occur: the geometric standard deviation of the bed material, for example, is suggested to be greater than 1.5; or the ratio D_{95}/D_5 should be greater than 5; Shields parameters for the D_{75} should not exceed 0.05; flow conditions should be between the limiting conditions of the least resistant particles and those of the most resistant particles; and so forth. The available sediment mixture in this study ($D_{50} = 3.3$ mm) ranges around the limiting values proposed by some authors:

- ratio $D_{95}/D_5 = 6 \text{ mm}/2.3 \text{ mm} = 2.6$ (not > 5)
- T_* for D_{75} (4.5 mm) = 0.055 (not < 0.05)
- comparison of the flow conditions for the least (1.1 mm) and the most (6.25 mm) resistant particles.

This comparison is difficult to approach, since critical values for various hydraulic parameters could be examined. In the case of this sediment mixture, the bottom velocities (very detailed measurements) can be considered for comparison as shown in Table 11. Critical shear velocities for incipient motion were approximated based on the Shields diagrams (there are difficulties in doing this, however, because the Shields approach uses average properties at a section). The resulting value for the smallest particles was 0.025 m/sec and that for the largest particles was 0.08 m/sec. As can be seen in Table 11, the critical shear velocities were just exceeded by the bottom velocities at the lowest discharge for both particle sizes. At higher discharges the bottom velocities stayed around zero. The low velocities at high flows provide the hydraulic conditions for armour layer formation. This might explain why coarsening of the upper sediment layer occurred by the washing-out of the fines. Another important factor that define incipient motion conditions is the tractive force exerted on the pool.

Table 11. Bottom velocities for a heterogeneous clearwater bed

Run	discharge <l/sec>	range of bottom velocities <m/sec>
4a	1.27	0.100
4b	2.92	0-0.086
4c	5.10	0
4d	7.60	0

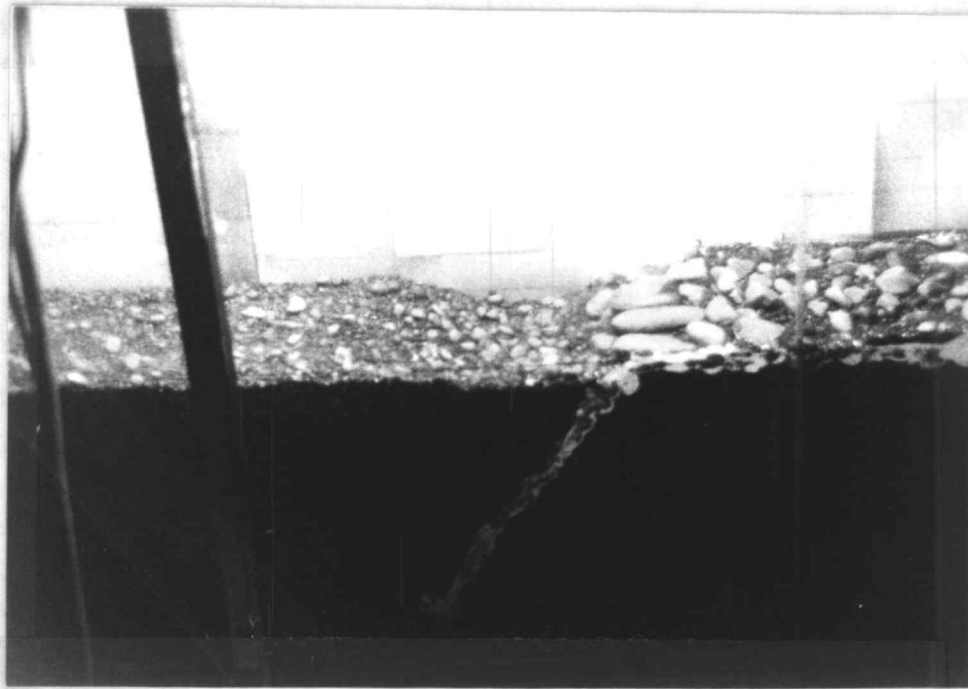
The tractive force could not be measured and the approach of using the mean shear stress did not seem appropriate under the gradually varied and rapidly varied flow conditions. Smaller turbulence, however, is assumed at lower discharges (observation of the 'needle fluctuation' at the velocity measuring device lead to this qualitative conclusion). This could be the reason why an extremely coarse pool surface was identified at the lowest discharge, even though the bottom velocities were at the entrainment limit.

Summarizing the considerations about 'prerequisites' for armouring processes, simple ratio approaches do not seem to describe the phenomenon sufficiently. The more general suggestion seems to apply that the hydraulic conditions should be between the limiting values for the smallest and the largest particle.

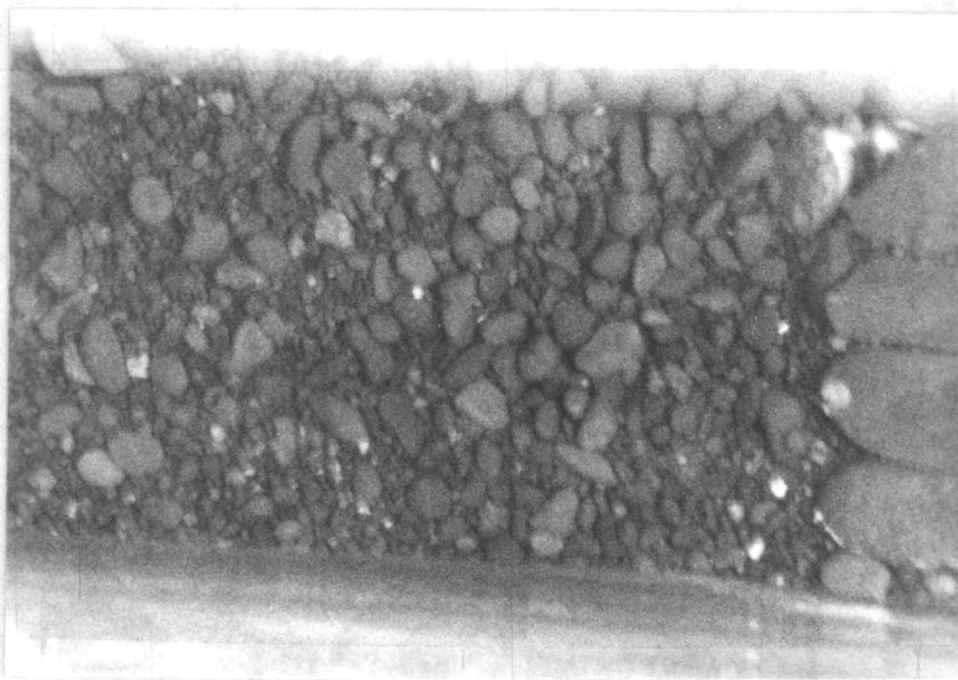
The small discharge seems to provide the right hydraulic conditions for the establishment of an optimal armour layer. This is supported by experimental observations. Figure 26 gives an impression of the exclusively coarse layer in the small pool formed during the lowest discharge step, where the fines were completely washed out.

Relationship between bedload transport rates and maximum scoured volumes

In the past, bedload transport rates were related to various hydraulic parameters such as discharge or maximum scour depth. In this study, a relationship between the maximum scoured volume of a pool at a specific discharge and the bedload transport rate was



top view



← flow

Fig. 26. Armour layer formation at the smallest discharge

established. Values for bedload transport rates were considered after the period of adjustment (preferably the last few measurements), so that a 'pseudo equilibrium' state could be assumed. The scour volume was considered, rather than the maximum 'equilibrium' scour depth, because the maximum depth itself does not give enough information about actual armouring effects in a pool. As I previously showed in the description of the pool shapes, the armoured pool can have a V-shape with a deep maximum depth and still inhibit erosion (indicated by the total scoured volume which was less than in the non-armoured case). Figure 27 illustrates the results for the four runs. Since the highest discharge in the experiment was reached in four steps, only four data points are provided for each run in this analysis. Nevertheless, trends are visible. Scour volume increases approximately linearly with an increase in bedload transport rates. Again, differences between the homogeneous and the heterogeneous bed were significant. In order to analyze the differences, the slopes of the trend curves were compared with each other. In the case of the homogeneous beds (runs 1 and 3), the increase in bedload transport rate with each increase in scour volume is tripled when additional sediment is supplied to the system (slope in run 1 = 0.0077; slope in run 3 = 0.0027). This implies that, in general, higher bedload transport rates can be expected in a riffle-pool-riffle system when sediment is supplied from upstream. The slope in the armoured clearwater case (0.032 in run 4) is even four times steeper than in the non-armoured (0.0077 in run 1). At the highest discharge, the total scoured volume in run 4 is approximately 10 % less than in run 1

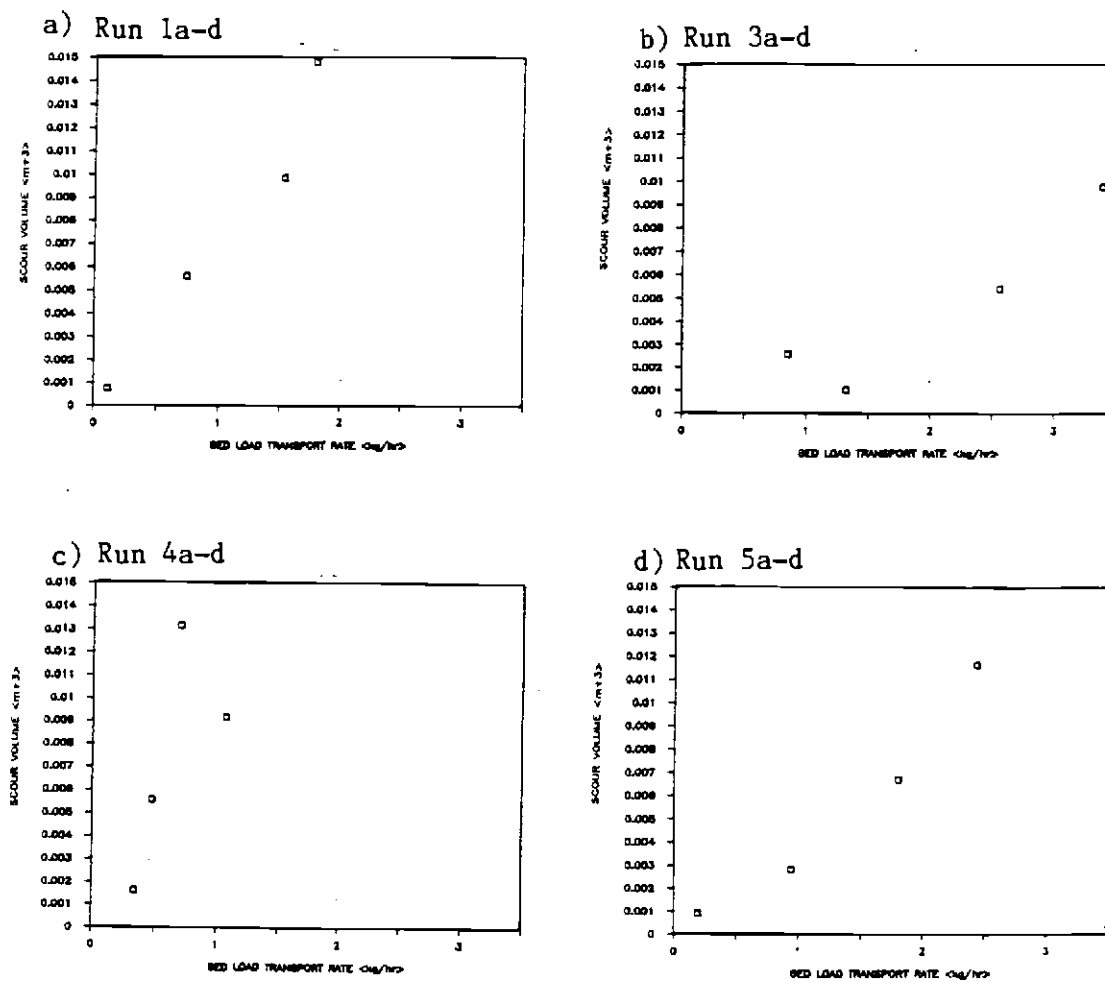


Fig. 27. Bedload transport rates vs. total scour volume over the range of discharges for runs 1, 3, 4, 5

(0.0132 m^3 , 0.0148 m^3). This leads to the conclusion that sediment stays in the system rather than being eroded. As already mentioned earlier, differences between the non-armoured bed (run 3) and the armoured bed (run 5) could not be identified so clearly when sediment was supplied at a steady rate. The total scoured volume was not decreased in the armoured bed. However, taking the slopes for comparison, it can be seen that the steeper slope in run 5 (0.0047, in comparison to 0.0027 in run 3) indicates lower bedload transport rates throughout the discharge steps.

Competence Reversal

An objective of this study was to investigate some hydraulic parameters which were used in field studies to explain the competence reversal hypothesis. The hypothesis tries to explain areal sorting mechanisms of bed material in pool-riffle systems. During a wide range of flows, mean velocities and shear stresses in pools are smaller than those on riffles. Larger particles are, therefore, entrained on the riffle and deposited in the pool. However, at low flow conditions, larger particles are often found deposited on the riffle, while the pool surface is characterized by finer bed material. The 'reversal' in hierarchy of shear stress values and velocities was suggested as one reason for this observation. Higher bottom velocities (Keller, 1971) or mean velocities (Richards, 1978) in the pool than on the riffle were suggested to be responsible for the

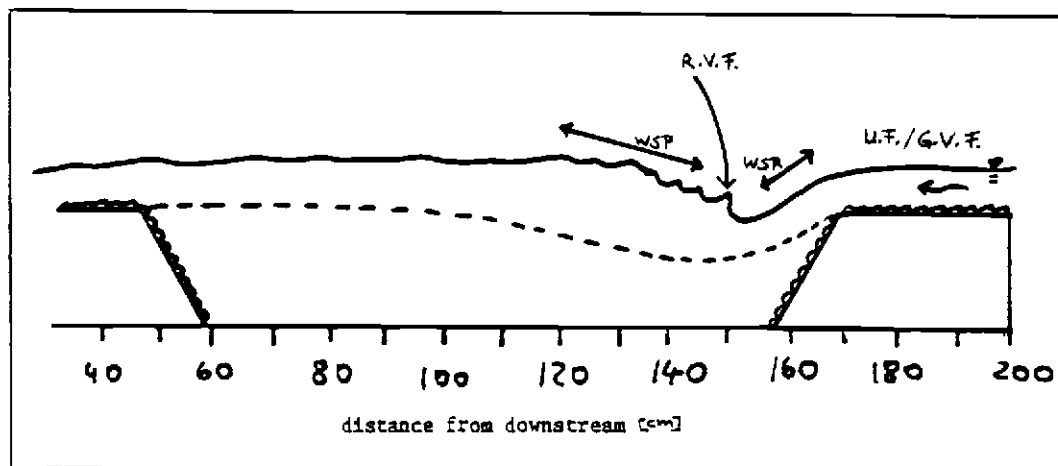
routing of larger material through the pool onto the riffle. Mean shear stresses in pools and on riffles were also compared over a range of discharges in order to find out whether the shear stress in the pool exceeds that on the riffle at certain discharges (Lisle, 1979). Detailed descriptions of individual studies on this subject were given in the literature review.

The results of the findings during this study are presented in the following sections and compared to ideas given in the literature. The first section presents the basic hydraulic characteristics in the pool and on the riffle in the context of the discharge magnitude and the changed parameters in the different runs. This leads to a basic understanding of the hydraulics in the modelled riffle-pool-riffle sequence. The second section traces the behaviour of velocities over four discharge steps during the simulated hydrograph. Velocity reversal never occurred during the experiments. Possible explanations are given referring to findings in the literature and to limits of the experimental apparatus. In the third section, considerations about the analysis of mean and bottom shear stresses lead to a comparison of results in this flume study with results obtained in field studies.

Hydraulic characteristics of the modelled riffle-pool-riffle sequence

The first important characteristic of the flume study was the gradually-varied to rapidly-varied steady flow in the studied riffle-pool section. For gradually varied steady flow, the depth varies

gradually along the length of the channel, the hydraulic characteristics at any point remain constant over the time interval under consideration ("steady") and the streamlines are practically parallel. For rapidly varied steady flow, there is a very pronounced curvature of the streamlines. The flow profile might be virtually broken, resulting, for example, in hydraulic jumps which serve as energy dissipators (Chow, 1959). The occurrence of gradually varied and rapidly varied flow situations is more typical of natural stream systems than is the often-modelled steady uniform flow. Especially in natural pool-riffle systems, these flow characteristics are predominant during a large range of flow conditions. Figure 28 illustrates the general appearance of the flow in this flume study throughout the chosen range of discharges. At higher flows, gradually varied flow (G.V.F.) occurred on the riffle in the form of a gently sloping water surface, whereas rapidly varied flow (R.V.F.) was present immediately below the upstream riffle. A hydraulic jump was found below the upstream riffle and acted as an energy dissipator. The main picture of the flow situation did not change over the range of the discharges. The riffle-pool-riffle sequence in the model was never completely submerged, a condition which occurs frequently in nature at high flows (see Figure 2 in Chapter II). This limitation was caused because of the limited flume discharge possible.



WSR = water surface slope above riffle

WSP = water surface slope above pool

U.F. = uniform flow

G.V.F. = gradually varied flow

R.V.F. = rapidly varied flow

 = fixed riffles

 = boundary of movable bed

 = direction of flow

Fig. 28. Flow conditions during the experiments

Froude number

Figure 29 shows the variation of the Froude number at the section of deepest pool depth and on the riffle. The Froude number — the ratio of inertial forces to gravity forces -- explains the effect of gravity upon the state of flow. The equation for calculation of Froude number is the following:

$$Fr = V/(gD)^{1/2} \quad [4-1]$$

where:

V = mean velocity (here:0.6 depth velocity) [LT⁻¹]

g = gravitational acceleration [LT⁻²]

D = hydraulic depth [L]
(cross sectional area of the water normal to the flow divided by the width of the free surface)

If Fr is less than unity, the flow is called subcritical; the gravity forces are more pronounced. If Fr is equal to unity, the flow is said to be in a critical state. If Fr is greater than unity, the flow is called supercritical.

In Figure 29 it can be seen that the Froude number on the riffle was larger than in the pool and generally increased with increasing discharge while the Froude number in the pool showed various tendencies. Froude numbers in the pool always stayed below those on the riffle. At high discharges, the Froude number on the riffle reached or exceeded unity and the flow became supercritical. At the interface between the fixed riffle (coarse gravel) and the pool (finer material), the flow profile was interrupted with a weak hydraulic

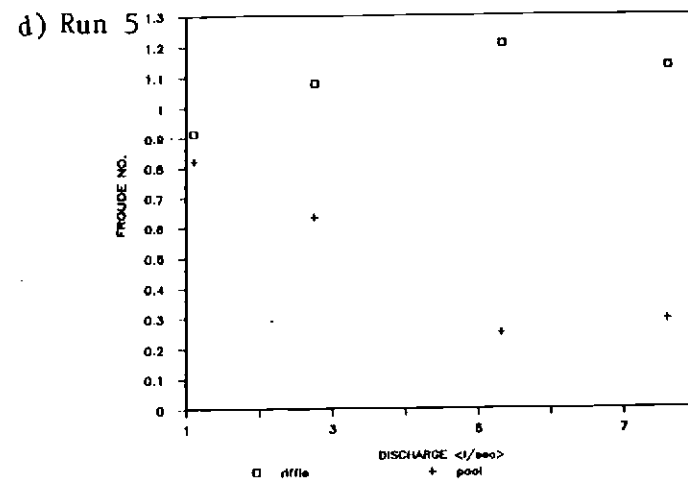
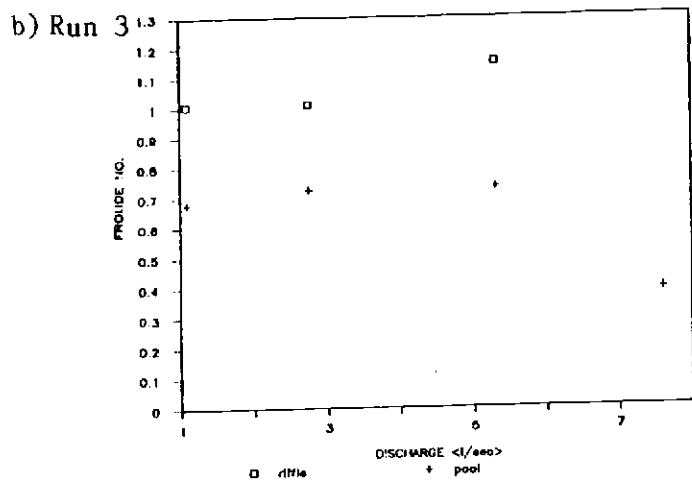
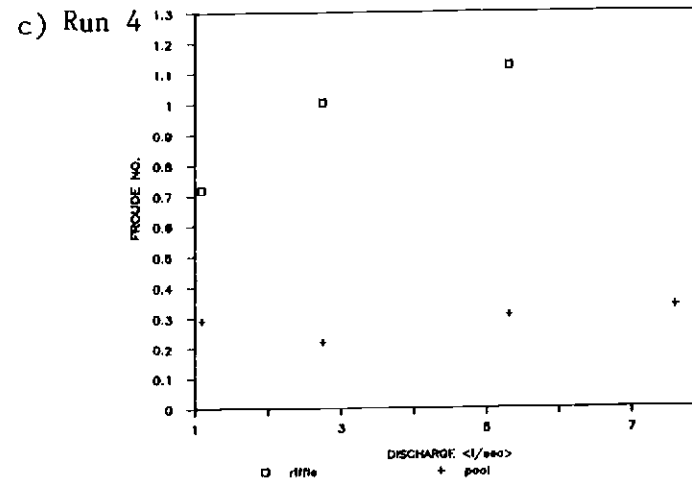
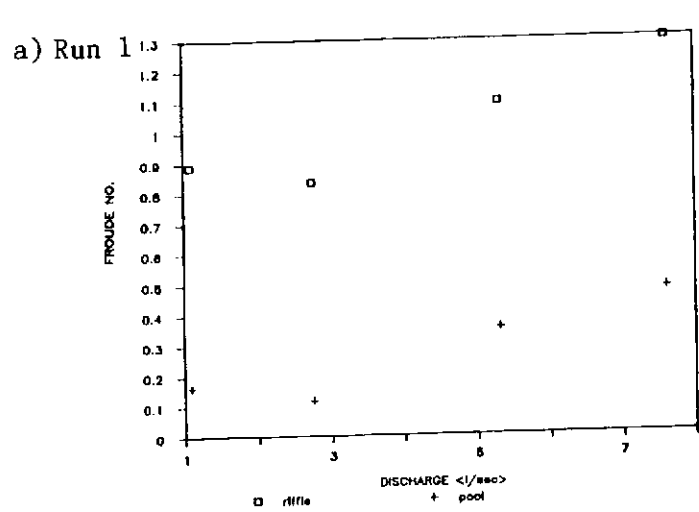


Fig. 29. Change of Froude numbers in pool and on riffle

jump, which caused a local zone of energy dissipation at the upper end of the pool.

Since the Froude number on the riffle ranged around unity (the highest value was 1.3) the hydraulic jump above the pool bed could be considered as an 'undulating jump' with weak effects on the downstream water surface; this represents the weakest form of a jump and should, therefore, not have affected the hydraulic results (Chow, 1959).

Hydraulic radius

In this study, as in nature (see Lisle data, 1979), the hydraulic radius of a pool always exceeded that of a riffle. This is because a pool usually has a constantly larger depth over a range of discharges. The hydraulic radius is calculated with the following equation:

$$R = A/W_p \text{ [L]} \quad [4-2]$$

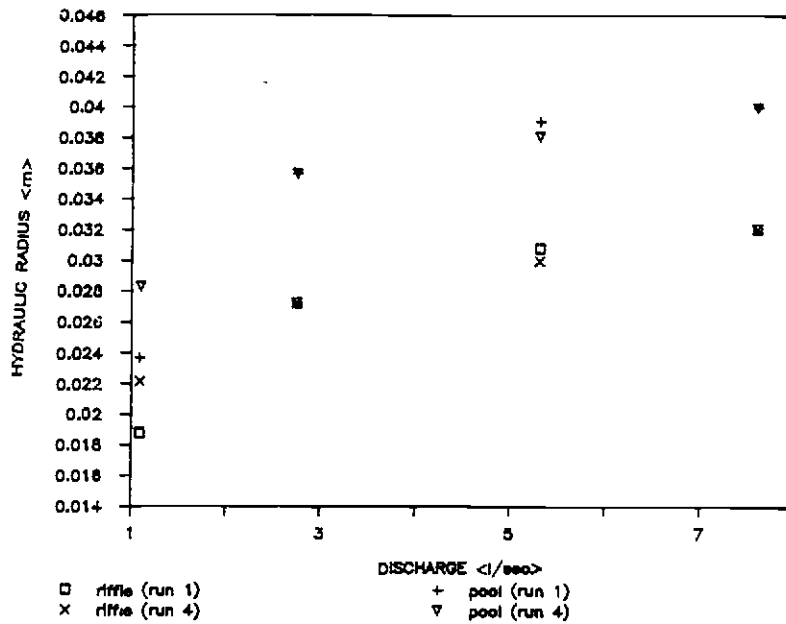
where:

A = cross sectional area [L^2]

W_p = wetted perimeter [L]

Figure 30 illustrates the variability in hydraulic radius in the pool and on the riffle over the different discharges. Figure 30a superimposes the hydraulic radius of the homogeneous-bed (run 1) and heterogeneous-bed (run 4) clearwater experiments. Figure 30b shows the homogeneous-bed (run 3) and heterogeneous-bed (run 5) experiments with sediment feed. Increases are proportional to the discharge, but occur at similar rates in pool and riffle.

a) Comparison of runs 1 and 4



b) Comparison of runs 3 and 5

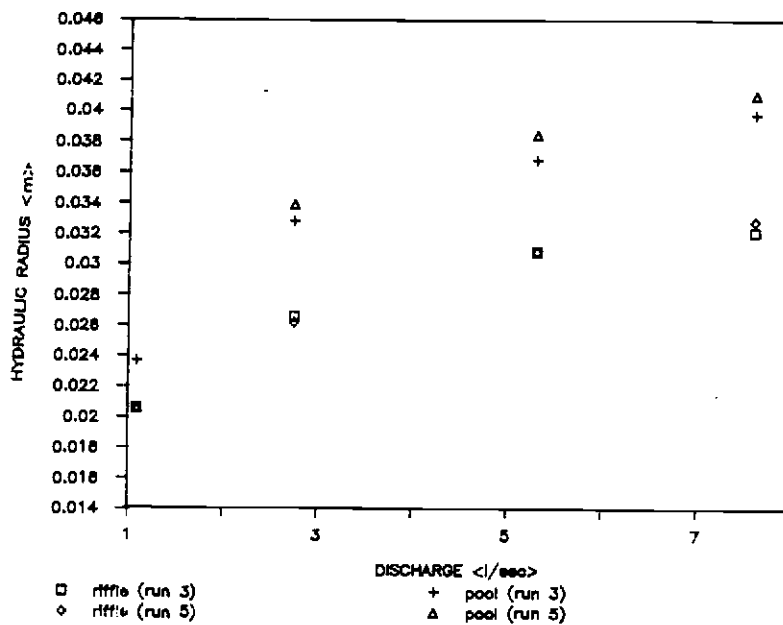


Fig. 30. Change of hydraulic radius in pools and on riffles

Velocity reversal

Detailed velocity profiles recorded during the experiments in this study give insight in the magnitude of the bottom and mean velocities over a range of discharges from 1 to 7.78 l/sec. Comparisons were made of velocities at different depths to find a possible riffle/pool velocity reversal relation. According to suggestions in the literature that mean velocities would be reversed in the pool and on the riffle, the mean velocities in the pool and on the riffle were used for the analysis. Measurements of velocities under field conditions mostly consider the velocity measured at 0.6 of the total water depth to represent the 'mean' velocity for a velocity profile. As already shown in the previous section about bed morphology changes, velocity profiles in pools cannot always be described by a logarithmic approach. The logarithmic profile, however, is the common basis for the choice of the 0.6-depth velocity as the representative 'mean' velocity. To check whether the choice of the arithmetic mean or the 0.6-depth mean of the velocities influences the outcome of the investigation, both types of 'mean' values were considered in this analysis.

1. The arithmetic mean was calculated from the velocity profiles on the riffle and at the deepest section of the pool and graphed versus discharge. The resulting trends are presented in Figure 31. The mean velocities in the pool stayed below those on the riffle at all discharges. The mean velocities on the riffle linearly increased with flow while the velocities in the pool did not show such a regular

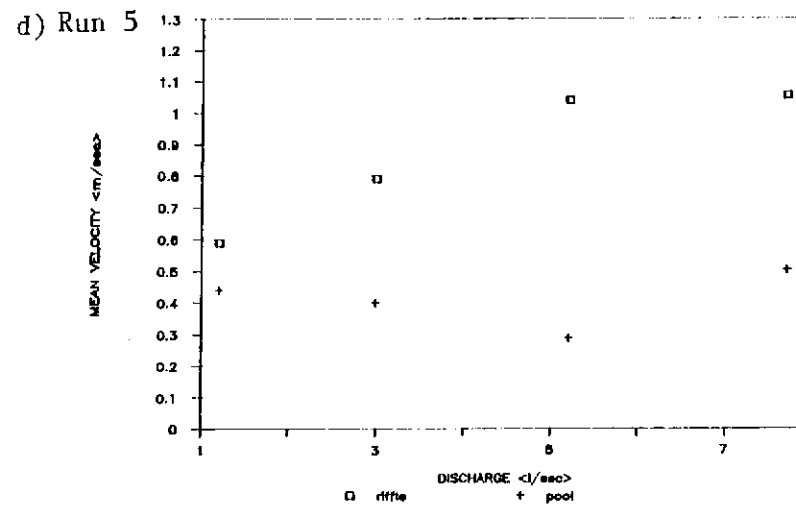
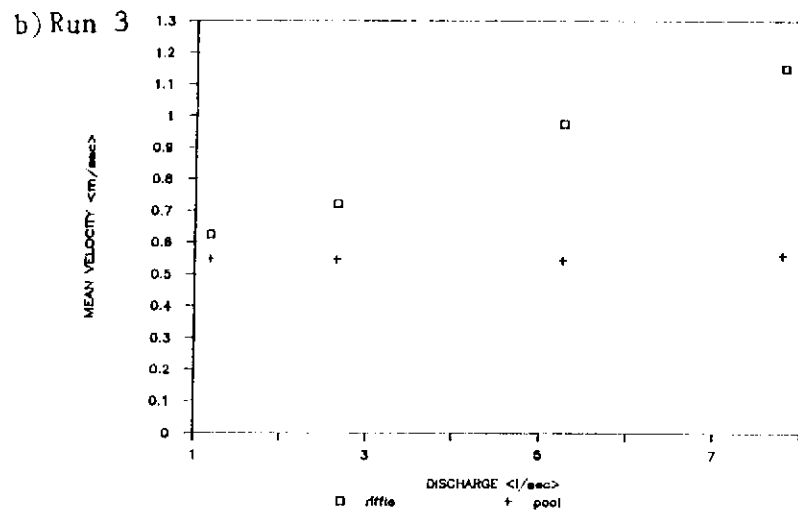
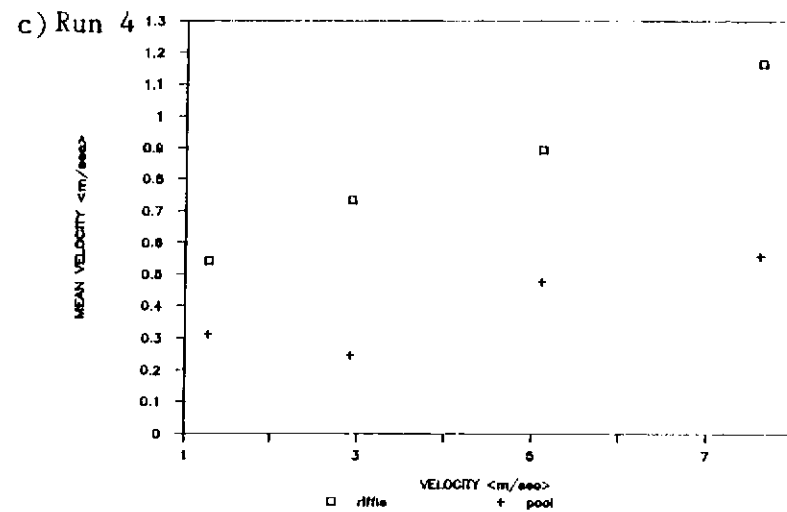
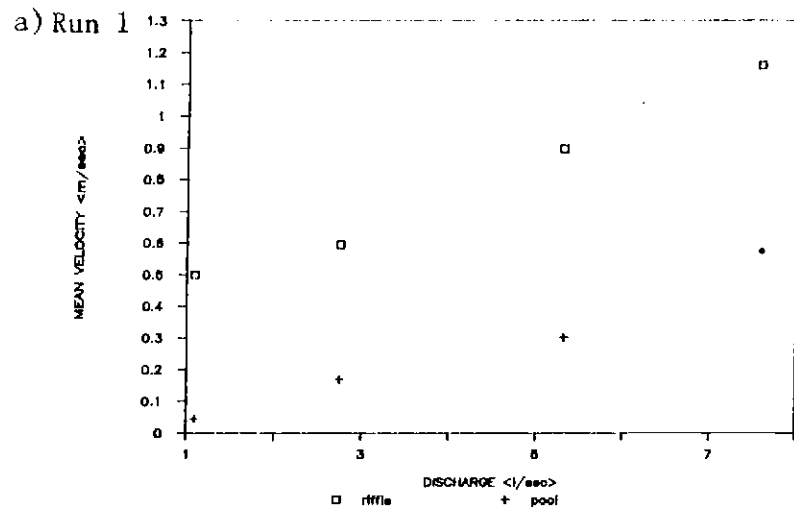


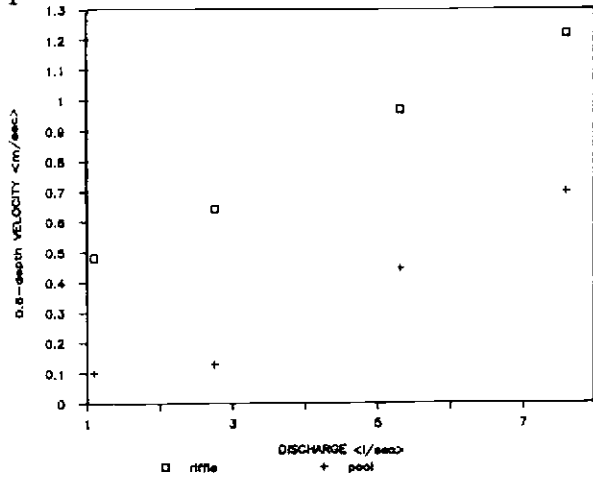
Fig. 31. Change in arithmetic mean velocities in pool and on riffle

pattern. Under steady sediment feed (runs 3 and 5), mean velocities in the pool seemed to roughly constant over the range of discharges: in the case of the homogeneous bed with sediment feed (run 3) this value was around 0.55 m/sec; in the case of the heterogeneous bed (run 5) this value was around 0.43 m/sec. This indicates very well that the arithmetic mean does not describe the hydraulic characteristics in a pool in an appropriate way. Negative or zero velocities near the bottom and higher velocities towards the water surface might 'cancel' each other in calculations of the mean. Local effects of higher velocities might be masked as well. The effects of increased discharge on mean velocity in the clearwater experiments (run 1 and run 4) showed similar patterns. A parallel trend can be concluded, meaning that the increases in bottom velocities in pool and riffle take place at similar rates.

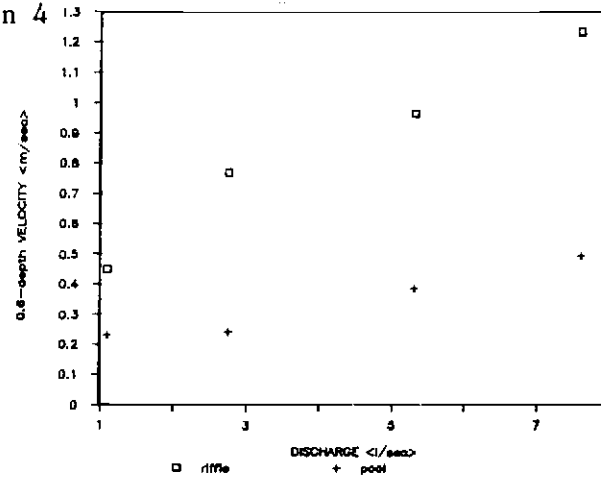
2. The 'mean' velocities obtained at the 0.6 depths at corresponding pool and riffle locations show similar tendencies. This is shown in Figure 32. Velocity reversal never occurred under this range of discharges. The 0.6-depth velocities on the riffle generally increased linearly. The values of the pool velocities in the clearwater experiments (runs 1 and 4) showed an increase parallel to the increase of the riffle velocities. In the case of the sediment feed experiments (runs 3 and 5), the pool velocities fluctuated throughout the range of discharges. A straight line approach does not seem appropriate for these four scattered data points.

Hence, in neither of the above comparisons could velocity reversal be concluded by taking any 'mean' for velocity values.

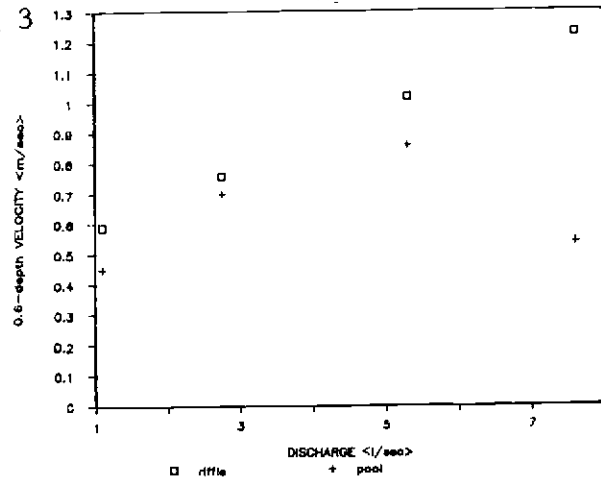
a) Run 1



c) Run 4



b) Run 3



d) Run 5

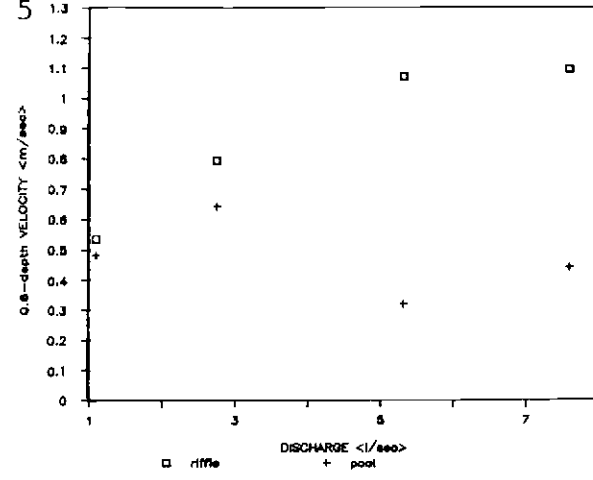


Fig. 32. Change in 0.6-depth 'mean' velocities in pool and on riffle

Since Keller (1971) measured velocities at distances of 0.05 ft (1.5 cm) above the stream bed, bottom velocities obtained in this experiment in the pool and on the riffle were analyzed next for further comparison. Results are given in Table 12. Throughout the whole set of experiments, bottom velocities in the deepest part of the pool never exceeded the bottom velocities on the riffle. This was true considering the bottom velocities measured at the deepest location in the pool as well as for values at any other location along the pool. Very small velocities (negative values or zero) were

Table 12. Bottom velocities in pool and on riffle

Run	bottom velocity in riffle <m/sec>	bottom velocity in pool <m/sec>
1a	0.482	0.102
1b	0.504	-0.086
1c	0.750	-0.171
1d	0.911	-0.150
3a	0.589	0.429
3b	0.536	0.268
3c	0.857	0.214
3d	0.857	-0.107
4a	0.450	0.107
4b	0.589	0.000
4c	0.804	0.000
4d	0.964	0.000
5a	0.536	0.482
5b	0.750	0.214
5c	0.857	0.643
5d	0.964	0.000

typical for the pool bottom, even up to the highest model discharge of 7.8 l/sec.

Summarizing the results concerning velocity behaviour in the pool and on the riffle over a range of discharges, it can be said that a reversal in hierarchy of velocity values did not occur in these experiments. The choice of whether to use mean values or bottom values did not affect the general trends. While velocities on the riffles increased linearly with increasing discharges, pool velocities were subject to more complex processes. For example, secondary currents and changing directions of the water flow within the pool resulted in very scattered values for velocities measured at similar depth intervals at different discharges. Straight line approaches to fit the data would be speculative. Figure 33 qualitatively illustrates some major flow directions in the pool at different depths.

One further reason why velocity reversal did not occur in the experiment, however, might be the choice of the discharges. The highest discharge (7.78 l/sec) might have still been too small to induce a reversal. The fact that the riffle-pool-riffle feature in the flume was never completely submerged might be the reason that the flow conditions necessary for reversal were never reached.

Considerations about shear stress reversal calculations

'Competence' reversal, possibly occurring at specific discharges, can be described by other hydraulic parameters than only velocities.

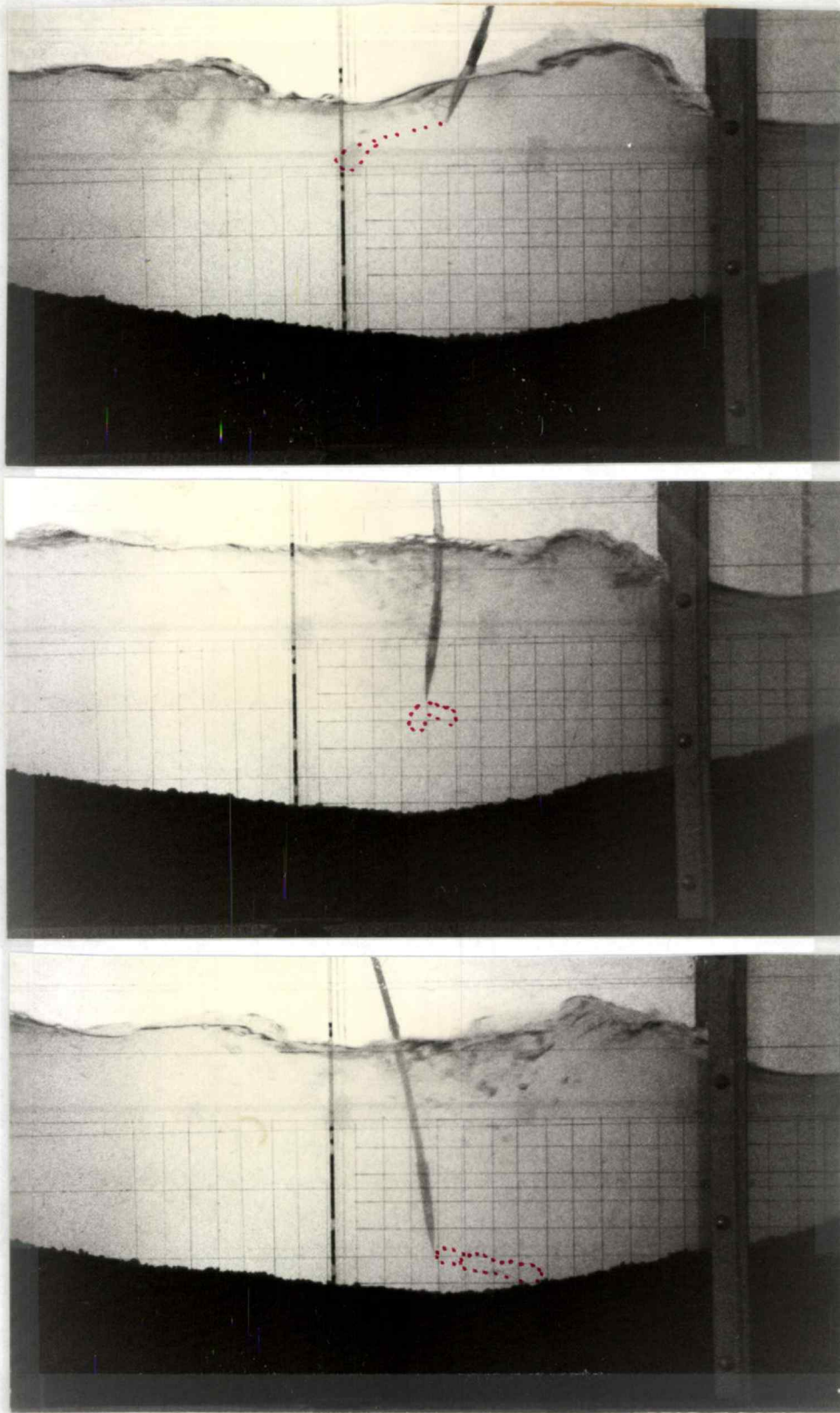


Fig. 33. Flow visualization in the pool at different depths
(flow from right to left; discharge: 5.1 l/sec)

25% COTTON FIBER

1.5 A

Shear stresses (bottom or average) are the most widely accepted parameters responsible for particle entrainment. Three ways of computing the boundary shear stresses are presented in the following paragraph: 1) calculation of the average boundary tractive force; 2) calculation of local shear stresses with local velocity profiles; and 3) calculation of local shear stresses using the assumption of a quadratic relationship between shear stress and mean velocity. These computational methods are related to the approaches used in the past in field investigations and to the restrictions in this flume study.

Lisle (1979) traced the mean shear stresses in pools and riffles over the range of increasing discharges (see Figure 5 , Chapter II). The general equation for the applicable average unit tractive force τ (average value per unit wetted perimeter) is given by:

$$\tau = \nu RS \text{ [ML}^{-1}\text{T}^{-2}\text{]} \quad [4-3]$$

where:

ν = specific weight of water $[\text{ML}^{-2}\text{T}^{-2}]$

R = hydraulic radius $[\text{L}]$

S = energy slope of water $[\text{L}\text{L}^{-1}]$.

In his field study, Lisle calculated mean shear stresses using the water surface slope over pool and riffle. The question that now arises is if the assumptions on which the choice of the water surface slope are based are still justified in the case of my flume study. In a uniform flow situation in a natural channel, the assumption can be made that the channel bottom slope equals the water surface slope and

the energy slope ($S_o = S_w = S_f$) (Chow, 1959). At high flows which submerge small scale bedforms like pools and riffles, the assumption that $S_w = S_f$ represents a good approach. Recalling the fact that submergence never occurred during the experiments in this study and that a hydraulic jump was present throughout all discharge magnitudes, it was not possible to make this assumption. The occurrence of the hydraulic jump caused the water surface slope of the riffle to remain very steep; the water surface slope of the pool stayed horizontal or, at higher flows, even became inverse because of the stronger influence of the jump (see also Figure 33). Because of the described appearance of the surface flow, water surface slopes could not be taken into consideration for a comparable mean shear stress computation. In addition, it could not be assumed that $S_o = S_f$, since, on the studied micro scale, the bottom slope in the pool changes markedly, even in its sign. These observations lead to the conclusion that the mean shear stress approach of the cited field study could not be applied for the situation in this flume study and therefore did not produce meaningful comparisons with field study results.

In a second approach, I tried to address the shear stress problem by means of the obtained velocity profiles. Four calculational methods are presented in the next paragraphs and their assumptions and limitations related to this flume study are demonstrated. The information was taken from Chow (1959), Gerhart and Gross (1985) and Vanoni (1975):

1. The use of local velocity gradients is a commonly accepted tool in order to translate measured point velocities into bottom shear

stress magnitudes. The shear stress in water under conditions of laminar flow is proportional to the velocity gradient; the constant of proportionality being the dynamic viscosity, μ .

$$\tau = \mu (dv/dy) \text{ [ML}^{-1}\text{T}^{-2}\text{]} \quad [4-4]$$

where:

$$\begin{aligned} \mu &= \text{dynamic viscosity [ML}^{-1}\text{T}^{-1}\text{]} \\ dv/dy &= \text{velocity gradient [T}^{-1}\text{]}. \end{aligned}$$

However, this formula is restricted to a laminar boundary layer; this implies that the stress in this layer is entirely due to viscosity and is constant. The laminar boundary layer is assumed to be very thin, considering the grain sizes of the bed material used in this study. The size of the velocity meter is too large to measure velocities within this layer. In addition, this viscous sublayer must be penetrated or disrupted if particles shall be moved in the first place. Therefore, the analysis of shear stresses in this layer would not be helpful in order to find reasons for the routing of large particles through pools and onto riffles.

2. Shear stress may also be expressed in terms of the usual frictional resistance equation which is applicable for laminar and turbulent flow conditions:

$$\tau = f/4 \rho v^2/2 \text{ [ML}^{-1}\text{T}^{-2}\text{]} \quad [4-5]$$

where:

$$\begin{aligned} \rho &= \text{density of water [ML}^{-3}\text{]} \\ f &= \text{Darcy-Weisbach friction factor} \\ V &= \text{average velocity [LT}^{-1}\text{]} \end{aligned}$$

The friction factor is not known for the situations we are dealing with. This value, obtained from the resistance diagram for flow in conduits (Moody diagram), must be increased by a factor that takes turbulent density currents into account. However, experimental information is insufficient to determine the dependence of this factor on the Reynolds number. Only direct measurement of turbulence near the bottom would help to get the necessary information. Because of the unavailability of suitable measurement devices, such measurements could not be conducted in the present study.

3. The bottom shear stress can also be assumed to be related to the shear velocity in the following manner:

$$\tau = (u_*)^2 \rho \quad [ML^{-1}T^{-2}] \quad [4-6]$$

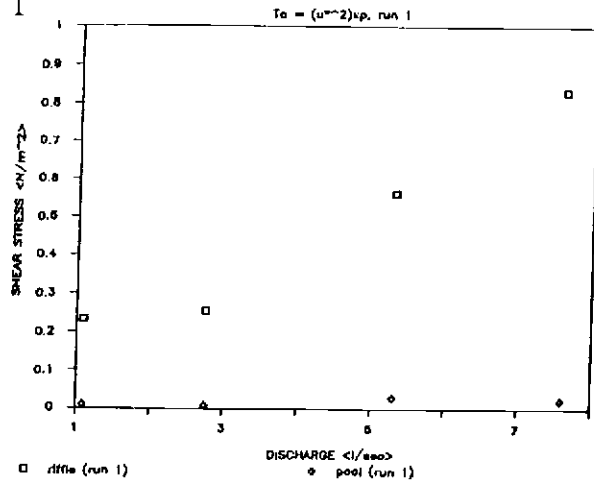
where:

τ = bottom shear stress

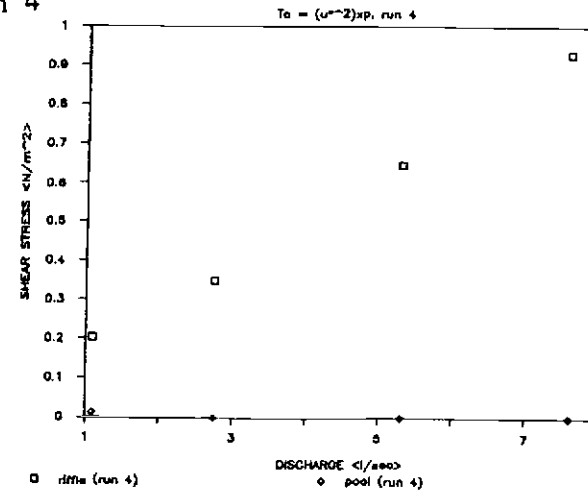
u_* = shear velocity $[LT^{-1}]$.

The gained data from the conducted experiments did not provide information about the real shear velocities within the laminar boundary layer. Assuming, however, that velocities measured close to the bed in different runs give an indication about the relative magnitude of the velocities, the bottom velocities were taken for a brief comparison. Figure 34 relates these bottom velocities to the bottom shear stresses calculated by equation 4-6 (ρ at $20^\circ C = 1 \text{ kg/m}^3$). As can be seen from Figure 34 the values of the bottom shear stresses in the pool never exceed those on the riffle. Even if 'convergence'

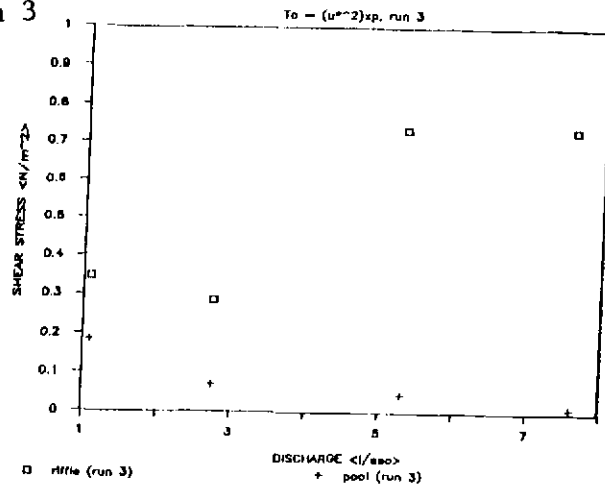
a) Run 1



c) Run 4



b) Run 3



d) Run 5

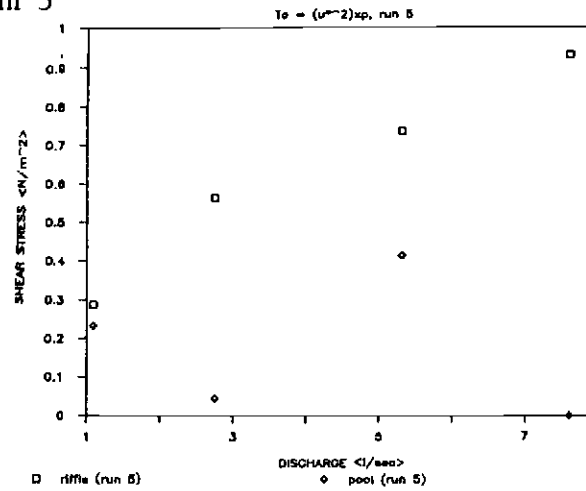


Fig. 34. Bottom shear stresses in pool and on riffle
 $(\tau = u_*^2 \times \epsilon)$

had occurred, this would not necessarily have proved that the shear stresses were converging at the same time. The reason for this is the fact that the magnitude of bottom shear stresses is influenced more by instantaneous stresses caused by turbulence than by the time-averaged velocities. These stresses are called Reynolds stresses and cannot be evaluated from viscosity and velocity gradients. The following paragraph explains the theoretical treatment of these stresses.

4. Assuming a full development of the turbulent boundary layer in uniform channel flow equation 4-7 represents another approach method:

$$\tau_{app} = \rho l^2 (dv/dy)^2 \quad [ML^{-1}T^{-2}] \quad [4-7]$$

where:

$$\tau_{app} = \text{time-averaged instantaneous apparent shear stress due to turbulent momentum transport } [ML^{-1}T^{-2}]$$

l = a characteristic length known as the mixing length, which must be determined in the experiment [L].

The deficiency of turbulence measurements in this study (and therefore also mixing length) does not make the use of this formula possible. The formula also assumes uniform flow, a condition which would not apply in the case of the highly non-uniform pool sections.

The different shear stress approaches introduced above turned out to be not really applicable for the problem under consideration. The only approach which can give reliable data and enhance further knowledge about transport mechanisms in small scale systems like pools and riffles is the approach of the apparent shear stress (No.4 above).

The best investigation is doubtless the direct measurement of the bottom shear stresses.

To tie together the results obtained in the bed morphology studies and the hydraulic characteristics of the modelled riffle-pool-riffle sequence, the following chapter provides a summary of the findings. Individual results and basic approaches are then discussed and related to those in the literature.

V. SUMMARY AND CONCLUSIONS

The first objective of this thesis was to investigate hydraulic influences on bed morphology changes in a riffle-pool-riffle sequence. The second objective was to verify hypotheses which state that a reversal in hierarchy of velocity and/or shear stress occurs in a pool-riffle system at discharges near bankfull flow. The objectives have been partly accomplished. Hydraulic influences on the bed morphology could be identified qualitatively and, to some degree, quantitatively evaluated. Reversal of the magnitude of velocities or tractive forces did not occur during the modelled discharges in the experiments.

Results of the flume study were presented under two major considerations related to the two objectives: bed morphology changes were quantified and analyzed. Second, results relating to competence reversal theories introduced in the literature review were presented and problems which arose in their analysis and interpretation were discussed. The following two paragraphs summarize and discuss the main findings under these two headings.

Bed morphology changes

Clearwater experiments revealed that the formation of an armour layer in a riffle-pool-riffle sequence with heterogeneous bed material affects the final shape of a pool as well as the bedload transport

rate through this system. Information on the maximum scour depth alone does not seem satisfactory to quantify the protective effect of the armour layer. Deep local scour could be identified due to the only partly-armoured bed surface which deflected and concentrated the shear forces at specific points. These results match findings by other researchers (see Chapter IV). In this study, the volume of scoured bed material in the armoured pool was around 10% less than for the non-armoured bed (see Table 6). The 'equilibrium' scour pools in the armoured bed (run 4) were V-shaped in horizontal distance while the non-armoured pools showed a U-shape longitudinally (see Figure 11). Bedload transport rates at the non-armoured bed increased with increasing discharge. The maximum rates for this homogeneous bed (run 1) were around 2 kg/hr, while the maximum rates for the heterogeneous bed (run 4) did not exceed 1.2 kg/hr (see Figure 22).

When sediment was supplied from upstream at a steady rate, the system had to find its new 'equilibrium' scour depth in accord with the energy consumed to transport sediment. Pools were shallower, because the limiting erosional capability was reached earlier. The total scoured volume in a homogeneous bed under clearwater conditions was up to 15 times greater than the scoured volume for a bed subject to sediment supply from upstream. This extreme difference occurred on the recession limb of the simulated hydrograph. Under clearwater conditions, the scour shape developed at high flow was maintained during the receding discharges. On the other hand, steady sediment supply on the recession limb caused the pools to fill in again until equilibrium was reached between sediment availability and erosional

capability. Recession-limb sediment feed rates similar to those during the rising limb of the hydrograph (which, in nature, would correspond to similar bedload transport from upstream) result in exactly the same 'equilibrium' pool shapes at similar discharges. The protective effect of an armour layer was not as evident in the sediment feed experiments as in the clearwater experiments. Even though coarsening of the upper layers could be identified, the conditions did not allow any obvious stable armour layer configuration. The larger particles of the heterogeneous mixture fed into the system caused additional shearing or impact forces which led to the immediate destruction of any prior armour layer. These results lead to the conclusion that the chosen sediment mixture only allowed relatively stable armour layer formation under certain limiting hydraulic conditions and that these conditions were exceeded in the experiments most of the time.

Bedload transport phenomena were investigated as well. Under steady flow conditions bedload transport was unsteady. The highest bedload transport rates were measured during the first hour of each run. After a time period of adjustment, the rates reached an 'equilibrium' state but differed from run to run, depending on the bed material and the sediment supply condition. In general, bedload transport rates in the runs with the homogeneous bed material were higher than in runs for heterogeneous beds. The protective effect of the armour layer became more important at higher discharges; in the clearwater experiments, decreases in bedload output rates by 70% (run 1d/4d, see Table 9) could be identified. During the experiments

with sediment feed, these differences were not so obvious; scoured volumes in the homogeneous and heterogeneous bed were equal. The armour layer might have been disturbed by the larger particles in the case of a heterogeneous sediment supply from upstream. This caused deeper pool scour. Another explanation may be that the formation of an armour layer in a natural stream system can require an appreciable amount of time. Reported laboratory experiments with a long flume continued for more than 50 hours before the size distribution of the armour layer stabilized; a 10-year period is reported for a natural stream (Andrews and Parker, 1987). The time of the experiments reported here (3 hours for each discharge step) might not have been long enough to make the effects visible. However, the final vertical profile through the bed after run 5 indicates that a coarsening of the upper gravel layer took place (Figure 20 and Figure 21).

Bedload transport rates after 'equilibrium' was reached were related to the final scour volumes and revealed the following difference between armoured and non-armoured beds: similar total scour volumes were associated with lower transport rates in the armoured and the non-armoured bed. Pulse-wise bedload transport was typical for the experiments with sediment feed. Several authors reported similar results and suggested explanations for the measured and observed pulse-wise transport (Beschta, 1987; Hayward, 1980; Klingeman and Emmett, 1982; Whittaker, 1987; Tacconi and Billi, 1987). Frequencies of passage of bedload bulks through the system could be identified for the two highest discharges; 30-minute intervals for discharges around 5 l/sec and 20-minute intervals for discharges around 7.7 l/sec.

Since frequencies and magnitude of bedload pulses vary under different hydraulic and morphologic conditions, however, it is difficult to find general predictive formulas for this phenomenon. However, several suggestions for an explanation of this phenomenon can be discussed and evaluated, including the new observations. One reason for sediment pulses was thought to be the poor reliability of the bedload measurement technique — spatial and temporal variation. Differences in the grain size distributions of the caught sediment samples in nature also seem to lead to distortions of the transport rates. Despite the high probability of inaccuracies in bedload measurement techniques, the carefully traced transport rates in this flume study, as well as in others (Whittaker, 1987), reveal that the phenomenon shows some regular pattern in some cases. The movement of sediment 'waves' through the system has been clearly shown by Whittaker and was also observed in this study. The existence of these waves can be initially caused in a natural system by bulk-wise sediment inputs (e.g., by landslides) or by rearrangement within smaller units like pool-riffle sequences, as shown in this study. Grain size distributions of the sediment sampled at the outlet of the flume were not analyzed; nevertheless, the results of the experiment with homogeneous bed material under steady sediment input suggest that pulse detection is not restricted to measurement inaccuracies. Hence, I suggest the following explanation for the presence of measured sediment pulses in a stream system. Measurable sediment pulses -- in intervals corresponding to various hydraulic conditions -- can be concluded for natural systems which provide bedforms on a smaller

scale (pools, riffles, steps, cascades, bars, etc.). Sediment 'waves' are initiated by variable sediment supply or by rearranging actions within the bedform system in order to reach a new 'equilibrium' state with minimum energy. Rather than having been caused by measurement errors, they seem to be 'system inherent' as another way of finding an equilibrium state between sediment availability and erosion capability. Rearrangement of bed material within small scale systems like pools and riffles can also occur in an abrupt manner. When the storage limit in a pool is exhausted or shear forces become larger than the resisting forces of the instable sediment accumulation, an additional sediment input might induce the sudden 'ejection' of the accumulated sediment (an observation made in this study).

Competence Reversal Hypothesis

One major objective of this thesis was to investigate whether or not a reversal in hierarchy of 'competence' to transport large particles through a pool onto a riffle would occur at specific discharges. Hydraulic conditions which define the magnitude of particle entrainment forces were, therefore, examined and analyzed during various flows. The choice of the hydraulic parameters to investigate was also oriented with respect to research efforts in the past, so that results could be compared and discussed. Competence reversal was hypothesized by Keller (1971), Richards (1978) and others who found that at discharges near bankfull the bottom velocities of

the pool approached the values of the riffle velocities. Lisle (1979) verified this hypothesis by a field study while Sullivan (1986) found reversal in some pool-riffle systems but not in others. Competence reversal could not be identified in the present flume experiments.

'Velocity reversal' was not occurring; bottom velocities showed negative or zero velocities at higher discharges. This was also due to the formation of deep scour holes that led to flow reflections at the downstream 'wall' of the pool and directed the flow back upstream. In the experiments with sediment feed, bottom velocities were in general higher than those measured under clearwater conditions; negative bottom velocities were not typical for the sediment feed experiments. On the other hand, changes of flow directions along the vertical velocity profile occurred more frequently during sediment feed experiments than in the clearwater experiments. The more irregular patterns of the flow profiles in the sediment feed experiments are thought to be characteristic for the situation where bedload transport consumes energy at various locations in the pool and bedload bulks are routed quickly through the system. 'Mean velocities' based on the 0.6-depth commonly measured in the field are point measurements in the sense that they do not give appropriate information about the complex vertical flow behavior in a pool. Despite this fact, I tried to provide a comparison to existing field data by calculating mean velocities. In this flume study both the 'mean' velocity at 0.6-depth and the arithmetic mean velocity (averaged over the entire vertical velocity profile) were used for the reversal analysis. Hence, the sensitivity of the results to the

choice of the different means was tested. Reversal did not occur in either case and the scatter of the mean values for the pool revealed two things. First, mean pool velocities do not provide information from which any conclusion or prediction can be made; second, the range of scatter includes a possible 'reversal potential' for the pool velocities under different circumstances. In other words, velocity reversal was not detected in this set of experiments but could as well have 'happened' at larger discharges than tested.

Shear stress reversal as found by Lisle (1979) could not be identified in this study. This was also due to the impossibility of calculating mean or bottom shear stresses given the flow conditions during the experiment. It is not correct to translate time-averaged bottom velocities into shear stresses. Instantaneous momentum exchange could cause spontaneous increases of shear forces above the 'critical' conditions for specific particle sizes. This, however, would not be registered by averaging the velocities over time.

The theory proposed by Bagnold (1954), that the magnitude of repulsive pressure might be responsible for the areal sorting mechanisms in pools and on riffles, was described in the literature review. The theory states that with an increase in concentration, grain diameter, and/or velocity gradient, an increase will result in the repulsive pressure between the grains of two layers. He further stated that the higher velocity gradient at the riffle would result in a higher repulsive pressure on the riffle than in the pool. This will lead to a relative depression of the pool and a relative raise of the

riffle. In this flume experiment, the upstream and downstream riffles were fixed, while the potential scour material between riffles was movable. Relative depression of the pool could, therefore, not be investigated. The amplification of the differences in velocity gradients between the pool and the adjacent riffle could be observed as the scour depths increased. According to Bagnold, this is responsible for further increase of the pressure effect. However, the experimental runs revealed that coarsening of the surface occurred also within the pool. This was mainly observed in the downstream half of the pool. The bigger material was washed out from upstream and also 'cleaned' from fines due to the hydraulic conditions at this location.

The results of the conducted experiments in this flume study in conjunction with already-existing field data lead directly to recommendations for future research. In the next chapter future research is suggested that should be done to enhance the quantification of bed morphology processes in pool-riffle systems. The next chapter also illustrates some implications of the findings in this study.

VI. IMPLICATIONS AND RECOMMENDATIONS

The first section of this chapter describes possible implications of changing hydraulic conditions on natural bedforms in a stream system such as pools and riffles. Implications are mainly considered under the aspect of the conservation of fish habitat. In the second section of this chapter recommendations are made for future research. I concentrate on the investigation of special parameters which could not be studied in this thesis but seem to enhance the knowledge about bed morphology changes in riffle-pool-riffle systems and competence reversal hypotheses in an important way.

Some implications of the research

Conservation of the diversity of fish habitat is a very important activity in the Pacific Northwest, involving multi-million dollar investments each year. Pools and riffles with their differing hydraulic conditions represent two different habitat forms. Major efforts are underway to increase the amount of pool space in streams by artificially 'constructing' pools (using log weirs, for example) or by inducing severe local scour (using deflector structures). Small velocities in the pool at low flow conditions give the pool the potential to act as a settling basin for sediment. Coarse spawning gravel tends to preferentially deposit on the riffles during high-flow bedload transport. There, the fines wash out due to higher bottom velocities (see Chapter IV).

It is necessary to increase the knowledge about the effects of sediment input on the shape of pools and riffles and on bed material composition. Both factors (shape and bed material composition) define the habitat quality for fish. Human activities might alter the habitat configuration and usability of these features. Besides the natural sediment load that a stream carries, additional input into a stream reach can originate from releases from upstream reservoirs. The reservoir functions as a sediment trap with the consequence of a deficit in bedload and suspended load downstream. This leads to increased scour of the stream bed; pools become deeper (short-term time scale) and the stream can degrade (long-term time scale). These effects are comparable to the clearwater scour modelled in this study. Flushing or sediment releases from the reservoir, on the other hand, can backfill the scoured areas. The effects of such measures on pool-riffle features were shown in the sediment feed experiments.

It is important to somehow quantify the scour and deposition processes for bedforms such as pools and riffles. This can, for example, allow one to estimate the effects on fish distribution. When the grain size distribution of the bed material and the degree of armouring in a stream are known approximately, predictions of the degradation or aggradation processes can be made.

Recommendations for future research

Some suggestions for necessary research can be made based on the conducted experiments and the literature review.

One of the next steps regarding the investigation of bed morphology changes in a riffle-pool-riffle system is the additional systematic quantification of these processes.

A modelling approach is suggested which involves a series of experiments that exceed the scope of experiments for this thesis. A predictive model could not be developed in this study, because of insufficient data. In the future, prediction models could be developed by conducting more experiments that cover more hydraulic parameters --such as slope, different grain size distributions for the sediment mixture in the pool, different steady sediment feed rates, different application times for sediment feed, and so forth. A long series of several pools and riffles could provide a physical model so that empirical models could be developed to predict scoured volumes or depths when sediment discharge and grain size distribution are known for a specific reach.

Regarding the investigation of the 'competence reversal' hypotheses, shear stresses and turbulences near the bottom of pools and riffles should be measured in more detail. The quantification of Reynolds stresses within a riffle-pool-riffle sequence might be a big step towards clarification of the 'reversal' question, since local

velocity measurements in the field do not seem to give consistent results. The experiments in this study also revealed that velocities alone do not give enough information to clarify this question.

VII. BIBLIOGRAPHY

- Andrews, E. D. and G. Parker, 1987. Formation of a Coarse Surface layer as the Response of Gravel Mobility. *Sediment Transport in Gravel-Bed Rivers*. John Wiley and Sons: 269-325.
- Bagnold, R. A., 1954. Experiments on a Gravity-free Dispersion of Large Solid Spheres in a Newtonian Fluid Under Shear. *Proc. Royal Soc. London. A* 225: 49-63.
- Bagnold, R. A., 1966. Sediment Discharge and Stream Power. USGS Circular 421. Washington D.C.
- Bagnold, R. A., 1968. Deposition in the Process of Hydraulic Transport. *Sedimentology* 10:45-56.
- Bagnold, R. A., 1980. An Empirical Correlation of Bedload Transport Rates in Flumes and Natural Channels. *Proc. R. Soc. London. A* 372. 453-473.
- Beschta, R. L., 1983. The Effects of Large Woody Debris upon Channel Morphology: A Flume Study. *Proc. of the D. B. Simons Symposium on Erosion and Sedimentation*, Simons, Li and Assoc. Fort Collins, Co. pp.8-63 to 8-78.
- Beschta, R. L., 1987. Conceptual Models of Sediment Transport in Streams. *Sediment Transport in Gravel Bed-Rivers*. John Wiley and Sons: 387-419.
- Beschta, R. L. and Platts, W. S., 1986. Morphological Features of Small Streams: Significance and Function. *Wat. Resour. Bull.* 22(3): 369-379.
- Bishnu, P. D. and R. D. Townsend, 1981. Shear Stress Distribution at Channel Constrictions. *J. Hyd. Div., Proc. ASCE* 107 (HY12): 1695-1711.
- Breusers, H. N. C., 1975. Computation of Velocity Profiles in Scour Holes. *IAHR* 1975: 300-306.
- Campbell, A. J. and R. C. Sidle, 1985. Bed-Load Transport in a Pool-Riffle Sequence. *Wat. Resour. Bull.* 21(4): 579-590.
- Chapra, S. C. and R. P. Canale, 1985. *Numerical Methods for Engineers - with personal computer applications -*. McGraw Hill Book Co.
- Cherkauer, D. S., 1973. Minimization of Power Expenditure in a Riffle-Pool Alluvial Channel. *Wat. Resour. Res.* 9: 1613-1628.

- Chow, V. T., 1959. Open Channel Hydraulics. McGraw-Hill Civil Engineering Series.
- Crickmore, M. J., 1970. Effect of Flume Width on Bed-Form Characteristics. J. Hyd. Div., Proc. ASCE 96 (HY2): 473-496.
- Christensen, B. A., 1975. International Association for Hydraulic Research on the Stochastic Nature of Scour Initiation. IAHR 1975: 65-72.
- Dietrich, W. E., Smith, J. D. and T. Dunne, 1984. Boundary Shear Stress, Sediment Transport and Bed Morphology in Sand-Bedded River Meander during High Flow and Low Flow. River Meandering (ed. by C. M. Elliot). ASCE. New York. 632-639.
- Dolling, R. K., 1968. Occurrence of Pools and Riffles: an Element in the Quasi-Equilibrium State of River Channels. Ontario Geogr. 2: 3-11.
- Ervine, D. A. and H. T. Falvey, 1987. Behavior of Turbulent Water Jets in the Atmosphere and in Plunge Pools. Proc. Inst. Civ. Eng. 83: 295-314.
- Gerhart, P. M. and R. J. Gross, 1985. Fundamentals of Fluid Mechanics. Addison-Wesley Publishing Company.
- Gessler, J., 1975. Critical Shear Stress for Sediment Mixtures. IAHR 1975: C-1: 3-8.
- Goldstein, R. J., 1983. Fluid Mechanics Measurements. Hemisphere Publishing Corporation.
- Hayward, J. A., 1980. Hydrology and Stream Sediments in a Mountain Catchment. Tussock Grasslands and Mountain Lands Institute Special Publication No. 17.
- Hirsch, P. J. and A. D. Abrahams, 1981. The Properties of Bed Sediments in Pools and Riffles. J. Sed. Pet. 51(3): 757-760.
- Jackson, W. L., 1980. Bed Material Routing and Streambed Composition in Alluvial Channels. PhD Dissertation. Oregon State University, Corvallis, Oregon. 160 pp.
- Jackson, W. L. and R. L. Beschta, 1984. Influence of Increased Sand Delivery on the Morphology of Sand and Gravel Channels. Wat. Resour. Bull. 20(4): 527-533.
- Keller, E. A., 1971. Areal Sorting and Bed-Load Material: The Hypothesis of Velocity Reversal. Geol. Soc. Am. Bull. 82: 753-756.

- Kellerhals, R., M. Church and D. I. Bray, 1976. Classification and Analysis of River Processes. J. Hyd. Div., Proc. ASCE 102 (HY7): 813-829.
- Klingeman, P. C. and W. W. Emmett, 1982. Gravel Bed-Load Transport Processes. Gravel-Bed Rivers. John Wiley and Sons: 141-179.
- Laronne, J. B. and M. A. Carson, 1975. Interrelationships between Bed Morphology and Bed Material Transport for Small, Gravel-Bed Channel. Sedimentology 23: 67-85.
- Leopold, and Langbein, 1962. The Concept of Entropy in Landscape Evolution. USGS Prof. Pap. 500-A.
- Lisle, T. E., 1979. A Sorting Mechanism for a Riffle-Pool Sequence. Bull. Geol. Soc. Am. 90: 1142-1157.
- Lisle, T. E., 1982. Effects of Aggradation and Degradation on Riffle-Pool Morphology in Natural Gravel Channels, Northwestern California. Wat. Resour. Res. 18(6): 1643-1651.
- Matin, H., 1986. Micro-Computer Use for Solution of Sediment Transport Problems. M.S. Thesis, Oregon State University, Corvallis, Oregon. 264 pp.
- McCorquodale, J. A., 1973. Flow over Natural and Artificial Ripples. IAHR 1973: A 22-1 to A 22-6.
- Milhous, R. T., 1973. Sediment Transport in a Gravel-Bottomed stream. PhD Dissertation, Oregon State University, Corvallis, Oregon. 232 pp.
- Milne, J. A., 1982. Bed-Material Size and the Riffle-Pool Sequence. Sedimentology 29: 267-278.
- _____, 1982. Bed Forms and Bend-Arc Spacings of Some Coarse Bedload Channels in Upland Britain. Earth Surface Processes and Landforms 7(3): 227-248.
- Mueller, A. and A. Gyr, 1986. On the Vortex Formation in the Mixing Layer Behind Dunes. J. Hyd. Res. 24(5): 359-375.
- Novak, P. and J. Cabelka, 1981. Models in Hydraulic Engineering. Pitman Advanced Publishing Program.
- O'Neill, M. P. and A. D. Abrahams, 1984. Objective Identification of Pools and Riffles. Wat. Resour. Res. 20(7): 921-926.
- O'Connor, J. E., Webb, R. H. and V. R. Baker, 1986. Paleohydrology of Pool-Riffle Pattern Development: Boulder Creek, Utah. Bull. Geol. Soc. Am. 97: 410-420.

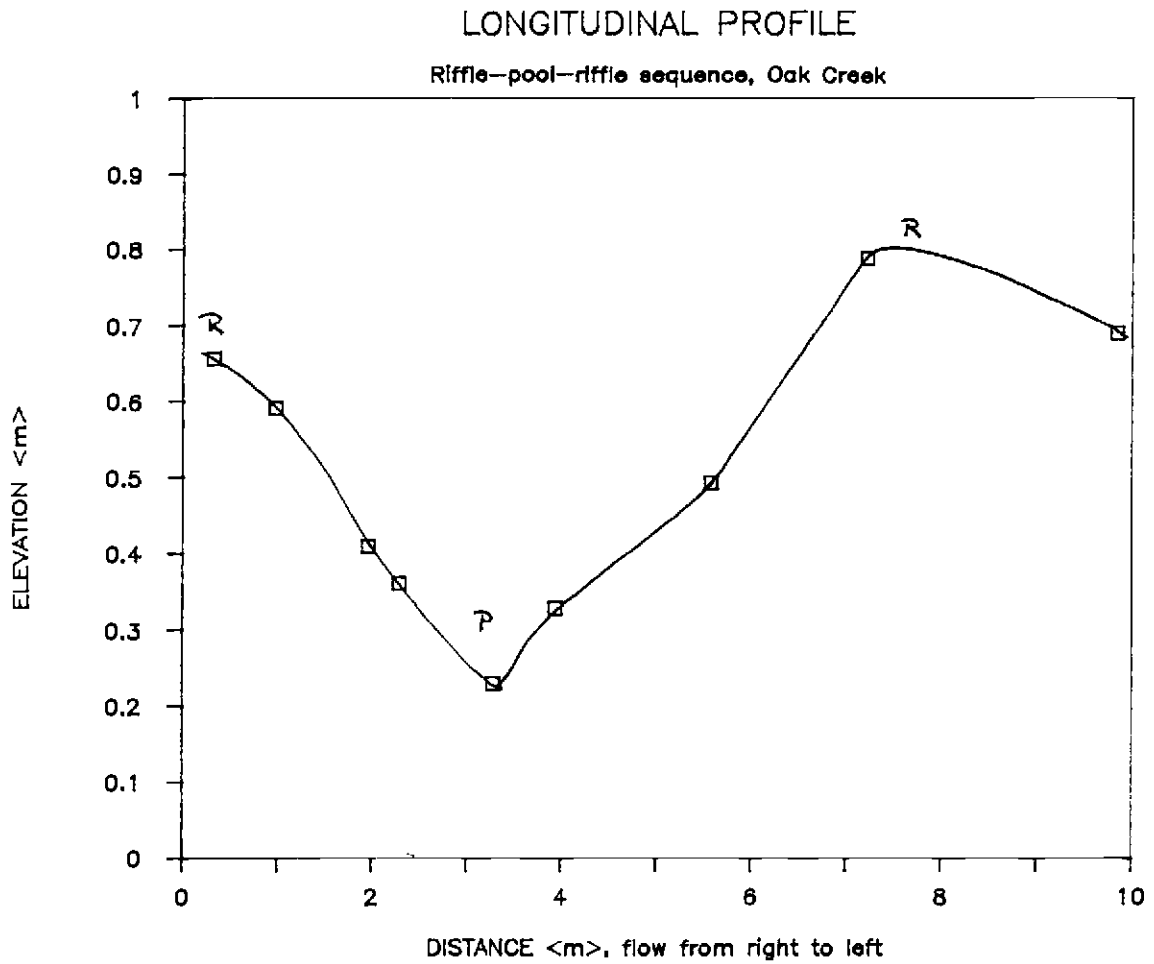
- Richards, K. S., 1976a. The Morphology of Riffle-Pool Sequences. *Earth Surface Processes* 1: 71-88.
- _____, 1976b. Channel Width and the Riffle-Pool Sequence. *Bull. Geol. Soc. Am.* 87: 883-890.
- _____, 1978. Simulation of Flow Geometry in a Riffle-Pool Stream. *Earth Surface Processes* 3: 345-354.
- Rosgen, D. L., 1986. A Stream Classification System. Symposium: *Riparian Ecosystems and their Management: Reconciling Conflicting Uses*. Tucson, Arizona.
- Simons, D. B., Al-Shalk-All, K. S. and R.-M. Li, 1979. Flow Resistance in Cobble and Boulder Riverbeds. *J. Hyd. Div., Proc. ASCE* 105 (HY5): 477-488.
- Simons, D. B. and R. K. Simons, 1987. Differences between Gravel- and Sand-bedded Rivers. *Sediment Transport in Gravel Bed Rivers 1987*. John Wiley and Sons: 3-17.
- Sullivan, K., 1986. Hydraulics and Fish Habitat in Relation to Channel Morphology. PhD Dissertation, John Hopkins University, Baltimore, Maryland. 409 pp.
- Sutherland, A. J., 1987. Static Armour Layers by Selective Erosion. *Sediment Transport in Gravel-Bed Rivers*. John Wiley and Sons: 243-267.
- Tacconi, P. and P. Billi, 1987. Bedload Transport Measurements by the Vortex-Tube Trap on Virginio Creek. *Sediment Transport in Gravel-Bed Rivers*. John Wiley and Sons: 583-616.
- Thompson, A., 1986. Secondary Flows and the Pool-Riffle Unit: A Case Study for the Processes of Meander Development. *Earth Surface Processes and Landforms* 11(6): 631-642.
- Tinkler, K. J., 1970. Pools, Riffles and Meanders. *Bull. Geol. Soc. Am.* 81: 547-552.
- Vanoni, V. A., 1975. *Sedimentation Engineering*. ASCE Manuals and Reports on Engineering Practice-No.54.
- Whittaker, J. G., 1987. Sediment Transport in Step-Pool Streams. *Sediment Transport in Gravel-Bed Rivers*. John Wiley and Sons: 545-579.
- Whittaker, J. G. and M. N. R. Jaeggi, 1982. Origin of Step-Pool Systems in Mountain Streams. *J. Hyd. Div., Proc. ASCE* 100 (HY6): 758-773.

Yalin, M. S., 1971. Theory of Hydraulic Models. Macmillan Civil Engineering Hydraulics.

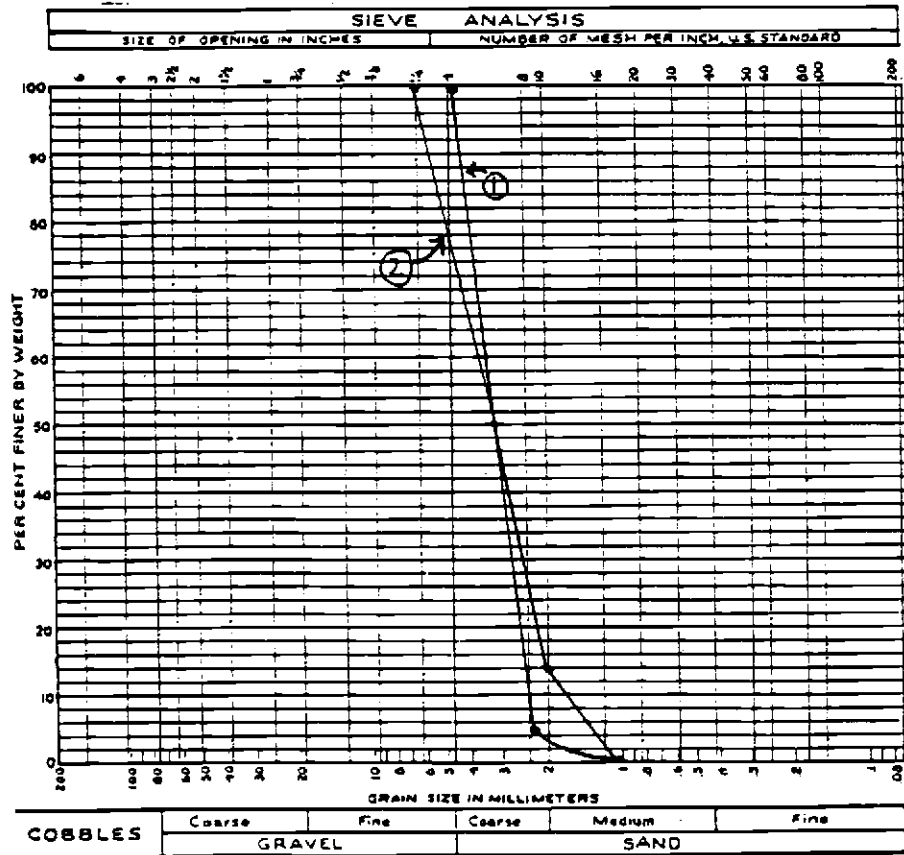
Yang, C. T. Y., 1971. Formation of Riffles and Pools. Wat. Resour. Res. 7(6): 1567-1574.

APPENDICES

APPENDIX A: Oak Creek field site data



APPENDIX B: Laboratory sediment characteristics



APPENDIX C: Bedload transport calculations using the HEC-6 computer program

The computer program calculates water surface and sediment bed surface profiles using a one-dimensional sediment transport model approach. Interactions between the sediment material in the stream bed and the flowing water-sediment mixture have to be computed. For each cross section, the total bed load along with the trap efficiencies for clay, silt and sands as well as the changes in bed -, water surface - and thalweg elevation are also calculated. Furthermore, the simulation of dredging and in-stream gravel mining operations and the analysis of reservoir deposition can be conducted (Matin, 1987).

For the purpose of this project the main interest was in the calculation of the total bed load. In order to perform this task, the modified program provides the choice of seven different bedload calculation procedures:

1. Schoklitsch 1934
2. Schoklitsch 1943
3. Meyer-Peter 1934
4. Meyer-Peter and Mueller 1948
5. Shields 1936
6. Laursen 1957
7. Einstein 1950

Three formulas treat the bedload transport process as a function of discharge (1,2,3). Two formulas are based on tractive force in order to determine critical values for bedload movement (4,5). The last two formulas (6,7) use relative roughness-based on the ratio of grain diameter to depth of flow- to compute total bedload. The following overview summarizes three approaches chosen for the bedload computations in the experiment as representants of the different concepts (all the formulas are given in metric units). The information was taken from Vanoni (1975) and Matin (1987):

SCHOKLITSCH 1943:

$$G = C(Q - Q_{cr})$$

with:

$$C = 2500 S^{3/2}$$

where:

G = bedload in kg/sec/m

Q = discharge in m^3 /sec/m

Q_{cr} = the critical discharge in m^3 /sec/m

The equations were derived for uniform grain material. Since the particle diameter does not appear in this formula, the calculation for the sediment mixture, used in some of the runs, might show some less precise results.

MEYER-PETER and MUELLER 1948:

$$(k_r/k_{r'})^{3/2} R_b S =$$

$$0.047(y_s - y)d_m + 0.25(y/g)^{1/3} [(y_s - y)/y]^{2/3} (g_s)^{2/3}$$

in which:

$$k_r/k_{r'} = (f'_b/y)^{1/2} [V/(gR_b S)^{1/2}]$$

where:

- y = specific unit weight of water
- y_s = specific weight of sediment
- d_m = weighted mean grain diameter for a mixture of sizes
- R_b = hydraulic radius with respect to the bed
- g = acceleration of gravity
- f'_b = Darcy-Weisbach bed friction factor
- y_s = specific unit weight of sediment particles
- g_s = bedload transport in weight per unit channel width
- V = mean velocity of the stream

This formula was developed in a flume study with graded and sorted river sediments. The advantage of this formula is that it can be used for graded sediments under flow conditions that give rise to dunes and other bed forms, which is appropriate for this project.

EINSTEIN 1950:

The Einstein method calculates the sediment discharge for individual size fractions of the bed material. The equations involved go over a sequence of hydraulic calculations to the final total load computations. The elaborate computation process can be summarized as follows:

$$g_s = g_{si}$$

$$G_s = bg_s$$

$$g_i = g_s b_i [(pr)(I1) + I2 + 1]$$

where:

g_s = bed sediment discharge rate in weight per unit channel width

g_{si} = discharge of bed sediment of mean size d_{si} (i.e., the i th size fraction), in weight per unit channel width

$g_s b_i$ = discharge of bedload of mean size d_{si} in weight per unit channel width

G_s = total bed sediment discharge in weight per unit time

b = width of the stream bed

g_i = the sum of g_{si} for all size fractions

pr = a parameter of total transport

$I1, I2$ = integral values

APPENDIX D: Experimental data

BED ELEVATION CHANGES #1:

Distance from upstream	Reading init.bed	Reading #1a	Reading #1b	Reading #1c	Reading #1d	Reading #1e	Reading #1f	Reading 2 hrs.
<m>	<m>	<m>	<m>	<m>	<m>	<m>	<m>	<m>
1.70	0.0000	0.0000	0.0000	0.0000	0.0000	0.0000	0.0000	0.0000
1.68	-0.0003	-0.0232	-0.0362	-0.0181	-0.0169	-0.0210	-0.0236	-0.0449
1.66	-0.0005	-0.0280	-0.0724	-0.0358	-0.0337	-0.0419	-0.0472	-0.0894
1.64	-0.0008	-0.0299	-0.0783	-0.0539	-0.0506	-0.0629	-0.0713	-0.1433
1.62	-0.0011	-0.0252	-0.0819	-0.0717	-0.0674	-0.0839	-0.0949	-0.1791
1.60	-0.0013	-0.0232	-0.0878	-0.0898	-0.0843	-0.0917	-0.0996	-0.1457
1.58	-0.0016	-0.0213	-0.0906	-0.0961	-0.0953	-0.0992	-0.1055	-0.1126
1.56	-0.0019	-0.0165	-0.0992	-0.1024	-0.1063	-0.1059	-0.1142	-0.1177
1.54	-0.0021	-0.0165	-0.1051	-0.1091	-0.1118	-0.1126	-0.1228	-0.1232
1.52	-0.0024	-0.0146	-0.1098	-0.1154	-0.1177	-0.1169	-0.1260	-0.1303
1.50	-0.0027	-0.0197	-0.1118	-0.1217	-0.1232	-0.1217	-0.1291	-0.1374
1.44	-0.0035	-0.0079	-0.1161	-0.1226	-0.1378	-0.1354	-0.1378	-0.1382
1.42	-0.0037	-0.0114	-0.1165	-0.1232	-0.1406	-0.1413	-0.1433	-0.1394
1.40	-0.0040	-0.0114	-0.1122	-0.1232	-0.1433	-0.1476	-0.1488	-0.1409
1.38	-0.0043	-0.0114	-0.1075	-0.1260	-0.1480	-0.1524	-0.1520	-0.1433
1.36	-0.0045	-0.0114	-0.1024	-0.1287	-0.1528	-0.1567	-0.1555	-0.1476
1.34	-0.0048	-0.0114	-0.0969	-0.1311	-0.1543	-0.1614	-0.1610	-0.1551
1.32	-0.0051	-0.0114	-0.0894	-0.1339	-0.1563	-0.1634	-0.1650	-0.1594
1.30	-0.0053	-0.0114	-0.0850	-0.1366	-0.1587	-0.1657	-0.1689	-0.1634
1.28	-0.0056	-0.0114	-0.0791	-0.1339	-0.1610	-0.1677	-0.1677	-0.1661
1.26	-0.0059	-0.0114	-0.0717	-0.1315	-0.1634	-0.1665	-0.1654	-0.1685
1.24	-0.0061	-0.0114	-0.0634	-0.1287	-0.1638	-0.1661	-0.1669	-0.1681
1.22	-0.0064	-0.0114	-0.0563	-0.1260	-0.1646	-0.1657	-0.1654	-0.1677
1.20	-0.0067	-0.0114	-0.0512	-0.1232	-0.1650	-0.1657	-0.1638	-0.1673
1.18	-0.0069	-0.0114	-0.0480	-0.1209	-0.1638	-0.1654	-0.1626	-0.1665
1.16	-0.0072	-0.0114	-0.0433	-0.1181	-0.1630	-0.1640	-0.1618	-0.1650
1.14	-0.0075	-0.0114	-0.0425	-0.1154	-0.1626	-0.1626	-0.1610	-0.1634
1.12	-0.0077	-0.0114	-0.0386	-0.1130	-0.1618	-0.1612	-0.1602	-0.1614
1.10	-0.0080	-0.0114	-0.0378	-0.1102	-0.1614	-0.1598	-0.1594	-0.1606
1.04	-0.0088	-0.0114	-0.0319	-0.1024	-0.1559	-0.1551	-0.1547	-0.1547
1.00	-0.0093	-0.0114	-0.0307	-0.0858	-0.1547	-0.1504	-0.1500	-0.1488
0.90	-0.0107	-0.0114	-0.0291	-0.0697	-0.1354	-0.1413	-0.1406	-0.1382
0.80	-0.0120	-0.0118	-0.0283	-0.0598	-0.1165	-0.1299	-0.1287	-0.1307
0.70	-0.0133	-0.0134	-0.0157	-0.0504	-0.0992	-0.1091	-0.1110	-0.1110
0.60	-0.0147	-0.0146	-0.0213	-0.0449	-0.0858	-0.0902	-0.0917	-0.0917
0.50	-0.0160	-0.0161	-0.0173	-0.0394	-0.0610	-0.0646	-0.0669	-0.0669
0.46	-0.0165	-0.0165	-0.0157	-0.0165	-0.0165	-0.0165	-0.0165	-0.0164

```

#####
# RUN #1
#
# SED. PROPERTIES: K4-08 (DS0+3.2km)
#####
    
```

VELOCITY #1: 0.9 17/sec:			VELOCITY #1b(2.75 17/sec):			VELOCITY #1c: 5.51 17/sec:						
Distance	Total Depth	Depth	Hertz	Velocity	Distance	Total Depth	Depth	Hertz	Velocity	Distance	Total Depth	Depth
(m)	(m)	(m)		(m/sec)	(m)	(m)	(m)		(m/sec)	(m)	(m)	(m)
1.90	0.025	0.010	45.0	0.482	1.90	0.035	0.010	47	0.504	1.90	0.075	0.010
		0.015	50.0	0.524			0.015	52	0.557			0.025
		0.025	50.0	0.534			0.020	60	0.643			0.035
1.86	0.074	0.010	9.5	0.102			0.030	58	0.621			0.050
		0.019	12.0	0.124			0.035	58	0.621			0.045
		0.024	55.0	0.589			0.045	63	0.675			0.075
		0.024	55.0	0.589			0.055	63	0.675			0.010
1.62	0.040	0.040	2.0	0.021	1.70	0.020	0.010	70	0.944	1.70	0.055	0.025
		0.020	4.0	0.044			0.011	70	0.944			0.035
		0.020	12.0	0.129			0.018	70	0.944			0.045
		0.040	12.0	0.129			0.028	70	0.944			0.055
1.58	0.077	0.020	17.0	0.182	1.64	0.070	0.010	-10	-0.107	1.60	0.090	0.010
		0.010	20.0	0.214			0.020	-4	-0.064			0.020
		0.021	28.0	0.290			0.020	-4	-0.064			0.030
		0.021	28.0	0.290			0.040	-55	-0.589			0.040
1.50	0.027	0.010	14.0	0.284			0.050	-80	-0.857			0.050
		0.014	15.0	0.275			0.060	-105	-1.125			0.080
		0.017	18.0	0.407			0.070	-105	-1.125			0.090
		0.027	18.0	0.407	1.35	0.075	0.010	-16	-0.171	1.50	0.140	0.010
1.40	0.022	0.010	48.0	0.514			0.025	-16	-0.171			0.020
		0.017	52.0	0.557			0.032	-10	-0.107			0.040
							0.045	0	0.000			0.050
							0.055	50	0.524			0.080
							0.065	100	1.071			0.070
							0.075	100	1.071			0.080
					1.54	0.100	0.010	-14	-0.171			0.100
							0.020	-7	-0.075			0.115
							0.020	-5	-0.054			0.140
							0.040	-3	-0.032	1.40	0.175	0.010
							0.030	-7	-0.072			0.035
							0.060	20	0.234			0.055
							0.070	70	0.721			0.075
							0.090	50	0.524			0.085
							0.100	50	0.524			0.105
					1.50	0.125	0.010	-14	-0.171			0.125
							0.025	-1	-0.011			0.155
							0.035	-8	-0.094			0.175
							0.045	-10	-0.107	1.20	0.150	0.010
							0.055	0	0.000			0.030
							0.065	0	0.000			0.050
							0.075	18	0.171			0.070
							0.085	20	0.214			0.100
							0.095	70	0.721			0.130
							0.105	40	0.429			0.140
							0.115	50	0.524			0.145
							0.125	50	0.524			0.160
					1.44	0.120	0.010	-8	-0.084	0.94	0.140	0.010
							0.020	-4	-0.044			0.030
							0.040	-4	-0.064			0.070
							0.050	0	0.000			0.100
							0.060	12	0.129			0.120
							0.074	20	0.214			0.130
							0.090	74	0.344			0.140
							0.090	45	0.482	0.70	0.115	0.020
							0.110	70	0.750			0.045
							0.120	70	0.750			0.065
					1.34	0.120	0.010	0	0.000			0.075
							0.020	0	0.000			0.105
							0.050	14	0.150			0.115
							0.060	22	0.224	0.45	0.080	0.010
							0.080	40	0.429			0.030
							0.100	30	0.324			0.050
							0.110	50	0.524			0.070
							0.120	50	0.524			0.080
					1.28	0.095	0.010	0	0.000			
							0.025	16	0.171			
							0.045	30	0.221			
							0.065	50	0.524			
							0.085	40	0.443			
							0.095	40	0.445			
					1.10	0.065	0.010	45	0.482			
							0.025	50	0.589			
							0.035	50	0.589			
							0.045	55	0.589			
							0.055	55	0.589			
							0.065	55	0.589			
					0.80	0.060	0.010	55	0.589			
							0.020	65	0.694			
							0.040	65	0.694			
							0.050	65	0.694			
							0.060	65	0.694			
					0.45	0.055	0.010	55	0.589			
							0.025	65	0.694			
							0.035	65	0.694			
							0.045	65	0.694			

BED ELEVATION CHANGES #3:

Distance from upstream (m)	Reading flat bed (m)	Reading #3a (m)	Reading #3b (m)	Reading #3c (m)	Reading #3d (m)	Reading #3e 19.05 (m)	Reading #3f 19.15 (m)	Reading #3g 19.25 (m)	Reading #3h 21.30 (m)	Reading #3i 22.27 (m)	Reading #3j 23.00 (m)	Reading #3k 0.50 (m)
1.70	0.0000	0.0000	0.0000	0.0000	0.0000	0.0000	0.0000	0.0000	0.0000	0.0000	0.0000	0.0000
1.68	-0.0003	-0.0169	-0.0295	-0.0295	-0.0283	-0.0295	-0.0295	-0.0295	-0.0295	-0.0295	-0.0295	-0.0295
1.66	-0.0005	-0.0228	-0.0406	-0.0358	-0.0457	-0.0638	-0.0638	-0.0638	-0.0398	-0.0713	-0.0555	-0.0303
1.64	-0.0008	-0.0268	-0.0476	-0.0496	-0.0528	-0.0697	-0.0697	-0.0697	-0.0496	-0.0760	-0.0614	-0.0350
1.62	-0.0011	-0.0268	-0.0563	-0.0594	-0.0634	-0.0803	-0.0803	-0.0803	-0.0598	-0.0850	-0.0685	-0.0335
1.60	-0.0013	-0.0232	-0.0591	-0.0693	-0.0713	-0.0929	-0.0929	-0.0929	-0.0675	-0.0858	-0.0732	-0.0299
1.58	-0.0016	-0.0224	-0.0638	-0.0791	-0.0791	-0.1028	-0.1028	-0.1028	-0.0756	-0.0870	-0.0701	-0.0240
1.56	-0.0019	-0.0217	-0.0571	-0.0870	-0.0862	-0.1114	-0.1114	-0.1114	-0.0850	-0.0850	-0.0650	-0.0240
1.54	-0.0021	-0.0169	-0.0634	-0.0917	-0.0929	-0.1205	-0.1205	-0.1205	-0.0890	-0.0846	-0.0535	-0.0213
1.52	-0.0024	-0.0146	-0.0614	-0.1000	-0.1028	-0.1283	-0.1283	-0.1283	-0.0909	-0.0776	-0.0445	-0.0173
1.50	-0.0027	-0.0130	-0.0575	-0.1094	-0.1189	-0.1283	-0.1283	-0.1185	-0.0890	-0.0740	-0.0299	-0.0142
1.44	-0.0035	-0.0130	-0.0406	-0.1008	-0.1362	-0.1224	-0.1195	-0.1087	-0.0709	-0.0705	-0.0220	-0.0142
1.42	-0.0037	-0.0130	-0.0366	-0.1008	-0.1374	-0.1205	-0.1141	-0.0929	-0.0654	-0.0685	-0.0220	-0.0134
1.40	-0.0040	-0.0130	-0.0299	-0.1008	-0.1425	-0.1185	-0.1087	-0.0850	-0.0598	-0.0575	-0.0201	-0.0134
1.38	-0.0043	-0.0130	-0.0240	-0.0988	-0.1461	-0.1126	-0.0772	-0.0732	-0.0520	-0.0528	-0.0181	-0.0122
1.36	-0.0045	-0.0130	-0.0260	-0.0988	-0.1461	-0.1067	-0.0693	-0.0634	-0.0476	-0.0457	-0.0201	-0.0102
1.34	-0.0048	-0.0122	-0.0240	-0.0933	-0.1461	-0.1000	-0.0654	-0.0535	-0.0417	-0.0417	-0.0201	-0.0102
1.32	-0.0051	-0.0122	-0.0205	-0.0890	-0.1472	-0.0980	-0.0575	-0.0437	-0.0366	-0.0366	-0.0200	-0.0102
1.30	-0.0053	-0.0122	-0.0213	-0.0835	-0.1520	-0.0961	-0.0535	-0.0409	-0.0339	-0.0339	-0.0199	-0.0102
1.28	-0.0056	-0.0146	-0.0197	-0.0799	-0.1488	-0.1051	-0.0457	-0.0382	-0.0319	-0.0319	-0.0198	-0.0102
1.26	-0.0059	-0.0161	-0.0201	-0.0744	-0.1429	-0.1264	-0.0398	-0.0354	-0.0280	-0.0280	-0.0197	-0.0102
1.24	-0.0061	-0.0146	-0.0181	-0.0701	-0.1437	-0.1409	-0.0378	-0.0327	-0.0252	-0.0252	-0.0196	-0.0102
1.22	-0.0064	-0.0138	-0.0220	-0.0669	-0.1437	-0.1429	-0.0358	-0.0299	-0.0244	-0.0244	-0.0195	-0.0102
1.20	-0.0067	-0.0130	-0.0201	-0.0634	-0.1382	-0.1406	-0.0331	-0.0291	-0.0220	-0.0220	-0.0194	-0.0102
1.18	-0.0069	-0.0130	-0.0217	-0.0543	-0.1362	-0.1429	-0.0331	-0.0287	-0.0252	-0.0252	-0.0193	-0.0102
1.16	-0.0072	-0.0130	-0.0201	-0.0528	-0.1373	-0.1307	-0.0319	-0.0280	-0.0248	-0.0248	-0.0192	-0.0102
1.14	-0.0075	-0.0130	-0.0201	-0.0484	-0.1350	-0.1283	-0.0339	-0.0276	-0.0260	-0.0260	-0.0191	-0.0102
1.12	-0.0077	-0.0130	-0.0201	-0.0441	-0.1268	-0.1213	-0.0535	-0.0268	-0.0264	-0.0264	-0.0190	-0.0102
1.10	-0.0080	-0.0130	-0.0201	-0.0417	-0.1283	-0.1205	-0.0701	-0.0264	-0.0240	-0.0240	-0.0189	-0.0102
1.04	-0.0088	-0.0130	-0.0201	-0.0354	-0.1140	-0.1031	-0.0972	-0.0335	-0.0240	-0.0240	-0.0186	-0.0120
1.00	-0.0093	-0.0157	-0.0201	-0.0291	-0.0996	-0.0858	-0.0858	-0.0335	-0.0240	-0.0240	-0.0184	-0.0132
0.90	-0.0107	-0.0157	-0.0201	-0.0264	-0.0673	-0.0555	-0.0555	-0.0575	-0.0240	-0.0240	-0.0179	-0.0161
0.80	-0.0120	-0.0161	-0.0220	-0.0264	-0.0457	-0.0299	-0.0299	-0.0480	-0.0240	-0.0240	-0.0174	-0.0161
0.70	-0.0133	-0.0161	-0.0240	-0.0264	-0.0339	-0.0264	-0.0264	-0.0386	-0.0240	-0.0240	-0.0169	-0.0161
0.60	-0.0147	-0.0161	-0.0220	-0.0240	-0.0299	-0.0240	-0.0240	-0.0291	-0.0240	-0.0240	-0.0164	-0.0157
0.50	-0.0160	-0.0161	-0.0201	-0.0199	-0.0299	-0.0199	-0.0199	-0.0197	-0.0240	-0.0240	-0.0159	-0.0157
0.46	-0.0165	-0.0165	-0.0157	-0.0157	-0.0157	-0.0157	-0.0157	-0.0157	-0.0157	-0.0157	-0.0157	-0.0157

SEDIMENT OUTPUT #3:

time (min)	rate #3a kg/hr	rate #3b kg/hr	rate #3c kg/hr	rate #3d kg/hr	rate #3e kg/hr
5	4.71	2.41	3.82	4.65	3.52
15	4.71	2.41	3.14	3.50	3.52
27	2.32	1.68	2.79	2.50	3.52
30	0.92	0.85	3.04	2.64	3.65
36	1.31	0.85	3.04	2.70	3.63
45	1.67	0.85	4.15	3.29	3.63
60	1.08	0.85	2.28		1.04
75	1.08	0.85	2.26		0.89
77	1.45		2.62		0.95
90	1.79		2.24		0.82
93	1.79		2.26		0.85
103	1.09		2.87		0.65
120	1.09		1.53		0.85
127	1.11		3.49		
150	1.22		2.56		
180	1.32				

```

*****
# RUN #3
# SED.PROPERTIES: #4 - #8 (DSO=3.2ae) #
*****

```

VELOCITY #3a(1.18 1/sec):				VELOCITY #3b(2.65 1/sec):				VELOCITY #3c(5.25 1/sec):			
Distance	total Depth	Depth	Hertz Velocity	Distance	total Depth	Depth	Hertz Velocity	Distance	total Depth	Depth	Hertz Velocity
(m)	(m)	(m)	(m/sec)	(m)	(m)	(m)	(m/sec)	(m)	(m)	(m)	(m/sec)
1.90	0.030	0.010	55.0	1.90	0.052	0.010	50	1.90	0.075	0.010	0.536
		0.015	58.0			0.017	70			0.020	0.750
		0.020	62.0			0.032	75			0.030	0.804
		0.030	62.0			0.042	75			0.045	0.804
1.64	0.040	0.010	40.0	1.64	0.055	0.010	35	1.64	0.105	0.010	0.804
		0.015	45.0			0.025	65			0.075	0.804
		0.020	60.0			0.045	90			0.085	0.804
		0.030	60.0			0.055	90			0.105	0.804
		0.040	60.0			0.090	25			0.020	0.964
1.54	0.028	0.010	35.0	1.54	0.090	0.010	25	1.54	0.135	0.010	0.268
		0.013	40.0			0.020	40			0.045	0.429
		0.018	40.0			0.030	60			0.065	0.429
		0.028	40.0			0.040	65			0.105	0.429
1.30	0.025	0.010	48.0	1.50	0.080	0.090	65	1.50	0.135	0.010	0.696
		0.012	50.0			0.010	45			0.025	0.696
		0.015	55.0			0.020	50			0.045	0.696
		0.025	55.0			0.030	50			0.065	0.696
0.46	0.028	0.010	43.0			0.040	40			0.095	0.536
		0.013	55.0			0.050	30			0.135	0.429
		0.018	60.0			0.060	10	1.30	0.130	0.010	0.321
		0.028	60.0			0.070	7			0.030	0.107
						0.070	7			0.050	0.075
						0.080	7			0.070	0.075
				0.46	0.040	0.010	65			0.090	0.496
						0.015	80			0.120	0.857
						0.020	80			0.130	0.857
						0.025	85	0.90	0.085	0.010	0.911
						0.030	85			0.035	0.911
						0.040	85			0.055	0.911
										0.075	0.911
										0.085	0.911
								0.46	0.070	0.010	0.496
										0.020	0.857
										0.040	0.857
										0.060	0.911
										0.070	0.911

BED ELEVATION CHANGES:

Distance from upstream <m>	Reading flat bed <m>	Reading #4a <m>	Reading #4b <m>	Reading #4c <m>	Reading #4d <m>	Reading #4e 18.05 <m>	Reading 18.30 <m>	Reading 20.30 <m>	Reading #4f <m>
1.70	0.0000	0.0000	0.0000	0.0000	0.0000	0.0000	0.0000	0.0000	0.0000
1.68	-0.0003	-0.0169	-0.0307	-0.0287	-0.0258	-0.0386	-0.0425	-0.0425	-0.0445
1.66	-0.0005	-0.0394	-0.0614	-0.0575	-0.0516	-0.0772	-0.0850	-0.0850	-0.0890
1.64	-0.0008	-0.0445	-0.0693	-0.0654	-0.0614	-0.0811	-0.0890	-0.0890	-0.0870
1.62	-0.0011	-0.0504	-0.0701	-0.0752	-0.0752	-0.0961	-0.0969	-0.0929	-0.0937
1.60	-0.0013	-0.0484	-0.0831	-0.0843	-0.0815	-0.1047	-0.1047	-0.1008	-0.0988
1.58	-0.0016	-0.0461	-0.0831	-0.0949	-0.0890	-0.1130	-0.1126	-0.1087	-0.1043
1.56	-0.0019	-0.0406	-0.0929	-0.0988	-0.0984	-0.1244	-0.1165	-0.1118	-0.1106
1.54	-0.0021	-0.0307	-0.0961	-0.1067	-0.1087	-0.1441	-0.1244	-0.1185	-0.1205
1.52	-0.0024	-0.0228	-0.0988	-0.1106	-0.1126	-0.1516	-0.1283	-0.1244	-0.1264
1.50	-0.0027	-0.0209	-0.1039	-0.1165	-0.1185	-0.1520	-0.1362	-0.1283	-0.1323
1.44	-0.0035	-0.0189	-0.1055	-0.1185	-0.1370	-0.1528	-0.1500	-0.1362	-0.1480
1.42	-0.0037	-0.0169	-0.1008	-0.1264	-0.1390	-0.1500	-0.1500	-0.1488	-0.1508
1.40	-0.0040	-0.0169	-0.0996	-0.1323	-0.1480	-0.1500	-0.1500	-0.1520	-0.1539
1.38	-0.0043	-0.0169	-0.0961	-0.1323	-0.1579	-0.1461	-0.1500	-0.1524	-0.1539
1.36	-0.0045	-0.0169	-0.0890	-0.1362	-0.1602	-0.1441	-0.1441	-0.1551	-0.1539
1.34	-0.0048	-0.0169	-0.0866	-0.1362	-0.1646	-0.1394	-0.1441	-0.1563	-0.1539
1.32	-0.0051	-0.0169	-0.0732	-0.1362	-0.1717	-0.1354	-0.1480	-0.1520	-0.1539
1.30	-0.0053	-0.0169	-0.0693	-0.1343	-0.1748	-0.1323	-0.1461	-0.1539	-0.1539
1.28	-0.0056	-0.0169	-0.0654	-0.1315	-0.1732	-0.1283	-0.1421	-0.1591	-0.1539
1.26	-0.0059	-0.0169	-0.0618	-0.1303	-0.1732	-0.1264	-0.1402	-0.1500	-0.1547
1.24	-0.0061	-0.0169	-0.0587	-0.1264	-0.1705	-0.1354	-0.1394	-0.1500	-0.1520
1.22	-0.0064	-0.0169	-0.0555	-0.1228	-0.1685	-0.1512	-0.1441	-0.1520	-0.1539
1.20	-0.0067	-0.0169	-0.0535	-0.1173	-0.1657	-0.1638	-0.1500	-0.1520	-0.1539
1.18	-0.0069	-0.0169	-0.0535	-0.1126	-0.1618	-0.1677	-0.1618	-0.1618	-0.1598
1.16	-0.0072	-0.0169	-0.0535	-0.1087	-0.1618	-0.1669	-0.1669	-0.1657	-0.1630
1.14	-0.0075	-0.0169	-0.0496	-0.1012	-0.1559	-0.1638	-0.1638	-0.1657	-0.1598
1.12	-0.0077	-0.0169	-0.0457	-0.0976	-0.1555	-0.1591	-0.1591	-0.1618	-0.1563
1.10	-0.0080	-0.0169	-0.0378	-0.0949	-0.1551	-0.1575	-0.1575	-0.1618	-0.1563
1.04	-0.0088	-0.0169	-0.0339	-0.0819	-0.1374	-0.1449	-0.1449	-0.1449	-0.1488
1.00	-0.0093	-0.0169	-0.0339	-0.0713	-0.1323	-0.1323	-0.1323	-0.1323	-0.1402
0.90	-0.0107	-0.0169	-0.0319	-0.0575	-0.1047	-0.1047	-0.1047	-0.1047	-0.1134
0.80	-0.0120	-0.0169	-0.0291	-0.0496	-0.0921	-0.0921	-0.0921	-0.0921	-0.1008
0.70	-0.0133	-0.0169	-0.0291	-0.0457	-0.0783	-0.0783	-0.0783	-0.0783	-0.0732
0.60	-0.0147	-0.0169	-0.0264	-0.0437	-0.0693	-0.0693	-0.0693	-0.0693	-0.0654
0.50	-0.0160	-0.0169	-0.0260	-0.0319	-0.0496	-0.0496	-0.0496	-0.0496	-0.0535
0.46	-0.0165	-0.0165	-0.0157	-0.0157	-0.0157	-0.0157	-0.0157	-0.0157	-0.0157

SEDIMENT OUTPUT #4:

time <min>	rate #4a <kg/hr>	rate #4b <kg/hr>	rate #4c <kg/hr>	rate #4d <kg/hr>
15	4.22	15.13	7.92	8.18
30	0.69	1.34	2.48	1.29
45	0.34	0.48	1.07	0.70
225	0.00	0.06	0.34	0.03
585	0.00	0.00	0.00	0.00

BED ELEVATION CHANGES #5:

Distance	Reading init.bed	Reading #5a	Reading #5b	Reading #5c	Reading #5d	Reading #5e	Reading #5f	Reading #5g	Reading #5h	Reading #5i
(m)	(m)	(a)	(m)	(m)	(m)	(a)	(a)	(a)	(a)	(m)
1.70	0.0000	0.0000	0.0000	0.0000	0.0000	0.0000	0.0000	0.0000	0.0000	0.0000
1.68	-0.0010	-0.0150	-0.0240	-0.0295	-0.0299	-0.0280	-0.0230	-0.0290	-0.0240	-0.0240
1.66	-0.0013	-0.0150	-0.0378	-0.0378	-0.0398	-0.0575	-0.0398	-0.0417	-0.0260	-0.0260
1.64	-0.0015	-0.0110	-0.0476	-0.0494	-0.0494	-0.0673	-0.0494	-0.0575	-0.0230	-0.0230
1.62	-0.0018	-0.0091	-0.0567	-0.0602	-0.0634	-0.0811	-0.0614	-0.0614	-0.0230	-0.0230
1.60	-0.0021	-0.0110	-0.0634	-0.0693	-0.0693	-0.0949	-0.0634	-0.0677	-0.0240	-0.0240
1.58	-0.0023	-0.0110	-0.0654	-0.0752	-0.0811	-0.1126	-0.0791	-0.0677	-0.0256	-0.0256
1.56	-0.0025	-0.0110	-0.0681	-0.0870	-0.0890	-0.1205	-0.0650	-0.0594	-0.0217	-0.0217
1.54	-0.0028	-0.0110	-0.0693	-0.1000	-0.1000	-0.1293	-0.0693	-0.0535	-0.0217	-0.0217
1.52	-0.0031	-0.0110	-0.0657	-0.1047	-0.1087	-0.1343	-0.0709	-0.0449	-0.0191	-0.0191
1.50	-0.0033	-0.0110	-0.0673	-0.1144	-0.1135	-0.1421	-0.0933	-0.0230	-0.0201	-0.0201
1.44	-0.0041	-0.0130	-0.0494	-0.1205	-0.1445	-0.1421	-0.0290	-0.0224	-0.0181	-0.0181
1.42	-0.0043	-0.0114	-0.0441	-0.1291	-0.1520	-0.1433	-0.0331	-0.0217	-0.0177	-0.0177
1.40	-0.0046	-0.0150	-0.0370	-0.1275	-0.1551	-0.1441	-0.0772	-0.0250	-0.0191	-0.0191
1.38	-0.0049	-0.0130	-0.0339	-0.1276	-0.1630	-0.1406	-0.0693	-0.0499	-0.0181	-0.0181
1.36	-0.0051	-0.0122	-0.0319	-0.1283	-0.1677	-0.1429	-0.0594	-0.0634	-0.0181	-0.0181
1.34	-0.0054	-0.0118	-0.0268	-0.1244	-0.1724	-0.1335	-0.0516	-0.0535	-0.0142	-0.0142
1.32	-0.0056	-0.0110	-0.0264	-0.1205	-0.1736	-0.1244	-0.0417	-0.0461	-0.0161	-0.0161
1.30	-0.0059	-0.0118	-0.0260	-0.1146	-0.1736	-0.1195	-0.0370	-0.0417	-0.0142	-0.0142
1.28	-0.0061	-0.0118	-0.0256	-0.1087	-0.1736	-0.1106	-0.0331	-0.0343	-0.0150	-0.0150
1.26	-0.0064	-0.0118	-0.0260	-0.1012	-0.1736	-0.1047	-0.0280	-0.0319	-0.0173	-0.0173
1.24	-0.0066	-0.0118	-0.0252	-0.0969	-0.1736	-0.1035	-0.0280	-0.0290	-0.0173	-0.0173
1.22	-0.0069	-0.0118	-0.0260	-0.0899	-0.1709	-0.1047	-0.0220	-0.0230	-0.0173	-0.0173
1.20	-0.0071	-0.0150	-0.0248	-0.0831	-0.1697	-0.1205	-0.0220	-0.0250	-0.0161	-0.0161
1.18	-0.0074	-0.0150	-0.0240	-0.0732	-0.1638	-0.1429	-0.0220	-0.0220	-0.0142	-0.0142
1.16	-0.0076	-0.0150	-0.0220	-0.0693	-0.1602	-0.1520	-0.0201	-0.0201	-0.0142	-0.0142
1.14	-0.0079	-0.0146	-0.0220	-0.0654	-0.1579	-0.1461	-0.0185	-0.0185	-0.0150	-0.0150
1.12	-0.0082	-0.0146	-0.0220	-0.0646	-0.1520	-0.1591	-0.0177	-0.0177	-0.0181	-0.0181
1.10	-0.0084	-0.0142	-0.0220	-0.0579	-0.1441	-0.1441	-0.0177	-0.0177	-0.0201	-0.0201
1.04	-0.0092	-0.0142	-0.0240	-0.0417	-0.1248	-0.1248	-0.0161	-0.0161	-0.0150	-0.0150
1.00	-0.0097	-0.0138	-0.0220	-0.0362	-0.1047	-0.1047	-0.0181	-0.0181	-0.0181	-0.0181
0.90	-0.0109	-0.0134	-0.0220	-0.0280	-0.0654	-0.0654	-0.0201	-0.0201	-0.0181	-0.0181
0.80	-0.0122	-0.0209	-0.0181	-0.0280	-0.0594	-0.0594	-0.0220	-0.0220	-0.0220	-0.0220
0.70	-0.0135	-0.0169	-0.0181	-0.0260	-0.0528	-0.0528	-0.0201	-0.0201	-0.0181	-0.0181
0.60	-0.0148	-0.0189	-0.0220	-0.0264	-0.0476	-0.0476	-0.0220	-0.0220	-0.0220	-0.0220
0.50	-0.0160	-0.0209	-0.0181	-0.0280	-0.0417	-0.0417	-0.0201	-0.0201	-0.0220	-0.0220
0.46	-0.0165	-0.0165	-0.0157	-0.0157	-0.0157	-0.0157	-0.0157	-0.0157	-0.0157	-0.0157

SEDIMENT OUTPUT #5:

time	rate #5a	rate #5b	rate #5c	rate #5d	rate #5e	rate #5f
min	kg/hr	kg/hr	kg/hr	kg/hr	kg/hr	kg/hr
7	0.51	1.55	1.39	2.40	0.85	0.36
15	0.44	1.45	1.55	2.82	0.85	0.35
30	0.17	0.94	1.35	2.39	0.82	0.36
42	0.15	1.30	2.11	2.14	0.82	0.36
51	0.15	1.42	2.04	2.25	0.82	0.36
61	0.14	1.05	1.98	2.42	0.82	0.36
71	0.14	1.00	2.04	1.98	0.82	0.36
81	0.16	0.94	2.26		0.82	0.36
90	0.17	1.34	1.80		0.85	0.36
102	0.18	0.97	1.80			0.36
120	0.19	0.94				0.36
150	0.19					0.25
160	0.19					

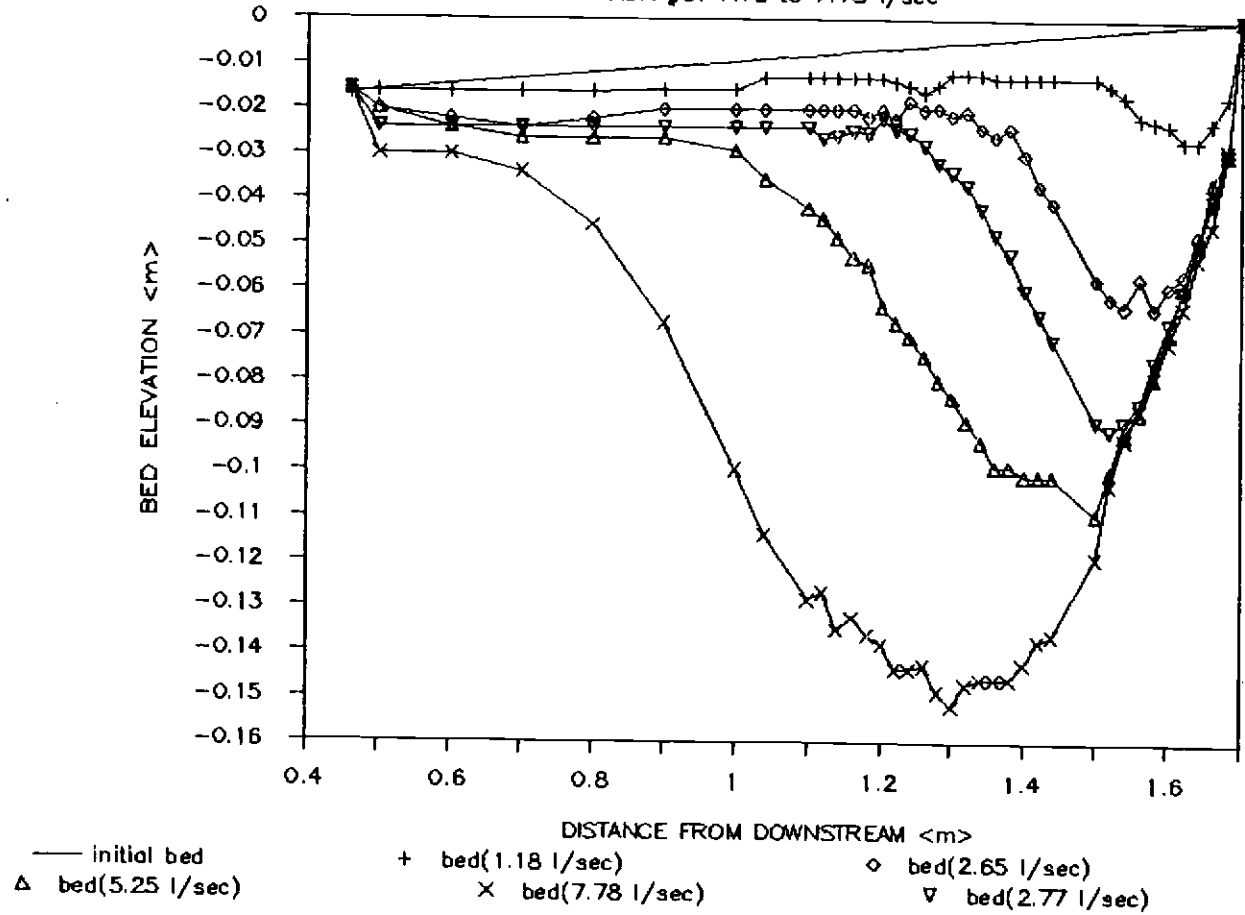
```

#####
# RUN 05
#
# SED.PROPERTIES:1/4' - #16 (D50=3.3mm)
#####
    
```

VELOCITY #Sa(1.2 l/sec):			VELOCITY #Sb(3.0 l/sec):				VELOCITY #Sc(5.2l l/sec):						
Distance	total Depth	Depth	Hertz	Velocity	Distance	total Depth	Depth	Hertz	Velocity	Distance	total Depth	Depth	Hertz
<m>	<m>	<m>		<m/sec>	<m>	<m>	<m>		<m/sec>	<m>	<m>	<m>	
1.90	0.030	0.010	50.0	0.536	1.90	0.050	0.010	70	0.750	1.90	0.075	0.010	80
		0.015	55.0	0.589			0.020	75	0.804			0.015	100
		0.020	60.0	0.643			0.030	75	0.804			0.025	100
		0.030	60.0	0.643			0.040	75	0.804			0.035	100
		0.010	45.0	0.482			0.050	75	0.804			0.045	100
1.66	0.030	0.015	50.0	0.536	1.64	0.055	0.010	10	0.107			0.055	100
		0.020	60.0	0.643			0.015	40	0.429			0.075	100
		0.030	60.0	0.643			0.025	50	0.536	1.60	0.095	0.010	20
		0.010	45.0	0.482			0.035	80	0.857			0.025	50
1.62	0.035	0.015	50.0	0.536			0.040	100	1.071			0.045	75
		0.020	40.0	0.429			0.045	100	1.071			0.055	110
		0.025	30.0	0.321			0.055	100	1.071			0.065	100
		0.035	30.0	0.321	1.54	0.100	0.010	20	0.214			0.095	100
1.30	0.030	0.010	45.0	0.482			0.020	50	0.536	1.40	0.160	0.010	60
		0.015	55.0	0.589			0.030	60	0.643			0.030	60
		0.020	65.0	0.696			0.050	60	0.643			0.050	80
		0.030	65.0	0.696			0.060	30	0.321			0.080	30
0.46	0.025	0.010	50.0	0.536			0.070	20	0.214			0.100	0
		0.015	65.0	0.696			0.090	20	0.214			0.120	-20
		0.025	65.0	0.696			0.100	20	0.214			0.150	-20
					1.42	0.075	0.010	45	0.482			0.160	-20
							0.025	45	0.482	1.24	0.130	0.010	60
							0.035	35	0.375			0.030	35
							0.045	25	0.268			0.050	45
							0.055	20	0.214			0.070	50
							0.065	15	0.161			0.090	50
							0.075	15	0.161			0.110	55
					1.10	0.050	0.010	60	0.643			0.120	55
							0.020	70	0.750			0.130	55
							0.030	70	0.750	0.90	0.075	0.010	70
							0.040	70	0.750			0.015	80
							0.050	70	0.750			0.025	80
					0.46	0.055	0.010	50	0.536			0.035	80
							0.015	65	0.696			0.045	80
							0.025	75	0.804			0.055	80
							0.035	75	0.804			0.065	70
							0.045	75	0.804			0.075	70
							0.055	75	0.804	0.46	0.080	0.010	80
												0.020	90
												0.030	90
												0.040	100
												0.050	100
												0.060	100
												0.070	100

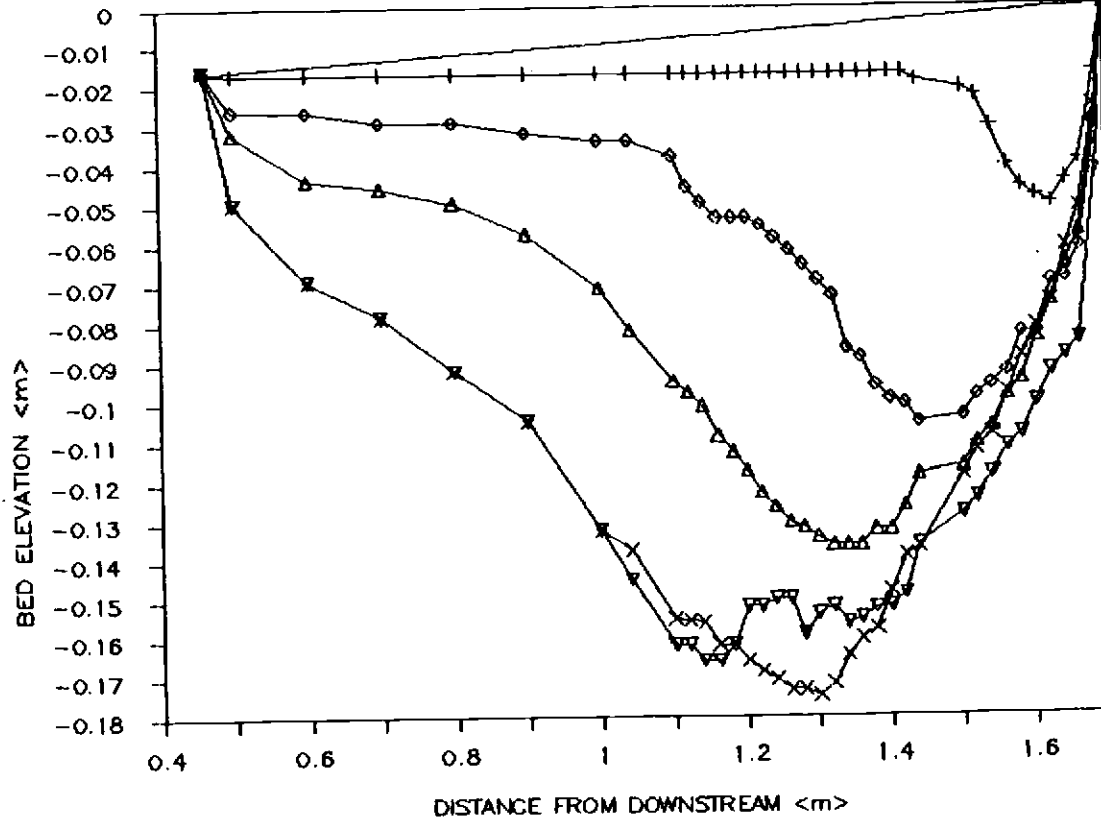
BED ELEVATION CHANGES

RUN #3: 1.18 to 7.78 l/sec



BED ELEVATION CHANGES

RUN #4: 1.27 to 7.6 l/sec



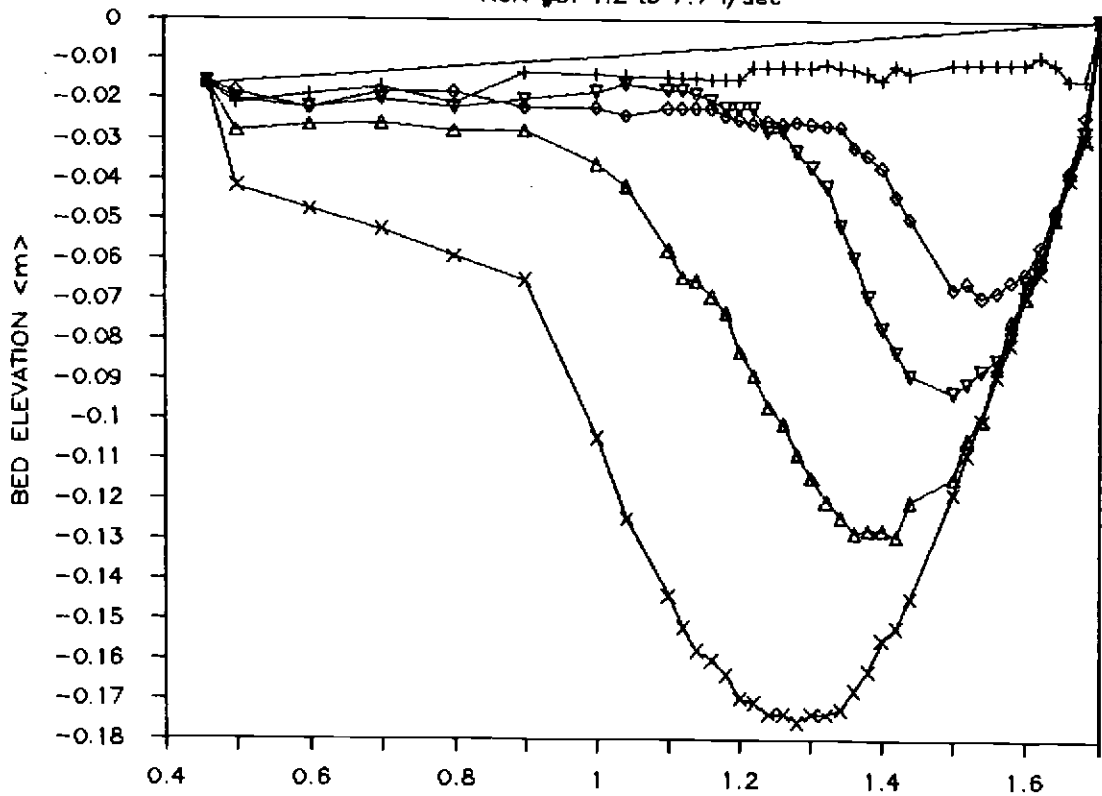
— initial bed
Δ bed(5.1 l/sec)

+ bed(1.27 l/sec)
x bed(7.6 l/sec)

◊ bed(2.92 l/sec)
▽ bed(3.05 l/sec)

BED ELEVATION CHANGE

RUN #5: 1.2 to 7.7 l/sec



— initial bed
Δ bed(5.21 l/sec) + bed(1.2 l/sec) o bed(3.0 l/sec)
x bed(7.7 l/sec) ∇ bed(3.42 l/sec)